Interplay between Ephaptic and Gap Junctional Coupling in Cardiac Conduction

Sharon Ann George

Dissertation submitted to the faculty of the Virginia Polytechnic Institute and State University in partial fulfillment of the requirements for the degree of

Doctor of Philosophy
In
Biomedical Engineering

Steven Poelzing
Robert Gourdie
William R. Huckle
Yong W. Lee
Soufian Almahameed

February 19th, 2016
Roanoke, VA

Keywords: Cardiac, Conduction, Gap junction, Ephaptic coupling, Ions

Interplay between Ephaptic and Gap Junctional Coupling in Cardiac Conduction

Sharon Ann George

ABSTRACT

Sudden cardiac death occurs due to aberrations in the multifactorial process that is cardiac conduction. Conduction velocity (CV) and its modulation by several determinants, like cellular excitability, tissue structure and electrical coupling by gap junctions (GJ), have been extensively studied. However, there are several discrepancies in cardiac electrophysiology research that have extended over decades, suggesting elements that are still not completely understood about this complex phenomenon. This dissertation will focus on one such mechanism, ephaptic coupling (EpC). The purpose of this work is twofold, 1) to identify ionic determinants of EpC, and its interactions with gap junctional coupling (GJC) and, 2) to investigate the possible role of serum ion modulation in cardiac arrhythmia therapy.

First, the effects of altering extracellular ion concentration – sodium, potassium and calcium at varying GJ protein expression were studied. Briefly, reducing sodium was related to CV slowing under conditions of reduced EpC (wide intercalated disc nanodomains – perinexi) and GJC (reduced GJ protein – Connexin43). On the other hand, increasing potassium slowed CV in hearts with wide perinexi independent of GJC. Elevating calcium, reduced perinexal width and was associated with fast CV during physiologic sodium concentration. However, under conditions associated with disease, like hyponatremia, elevating calcium still reduced perinexal width but slowed CV. These findings are the first to suggest that ionic modulators of EpC could modulate CV during health and disease.

Next, the potential of perfusate ion modulation in cardiac arrhythmia therapy was investigated. Briefly, in a model of myocardial inflammation, TNFα, a pro-inflammatory cytokine, slowed CV relative to control conditions and this was associated with widening of the perinexus (reduced EpC). Increasing extracellular calcium restored CV to control values by improving not only EpC but also GJC. Finally, in a model of metabolic ischemia in the heart, CV response due to solutions with varying sodium and calcium concentrations were tested. The solutions that were associated with wider perinexi and elevated sodium performed best during ischemia by attenuating CV slowing, reducing arrhythmias and increasing time to asystole. Taken together, these findings provide evidence for the possibility of ionic determinants of EpC in cardiac arrhythmia therapy.

Interplay between Ephaptic and Gap Junctional Coupling in Cardiac Conduction

Sharon Ann George

ABSTRACT (Public)

The serum level of various ions differs from person to person, as well as due to gender, age and species. However, these concentrations remain within a “normal” range when the individual is healthy. During diseases, this normal range is disrupted and the concentration of ions such as sodium, potassium and calcium is either greatly increased or decreased (disease range) and this can then have secondary effects on the normal functioning of the body.

We have identified here that variations in ion concentrations even within the normal healthy range can modify cardiac functioning. We proposed that these ionic fluctuations can alter electrical coupling between cardiac cells or the means by which each cardiac cell communicates with its neighbor. We specifically hypothesized that ionic fluctuations can alter a form of electrical coupling that is based on the development of electric fields between cells in the heart – Ephaptic coupling. We identified that varying the concentration of sodium, potassium and calcium ions can alter this process of cell to cell communication.

We then applied this data to identify the role of varying the concentration of these ions to preserve electrical activity in the heart during cardiac diseases such as inflammation and ischemia (heart attack). We have identified that maintaining efficient Ephaptic coupling during cardiac diseases can be a new target for cardiac disease therapy.

To all who’d dare to chance the road less travelled.

ACKNOWLEDGEMENTS

The completion of this work would not have been possible without the help, support and guidance of several individuals who have been by my side on this journey, from nearby and from across many miles.

First and foremost, I am grateful for the incredible mentor I received in Dr Steven Poelzing. His infectious enthusiasm and genuine curiosity for science have been crucial in inspiring me to unfold the unknown over the last several years. I would like to thank him for his guidance, motivation and friendship that have aided in molding me as a scientist and as a person.

I would also like to thank my committee members, Dr Robert Gourdie, Dr Soufian Alamahameed, Dr William Huckle and Dr Yong Lee for their scientific guidance as my project took shape. I am thankful to Dr Gourdie who spent time and effort in training and developing my skills in several techniques that I have familiarized. I am also deeply grateful to Drs Huckle and Lee, for not only taking time from their busy schedules to be available for me but also to put in the extra effort of traveling all the way to Roanoke. I would also like to thank Dr Almahameed for his constant reminder of how it is important for science to be translatable to patient care.

Next, I acknowledge the help of all past and present members of the Poelzing lab, all of who have contributed in one way or another to the development of me as a person and my project. I will have to specifically mention Amara Greer-Short, Rengasayee Veeraraghavan, Katie Sciuto, Mike Heidinger, Jeannette Eagen and Stephanie Hurt for their friendship, guidance, help and more importantly patience as I made my way through the many challenges over the last couple of years.

I would be remiss if I did not to acknowledge the support and training I received from Kathy Lowe at VetMed, who worked several hours on my electron microscopy samples and putting extra effort and work to keep up with my pace. I am also grateful for all the guidance provided by Dr James Smyth, who was always available to help me with my molecular biology questions and training. I would also like to thank Dr Rafael Davalos and Mohammad Bonakdar, who have provided their invaluable expertise while I set up the tissue impedance measurement technique in the lab.

Finally and probably more importantly, I would like to thank my family who have supported me all these years and have challenged me to not only follow but to achieve my dreams. The lessons I have learnt from them have been invaluable in motivating me through rough times and have taught me to constantly aspire to be better.

TABLE OF CONTENTS

Page

ABSTRACT ii

ABSTRACT (Public) iii

ACKNOWLEDGEMENTS v

LIST OF FIGURES ix

LIST OF TABLES x

LIST OF ABBREVIATIONS AND ACRONYMS xi

1. INTRODUCTION 1
   - Cardiac Conduction 2
   - Conduction Velocity 4
   - History of Perfusion Solutions 5
   - Ionic Composition and Conduction 6
   - Ephaptic Coupling 6
   - Research Objectives 7
   - References 9

2. PERFUSATE SODIUM AND POTASSIUM ION CONCENTRATIONS AS MODULATORS OF CONDUCTION VELOCITY 15
   - Introduction 16
   - Materials and Methods 16
   - Results 19
   - Discussion 22
   - Limitations 25
   - Conclusions 26
   - References 28

3. PERFUSATE CALCIUM ION CONCENTRATION AS A MODUALTOR OF CONDUCTION VELOCITY IN NORMAL AND DISEASE STATES 39
   - Introduction 40
   - Materials and Methods 41

- Results 44
- Discussion 49
- Limitations 52
- Conclusions 52
- References 54

4. PERFUSATE COMPSITION MODULATION DURING ACUTE TNFα EXPOSURE 67
   - Introduction 68
   - Materials and Methods 69
   - Results 72
   - Discussion 75
   - Limitations 77
   - Conclusions 78
   - References 79

5. PERFUSATE COMPOSITION MODULATION DURING METABOLIC ISCHEMIA 90
   - Introduction 91
   - Materials and Methods 92
   - Results 94
   - Discussion 98
   - Limitations 101
   - Conclusions 102
   - References 103
6. SUMMARY AND FUTURE DIRECTIONS 112
   - Perfusate Classification by Ionic Composition 114
   - Perfusate Ion Modulation in Cardiac Disease 115
   - Conclusions 117
   - Future Directions 117
   - References 118
7. APPENDIX A 121

LIST OF FIGURES

Figure Page

1.1 Conduction – Gap Junction Trend Plot …… 14

2.1 Modulation of Interstitial Volume by Perfusates …… 33

2.2 Modulation of Perinexus by Perfusates …….... 34

2.3 Modulation of Conduction by Perfusates …… 35

2.4 Conduction Velocity – Perinexal width Relationship …….. 36

2.5 Modulation of Conduction Velocity by altering Ionic Composition of Solution 1 …….. 37

2.6 Modulation of Conduction Velocity by altering Ionic Composition of Solution 2 ……..... 38

3.1 Extracellular Calcium – Perinexal Width Relationship during Normonatremia …….. 60

3.2 Extracellular Calcium modulates Conduction Velocity during Normonatremia …… 61

3.3 Extracellular Calcium – Perinexal Width Relationship during Hyponatremia …… 62

3.4 Extracellular Calcium modulates Conduction Velocity during Hyponatremia …… 63

3.5 Cx43 Expression during variation in Extracellular Sodium and Calcium Ion Concentration …….... 64

3.6 Tissue Impedance during variation in Extracellular Sodium and Calcium Ion Concentration …….... 65

3.7 Action Potential duration not affected by $[Na^+]_o$,$[Ca^{2+}]_o$ or Cx43 expression …… 66

4.1 Conduction Velocity Modulation by TNFα ……..... 83

4.2 Conduction Rescue by High Calcium …….. 84

4.3 Action Potential Parameters …… 85

4.4 ECG Parameters ……... 86

4.5 Modulation of Perinexal Width by TNFα …… 87

4.6 Cx43 Expression and Phosphorylation Modulation by TNFα ……..... 88

4.7 Cx43 Distribution Modulation by TNFα …….. 89

5.1 Conduction Velocity during Ischemia and Reperfusion …….. 107

5.2 Action Potential Characteristics …….. 108

5.3 Perinexal Width during Ischemia and Reperfusion …….. 109

5.4 Connexin43 expression and phosphorylation …….. 110

5.5 Arrhythmias …… 111

6.1 Perfusate Composition Modulates CV during Flecainide Exposure …….. 120

LIST OF TABLES

Table	Page
1.1 Ionic Composition of Common Perfusates ……..	13
2.1 Perfusate Composition ……..	32
3.1 Perfusate Osmolarity ……..	59
5.1 Ionic Composition of the Solutions used in the Ischemia Study in mM …….	106

LIST OF ABBREVIATIONS AND ACRONYMS

$[Na^+]_o$	Extracellular sodium ion concentration
$[K^+]_o$	Extracellular potassium ion concentration
WT	Wild type
HZ	Heterozygous
$[Ca^{2+}]_o$	Extracellular calcium ion concentration
Cx43	Connexin43
dV/dt_{max}	Maximum rate of rise of the action potential
I_{Na}	Sodium current
APD	Action potential duration
RMP	Resting membrane potential
CV	Conduction Velocity
CV_L	Longitudinal conduction velocity
CV_T	Transverse conduction velocity
V_m	Transmembrane potential
Φ_o	Extracellular potential
Φ_i	Intracellular potential
CVD	Cardiovascular Disease
AP	Action Potential
$Na_v1.5$	Cardiac isoform of the voltage gated sodium ion channel
I_{KATP}	ATP sensitive inward rectifier potassium channel
EpC	Ephaptic Coupling
GJ	Gap Junction
V_{IS}	Interstitial Volume
W_P	Perinexal Width
E_{Na}	Sodium Reversal potential
R_{GJ}	Gap junctional resistance
$pCx43^{Ser368}$	Connexin43 phosphorylated at serine 368
TNFα	Tumor Necrosis Factor alpha
ID	Intercalated Disc

CHAPTER 1

INTRODUCTION

"In 1960… first three causes of death alone - diseases of the heart, malignant neoplasms, and vascular lesions of the central nervous system - accounted for 66 percent of all deaths." – Vital Statistics of the United States, 1960.

"CVD [cardiovascular disease] is the leading global cause of death, accounting for 17.3 million deaths per year, a number that is expected to grow to >23.6 million by 2030." – Heart Disease and Stroke Statistics – 2015 Update.[1]

In 1960, the US Department of Health, Education and Welfare listed diseases of the heart as the leading cause of death and reported a death rate greater than two times that of the second highest cause of death in all studied groups – male and female, white and non-white. Today, the American Heart Association reports that cardiovascular disease still holds the position of leading cause of death, not only in the United States but worldwide, and the number of deaths due to CVD is projected to grow in 2030, despite decades of cardiovascular research.

Approximately 40-50% of CVD deaths today are attributable to sudden cardiac death.[2] Sudden cardiac death is a result of abnormal and uncoordinated conduction of electrical impulses through the myocardium leading to a lack of synchronous contraction, inefficient pumping of blood and tissue death.

CARDIAC CONDUCTION:

The myocardium was initially thought to be a syncytium, and the conduction of electrical excitation was explained by a model of linear cable theory.[3] Later, it was discovered that the myocardium is composed of individual myocytes surrounded by a cell membrane.[4] Thus conduction of electrical impulses through the myocardium requires the excitation of these individual myocytes and is dependent on several properties of the individual myocytes, its interaction with its neighbors as well as the environment as detailed below.

1. Excitability:

Excitability is usually referred to as the ability to trigger an action potential in a cell or tissue. The electrical signature of a cardiac myocyte excitation is recorded as an action potential (AP). A cardiac AP consists of five phases – Phase 0 to 4. Phase 4 is the resting state of the myocyte where the transmembrane potential (V_m) is set at approximately -90mV. The cell membrane is most permeable to potassium ions at this state[5] and potassium currents, like the inward rectifying potassium current, set the resting membrane potential (RMP).[6] Cells in this resting

state receive stimuli from neighboring myocytes which raise its V_m to the threshold for activation of the sodium ion channels. Current through the voltage gated sodium ion channels, Nav1.5, in cardiac myocytes, then depolarizes the myocyte and raises V_m to positive potentials.[5] This constitutes Phase 0 of the AP. At the end of this phase the sodium channels become inactivated and in some species, like humans and mice but not guinea pigs, this is followed by a slight drop in V_m due to activation of the transient outward potassium currents which forms a notch or Phase 1 of the AP.[7] Phase 2 is determined by a balance between the influx of calcium[8] and efflux of potassium ions[9] in opposite directions to maintain an almost constant V_m. This forms the plateau portion of the AP. During Phase 3, the calcium channels are inactivated leaving the outward potassium currents - delayed rectifier currents and the inward rectifying current to be the predominant determinants of V_m.[10] The cell then repolarizes and V_m returns to resting values. Thus, different phases of the AP are governed by different ionic currents and some of these currents are crucial in determining the excitability of the myocyte.

Nav1.5 availability has been identified as an important factor that can modulate excitability.[11] Reduction in the sodium current (I_{Na}) has been associated with slower rate of rise of the action potential upstroke (dV/dt_{max}).[12] Similarly, potassium currents, especially those that can alter the resting membrane potential, like the inward rectifier and ATP dependent inwardly rectifying potassium currents, can also affect excitability by modulating the number of available sodium ion channels during depolarization.[13] Specifically, elevated RMP results in more sodium ion channels remaining in an inactivated state rendering them unavailable during the next depolarization phase. Additionally, recent studies have also demonstrated a close relationship between the localization and function of the sodium and potassium ion channels where modulating one can affect the other, thereby having a cumulative effect on excitability.[14]

2. Tissue structure:

Conduction is successful only when excitation of individual myocytes is propagated in a fast and coordinated manner across the myocardium. Therefore, the tissue structure is another key determinant of cardiac conduction. Cardiac myocytes are roughly brick-shaped cells that abut end to end at the intercalated disc, making the organization anisotropic. Additionally, each layer of myocytes is then slightly rotated with respect to the one above and this gradual change is called rotational anisotropy.

The extracellular matrix in which the cells are organized is also important in modulating conduction. For example, extracellular fibrosis, which is increased during several diseases like

heart failure can detrimentally affect cardiac conduction.[15] Extracellular volume is another factor to consider. Previously, studies based on the cable theory of cardiac conduction, hypothesized that reducing the extracellular volume will slow cardiac conduction.[16] However, more recent studies have demonstrated that increasing the extracellular volume– both the bulk interstitium[17] as well as in nanodomains along the intercalated discs,[18] slows cardiac conduction, contrary to previous theories. This suggested the presence of additional factors that can affect cardiac conduction that were not previously accounted for.

3. Gap junctional coupling:

Individual myocytes placed in a suitable environment have to be connected to neighboring myocytes, to support efficient propagation of electrical excitation. Structural and electrical coupling between myocytes is achieved by gap junctions (GJ). Connexin43 (Cx43), the predominant ventricular gap junctional protein, forms gap junction plaques at the intercalated discs, which act as resistive pathways for the propagation of electrical impulses from one cell to the next.[19] Cx43 GJ channels are formed when two hemichannels from apposing cell membranes dock together.[20] The hemichannels are, in turn, composed of six connexin subunits and based on the presence of different connexin isoform in these hemichannels, they could be homomeric (same isoforms) or heteromeric (different isoforms). Similarly, based on the types of hemichannels that form a GJ channel, it could be either homotypic (same isoform hemichannels) of heterotypic (different isoform hemichannels).

Importantly, reduced Cx43 expression is associated with numerous cardiac diseases.[21-23] As a result, most contemporary studies seeking to explore changes in cardiac electrical propagation include some quantification of gap junction mRNA, protein expression, protein phosphorylation, protein distribution, and/or direct cell-to-cell conductance measurements. Several groups have also developed different genetic mouse models of Cx43 reduction to study the effect of Cx43 expression modulation on conduction. These models include total Cx43 knockout mice,[24] conditional knockout mice[25] with cardiac restricted Cx43 reduction,[26] chimeric mice[27] and C-terminus mutant mice.[28] These models have made it possible to study several functional consequences of varying degrees of functional Cx43 expression.

CONDUCTION VELOCITY:

Conduction velocity (CV), a well-established metric of cardiac conduction, has been extensively studied using these mouse models. Altering any of the determinants of conduction mentioned

above individually or in combination can significantly modulate CV.[25,29] CV slowing then forms a substrate for the development of abnormal conduction patterns in the heart or arrhythmias, which can be fatal.

Among all the above determinants of CV, the CV-GJ relationship has been a subject of intense research for many years. The trend plot in Figure 1.1 illustrates the number of scientific studies published that are based on conduction and Cx43 in the heart. However, various groups have reported differing results even with similar extents of Cx43 downregulation and *ex vivo* protocols.[24,26,29-31] These differing results were attributed to experimental differences.

We identified that one crucial and easily overlooked source for differences in these *ex vivo* isolated heart preparations is the ionic composition of the perfusates. Perfusates are used in these protocols as an artificial blood-like solution that is circulated through the heart to keep the heart alive over the experimental period. To understand the importance of these perfusates in physiology, we must first take a look at the history of these solutions.

HISTORY OF PERFUSION SOLUTIONS:

The origin of salt perfusion solutions in science and medicine can be traced to the early 19th century when Indian Blue Cholera spread to the northern regions of England. In 1831, William Brooke O'Shaughnessy reported "injection of highly-oxygenated salts into the venous system" as a new method to treat cholera. This new discovery led several others to use their own versions of salt solutions to treat cholera. However, it was Thomas Latta, in 1832, who identified the first solution that was most similar to blood composition. About 50 years later in 1883, Sydney Ringer created what is now referred to as the original Ringer's solution (130 mM [Na^+], 4 mM [K^+], 1.5mM [Ca^{2+}], 109mM [Cl^-] and 28mM Lactate) to bathe explanted frog hearts. Over the next century, the composition of solutions significantly diverged and the number of buffer solutions exploded because of the need to investigate single proteins, isolated cells, tissue cultures, organ preservation, organ perfusion and transplant.[32]

In 1895, Oskar Langendorff developed the method of perfusing explanted mammalian hearts to study the amplitude and rate of contraction.[33] The Langendorff method was then used to study the coronary vasculature and the effect of pharmacological interventions. Today, it has a wide range of applications in physiology, including the measurement of conduction velocity in explanted hearts. Tyrode's, Kreb's and Kreb's-Henseleit solutions are the most commonly used perfusates in explanted heart studies, and the individual solubilized components of these common buffers according to Cold Spring Harbor are listed in Table 1.1.

An important factor to consider when using various perfusion solutions is that the concentration of solutes in serum varies from species to species.[34] The physiological ranges of solutes in mouse and guinea pig serum, the species discussed here, are listed in Table 1.1.[34] Many groups have modified the original solutions to resemble the serum concentrations of the particular species in use. It was the observation that different groups used different perfusates that led us to hypothesize that perfusate composition may underlie the diverse CV-GJ relationships reported in the literature.

IONIC COMPOSITION AND CONDUCTION:

Serum ion concentration varies due to numerous factors like disease, circadian rhythm, species and gender. The relationship between extracellular ion concentration and CV has been previously reported. Increasing extracellular potassium ion concentration ($[K^+]_o$) has been shown to elicit a biphasic CV response.[35] Briefly, small increases in $[K^+]_o$ slightly raises RMP closer to threshold for sodium channel activation and thereby produces faster CV. However, further increasing $[K^+]_o$ raises RMP even more, which can then reduce the number of available sodium ion channels during depolarization and slow conduction. On the other hand, reducing extracellular sodium ion concentration ($[Na^+]_o$) can reduce the driving force for I_{Na} due to smaller chemical gradient across the cell membrane.[36] This can also result in CV slowing. The effect of modulating extracellular calcium ion concentration ($[Ca^{2+}]_o$) on CV has also been reported.[37] Increasing $[Ca^{2+}]_o$ has been demonstrated to have a myriad of effects on cellular functioning[38] which can then precipitate as CV slowing. Similarly, varying other ion concentrations may also modulate CV. However, the majority of these studies investigated pathophysiologic variations in ionic composition and its effects on CV. However, the effect of physiologic modulation of ionic composition on cardiac conduction and its mechanism of action are not fully understood.

EPHAPTIC COUPLING:

In 2002, Dr Sperelakis proposed an alternative form of electrical coupling between cardiac myocytes – ephaptic coupling (EpC), which simply means non-synaptic and non-gap junctional coupling. He proposed six different mechanisms by which ion accumulation or depletion in extracellular spaces can generate electric fields that electrically couple neighboring myocytes.[39] Ephaptic coupling is perhaps better accepted in the neural literature.[40-44] In the cardiac literature, the preponderance of work into ephaptic coupling has been largely confined to theoretical simulations [45-47] where it is often modeled as the generation of significant extracellular fields in small clefts between neighboring myocytes. By definition, excitable cells like cardiomyocytes

depolarize when V_m – the difference between the intracellular and extracellular potentials ($V_m = \Phi_i - \Phi_o$) – rises. V_m can rise by either increasing Φ_i or decreasing Φ_o. In turn, Φ_i can be elevated by charge transfer from a pre- to a post-junctional cell via GJ, while Φ_o can change in response to accumulation or depletion of charge within restricted extracellular clefts between myocytes. In cardiomyocytes, it has been proposed that ephaptic coupling can occur via activation of sodium ion channels in the actively depolarizing myocyte, inducing an inward flow of sodium ions into the cell, while simultaneously reducing the potential in the cleft between the myocytes. This decreases cleft potential (reduces Φ_o), raises V_m of the neighboring cell, which then activates the post-junctional sodium channels by depolarizing the membrane from the extracellular domain to initiate cellular depolarization.[45,46]

Our group recently provided experimental evidence supporting the theory of ephaptic coupling in guinea pig[17,48] whole-heart preparations. Further support for this hypothesis comes from the identification of intercalated disc microdomains such as the connexome[49] and perinexus[50] which meet the theoretically-predicted requirements of a cardiac ephapse: dense sodium channel localization in narrow intercellular clefts. We have demonstrated that CV slowing during pharmacologic reduction of gap junctions can be mitigated or exacerbated by altering the perinexus through interventions like albumin or mannitol perfusion. Broadly, we found that wide perinexi exacerbate the loss of GJs. Importantly, only computational models incorporating ephaptic coupling predict that increasing extracellular volume and/or conductivity decreases CV and exacerbates GJ uncoupling induced CV slowing.[46,48] However, the effects of ionic determinants of ephaptic coupling on conduction and its interactions with other factors that can modulate CV have not been characterized.

RESEARCH OBJECTIVES

This dissertation focuses on understanding the interaction between the two proposed forms of electrical coupling in cardiac myocytes – ephaptic and gap junctional coupling. In Chapters 1 and 2, ionic modulators of ephaptic coupling will be identified and its effect on CV will be demonstrated. Specifically, Chapter 1 will focus on physiologic variations in extracellular sodium and potassium ion concentrations and its interaction with perinexal width and gap junctional coupling. Modulation of CV under these conditions will be studied. Chapter 2 will include the effects of extracellular ion modulation of perinexal width and therefore CV. The differential CV response to calcium concentration during normal states and conditions of disease, like hyponatremia, will be determined.

In Chapters 3 and 4, the possibility of perfusate composition modulation as a therapy during cardiac diseases will be explored. Specifically, in Chapter 3 we will discuss the role of ionic composition in modulating ephaptic and gap junctional coupling and thereby CV in a model of myocardial inflammation. While in Chapter 4, the concept of CV modulation by perfusate composition will be applied to preserve conduction during metabolic ischemia in the heart.

REFERENCES:

1. Mozaffarian D, Benjamin EJ, Go AS, et al. Heart disease and stroke statistics--2015 update: a report from the American Heart Association. *Circulation.* 2015;131:e29-322.

2. Mehra R. Global public health problem of sudden cardiac death. *Journal of Electrocardiology.* 2007;40:S118-122.

3. Weidmann S. The electrical constants of Purkinje fibres. *The Journal of Physiology.* 1952;118:348-360.

4. Dewey MM, Barr L. Intercellular Connection between Smooth Muscle Cells: the Nexus. *Science.* 1962;137:670-672.

5. Hodgkin AL, Huxley AF, Katz B. Measurement of current-voltage relations in the membrane of the giant axon of Loligo. *The Journal of Physiology.* 1952;116:424-448.

6. Ibarra J, Morley GE, Delmar M. Dynamics of the inward rectifier K+ current during the action potential of guinea pig ventricular myocytes. *Biophysical Journal.* 1991;60:1534-1539.

7. Kenyon JL, Gibbons WR. 4-Aminopyridine and the early outward current of sheep cardiac Purkinje fibers. *The Journal of General Physiology.* 1979;73:139-157.

8. Reuter H. The dependence of slow inward current in Purkinje fibres on the extracellular calcium-concentration. *The Journal of Physiology.* 1967;192:479-492.

9. Yue DT, Marban E. A novel cardiac potassium channel that is active and conductive at depolarized potentials. *Pflugers Archiv : European Journal of Physiology.* 1988;413:127-133.

10. Sanguinetti MC, Jurkiewicz NK. Two components of cardiac delayed rectifier K+ current. Differential sensitivity to block by class III antiarrhythmic agents. *The Journal of General Physiology.* 1990;96:195-215.

11. Shaw RM, Rudy Y. Ionic mechanisms of propagation in cardiac tissue. Roles of the sodium and L-type calcium currents during reduced excitability and decreased gap junction coupling. *Circulation Research.* 1997;81:727-741.

12. Weidmann S. The effect of the cardiac membrane potential on the rapid availability of the sodium-carrying system. *The Journal of Physiology.* 1955;127:213-224.

13. Hodgkin AL, Huxley AF. The dual effect of membrane potential on sodium conductance in the giant axon of Loligo. *The Journal of Physiology.* 1952;116:497-506.

14. Milstein ML, Musa H, Balbuena DP, et al. Dynamic reciprocity of sodium and potassium channel expression in a macromolecular complex controls cardiac excitability and

arrhythmia. *Proceedings of the National Academy of Sciences of the United States of America.* 2012;109:E2134-2143.

15. Glukhov AV, Fedorov VV, Kalish PW, et al. Conduction remodeling in human end-stage nonischemic left ventricular cardiomyopathy. *Circulation.* 2012;125:1835-1847.

16. Spach MS, Heidlage JF, Barr RC, et al. Cell size and communication: role in structural and electrical development and remodeling of the heart. *Heart Rhythm.* 2004;1:500-515.

17. Veeraraghavan R, Salama ME, Poelzing S. Interstitial volume modulates the conduction velocity-gap junction relationship. *American Journal of Physiology. Heart and Circulatory Physiology.* 2012;302:H278-286.

18. Veeraraghavan R, Lin J, Hoeker GS, et al. Sodium channels in the Cx43 gap junction perinexus may constitute a cardiac ephapse: an experimental and modeling study. *Pflugers Archiv : European Journal of Physiology.* 2015;467:2093-2105.

19. Barr L, Dewey MM, Berger W. Propagation of Action Potentials and the Structure of the Nexus in Cardiac Muscle. *The Journal of General Physiology.* 1965;48:797-823.

20. Sohl G, Willecke K. Gap junctions and the connexin protein family. *Cardiovascular Research.* 2004;62:228-232.

21. Celes MR, Torres-Duenas D, Alves-Filho JC, et al. Reduction of gap and adherens junction proteins and intercalated disc structural remodeling in the hearts of mice submitted to severe cecal ligation and puncture sepsis. *Critical Care Medicine.* 2007;35:2176-2185.

22. Poelzing S, Rosenbaum DS. Altered connexin43 expression produces arrhythmia substrate in heart failure. *American Journal of Physiology. Heart and Circulatory Physiology.* 2004;287:H1762-1770.

23. Cascio WE, Yang H, Muller-Borer BJ, et al. Ischemia-induced arrhythmia: the role of connexins, gap junctions, and attendant changes in impulse propagation. *Journal of Electrocardiology.* 2005;38:55-59.

24. Guerrero PA, Schuessler RB, Davis LM, et al. Slow ventricular conduction in mice heterozygous for a connexin43 null mutation. *The Journal of Clinical Investigation.* 1997;99:1991-1998.

25. Stein M, van Veen TA, Remme CA, et al. Combined reduction of intercellular coupling and membrane excitability differentially affects transverse and longitudinal cardiac conduction. *Cardiovascular Research.* 2009;83:52-60.

26. Gutstein DE, Morley GE, Tamaddon H, et al. Conduction slowing and sudden arrhythmic death in mice with cardiac-restricted inactivation of connexin43. *Circulation Research.* 2001;88:333-339.

27. Gutstein DE, Morley GE, Vaidya D, et al. Heterogeneous expression of gap junction channels in the heart leads to conduction defects and ventricular dysfunction. *Circulation.* 2001;104:1194-1199.

28. Lubkemeier I, Requardt RP, Lin X, et al. Deletion of the last five C-terminal amino acid residues of connexin43 leads to lethal ventricular arrhythmias in mice without affecting coupling via gap junction channels. *Basic Research in Cardiology.* 2013;108:348.

29. Stein M, van Veen TA, Hauer RN, et al. A 50% reduction of excitability but not of intercellular coupling affects conduction velocity restitution and activation delay in the mouse heart. *PloS One.* 2011;6:e20310.

30. Eloff BC, Lerner DL, Yamada KA, et al. High resolution optical mapping reveals conduction slowing in connexin43 deficient mice. *Cardiovascular Research.* 2001;51:681-690.

31. Morley GE, Vaidya D, Samie FH, et al. Characterization of conduction in the ventricles of normal and heterozygous Cx43 knockout mice using optical mapping. *Journal of Cardiovascular Electrophysiology.* 1999;10:1361-1375.

32. Awad S, Allison SP, Lobo DN. The history of 0.9% saline. *Clinical Nutrition.* 2008;27:179-188.

33. Broadley KJ. The Langendorff heart preparation - Reappraisal of its role as a research and teaching model for coronary vasoactive drugs. *Journal of Pharmacological Methods.* 1979;2:143-156.

34. Research Animals Resources UoM. Reference Values for Laboratory Animals. Normal Hematology Values. 2009; www.ahc.umn.edu/rar/refvalues.html, 2013.

35. Kagiyama Y, Hill JL, Gettes LS. Interaction of acidosis and increased extracellular potassium on action potential characteristics and conduction in guinea pig ventricular muscle. *Circulation Research.* 1982;51:614-623.

36. Hodgkin AL, Huxley AF. Currents carried by sodium and potassium ions through the membrane of the giant axon of Loligo. *The Journal of Physiology.* 1952;116:449-472.

37. Pressler ML, Elharrar V, Bailey JC. Effects of extracellular calcium ions, verapamil, and lanthanum on active and passive properties of canine cardiac purkinje fibers. *Circulation Research.* 1982;51:637-651.

38. Zarain-Herzberg A, Fragoso-Medina J, Estrada-Aviles R. Calcium-regulated transcriptional pathways in the normal and pathologic heart. *International Union of Biochemistry and Molecular Biology Life.* 2011;63:847-855.

39. Sperelakis N, McConnell K. Electric field interactions between closely abutting excitable cells. *Institute of Electrical and Electronic Engineers - Engineering in Medicine and Biology Magazine.* 2002;21:77-89.

40. Arvanitaki A. Effects Evoked in an Axon by teh Activity of a Contiguous one. *Journal of Neurophysiology.* 1942;5:89-108.

41. Bokil H, Laaris N, Blinder K, et al. Ephaptic interactions in the mammalian olfactory system. *The Journal of Neuroscience.* 2001;21:RC173.

42. Anastassiou CA, Perin R, Markram H, et al. Ephaptic coupling of cortical neurons. *Nature Neuroscience.* 2011;14:217-223.

43. Su CY, Menuz K, Reisert J, et al. Non-synaptic inhibition between grouped neurons in an olfactory circuit. *Nature.* 2012;492:66-71.

44. Van der Goes van Naters W. Inhibition among olfactory receptor neurons. *Frontiers in Human Neuroscience.* 2013;7:690.

45. Lin J, Keener JP. Ephaptic coupling in cardiac myocytes. *Institute of Electrical and Electronic Engineers - Transactions on Bio-medical Engineering.* 2013;60:576-582.

46. Lin J, Keener JP. Microdomain effects on transverse cardiac propagation. *Biophysical Journal.* 2014;106:925-931.

47. Mori Y, Fishman GI, Peskin CS. Ephaptic conduction in a cardiac strand model with 3D electrodiffusion. *Proceedings of the National Academy of Sciences of the United States of America.* 2008;105:6463-6468.

48. Veeraraghavan R, Lin J, Hoeker GS, et al. Sodium channels in the Cx43 gap junction perinexus may constitute a cardiac ephapse: an experimental and modeling study. *Pflugers Archiv : European Journal of Physiology.* 2015; 467:2093-2105.

49. Agullo-Pascual E, Reid DA, Keegan S, et al. Super-resolution fluorescence microscopy of the cardiac connexome reveals plakophilin-2 inside the connexin43 plaque. *Cardiovascular Research.* 2013;100:231-240.

50. Rhett JM, Gourdie RG. The perinexus: a new feature of Cx43 gap junction organization. *Heart Rhythm.* 2012;9:619-623.

Table 1.1 Ionic Composition of Common Perfusates. The standard ionic composition (in mM) of commonly used perfusates in Langendorff preparations as published by Cold Spring Harbor Protocols is tabulated. Serum ion concentration in mice and guinea pigs are also listed. NR – not reported.

Ions	Tyrode	Krebs	Krebs-Henseleit		Mouse Physiologic Range	Guinea Pig Physiologic Range
Na^+	149.2	152.2	143		140 – 160	146 – 152
K^+	2.7	2.5	5.9		5 - 7.5	6.8 – 8.9
Mg^{2+}	1	1.2	1.2		NR	NR
Ca^{2+}	1.8	2.5	1.25		1.7 - 2.5	1.3 – 3
Cl^-	145.3	135.9	125.2		88 – 110	98.115
$H_2PO_4^-$	0.2	1.2	1.2		1.8 – 3	1 – 2.5
HCO_3^-	12	25	25		NR	NR
SO_4^{2-}			1.2		NR	NR
Glucose	5.5		11		3.4 - 9.8	3.3 – 7

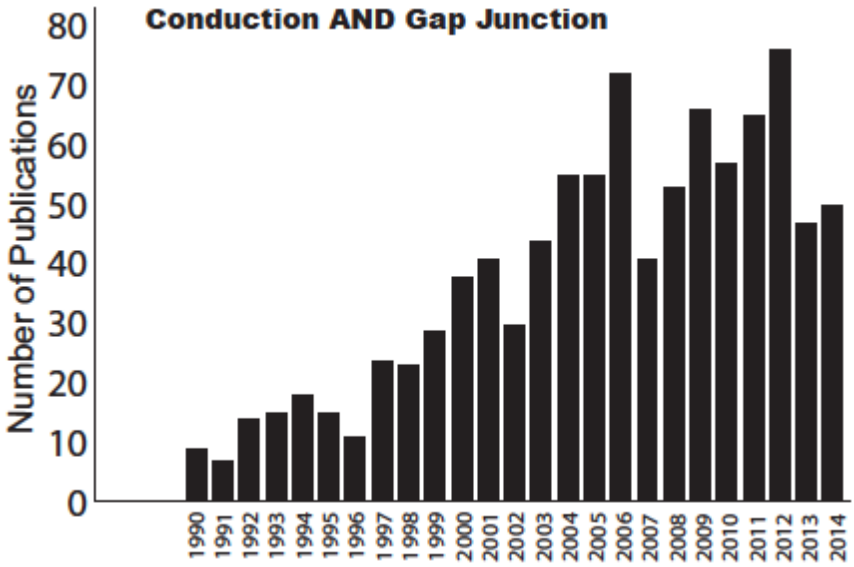

Figure 1.1: Conduction – Gap Junction Trend Plot. The number of studies that were identified by Pubmed with the search term “Conduction AND Gap Junction” since 1990 is plotted.

CHAPTER – 2

PERFUSATE SODIUM AND POTASSIUM ION CONCENTRATION AS MODULATORS OF CONDUCTION VELOCITY

INTRODUCTION

Gap junctional coupling is an important determinant of electrical impulse propagation through the heart and many other tissues. Gap junctions (GJ) are low resistance pathways between myocytes that aid in the transmission of electrical impulses from one myocyte to the next.[1] Remodeling of the principal ventricular GJ protein, Connexin43 (Cx43), is a hallmark of several cardiac diseases.[2-4] Due to its association with abnormal conduction and arrhythmogenesis, the conduction velocity–gap junction (CV–GJ) relationship has been the focus of intense study. [5-12] However, the results of these studies have not been in agreement, leading to interesting and as yet unresolved controversies.

In general, the conclusions of previous studies can be summarized in two categories: 1) substantial reduction in GJ expression (>50%) is required to change CV [5,9,10,13,14] or 2) CV slows secondary to an approximate 50% loss of Cx43 protein.[6,7,12] Comparing two specific studies [5,6] revealed that perfusate composition and conclusions drawn were different even though both groups used genotypically identical mice with heterozygous loss of GJa1 and a resultant 50% reduction in Cx43. It has been previously demonstrated that altering perfusate composition can change the interstitial volume (V_{IS}) in the heart and thereby modulate the CV-GJ relationship.[15] More recently, we found that variance in inter-membrane spacing within intercalated disc microdomains adjacent to GJ plaques termed the perinexus may modulate an alternative mode of electrical coupling that can explain how V_{IS} modulates the CV-GJ relationship.[16] We therefore hypothesized that perfusate ionic composition can modulate the CV-GJ relationships in a related manner. The specific aims of this study were to determine the differential effects of perfusate composition on perinexal spacing and how varying extracellular sodium and potassium modulates the CV-GJ relationship in the GJa1 heterozygous null mouse.

MATERIALS AND METHODS

The study protocols were approved by the Institutional Animal Care and Use Committee at Virginia Polytechnic Institute and State University and conform to the NIH Guide for the Care and Usage of Laboratory Animals.

Langendorff Perfusion System: Mice from the same lineage as in the aforementioned two studies[5-7] were genotyped by Transnetyx (Cordova, TN). These mice, generously provided by Dr Jeffery Saffitz of Harvard University, were on a C57BL/6 background (original breeders from

Jackson Laboratory) and were heterozygous for Cx43 null mutations (~50% Cx43 reduction compared to control [7]). Wild Type (WT) and heterozygous (HZ, ~50% Cx43) mice (10-30 weeks of age) were anesthetized by a lethal intraperitoneal injection of sodium pentobarbital (~325 mg/kg) and the hearts were quickly excised. The aorta was cannulated and retrogradely perfused as previously described.[5,6] Hearts were perfused with solutions (pH7.4) described in Table 2.1 in random order at a flow rate of 1 to 1.5 ml/min maintaining the perfusion pressure at approximately 65 mmHg. The temperature of the perfusate and the bath were maintained at 37ºC. The osmolarity of the solutions was measured using Precision Systems Micro Osmometer and are reported in Table 2.1.

All solutions were perfused in random order to minimize differences due to perfusion order and time. Each heart was perfused with a maximum of 4 solutions. Electrophysiology was quantified in hearts perfused with Solutions 1 and 2 (13 WT and 13 HZ animals). Electrophysiology was quantified in 5 hearts for every other solution except Solution 1A (n=9).

Histology: Hearts (n=8 per intervention, and N=32 total) were formalin fixed after one hour of perfusion and V_{IS} was quantified as previously described.[15] Fixed hearts were paraffin embedded, sectioned and Hematoxylin and Eosin (H&E) stained. Sections from the right ventricle were then digitally scanned using an Aperio ScanScope XT system (Vista, CA). A positive pixel algorithm was applied to whole slide images to segment cardiac myocytes and the interstitial (extracellular) volume (excluding blood and lymph vessels). The percent interstitial volume ($\%V_{IS}$) was determined as follows.

$$\% V_{IS} = \frac{(Total\ analysis\ area\ -\ Stained\ Area)}{Total\ analysis\ Area}\ X\ 100$$

Blood and lymph vessels that were greater than 100 μm^2 in area were excluded from the selected region.

Transmission Electron Microscopy: In another separate set of experiments (n=3 per intervention, N=24 samples, with 15 images per sample), $1mm^3$ cubes of right ventricular tissue perfused for 1 hour, were fixed in 2.5% Gluteraldehyde overnight at 4ºC and then transferred to PBS at 4ºC. The tissue was processed as previously described[16] initially in 1% Osmium Tetroxide (OsO_4) and 1.5% Potassium Ferricyanide (KFeCN) followed by rinse with H_2O. Samples were then transferred to ethanol at increasing concentrations (70, 95 and 100%) for 15

minutes at each concentration and then transferred to a 1:1 solution of 100% ethanol and acetonitrile for 10 minutes. Samples were then transferred to only acetonitrile for two 10 minute periods and then embedded in PolyBed 812 at increasing concentrations with Acetonitrile on a rotator. The samples were left in vacuum for ~3 hours and then left in PolyBed 812 overnight and transferred to flat molds and incubated at 60ºC for 2 days. The blocks were then sectioned using a microtome onto copper grids and stained with Uranyl acetate (Aq) for 40 minutes followed by Hanaichi Pb stain. Images were then collected using a transmission electron microscope (JEOL JEM1400). The images of the gap junctions and the perinexi were obtained at 150,000X magnification. The perinexal width (W_P) in these images was measured using ImageJ. Mean ± standard error is reported.

Optical Mapping: Hearts were optically mapped with the voltage sensitive dye, Di-4-ANEPPS at a concentration of 4 μM for approximately 5 minutes. Motion was reduced with the electromechanical uncoupler, 2,3-butanedione monoxime (BDM). Specific BDM concentrations matching the previous studies are detailed in Table 2.1. Hearts were stabilized against the front glass of the bath by applying slight pressure to the back of the heart. The center of the anterior ventricular surface was paced with a unipolar silver wire with a reference electrode at the back of the bath. Hearts were stimulated at ~1V for 1ms at a BCL of 150 ms.

The excitation light from a halogen light source (MHAB-150W, Moritex Corpration) was filtered by a 510 nm filter (Brightline Fluorescence Filter) before it reached the heart. The emitted light was filtered by a 610 nm filter (610FG01-50(T257), Andover Corporation) before it was recorded using a MiCam Ultima CMOS L-camera at a sampling rate of 1000 frames/sec. The camera captured optical signals from an area of 1 cm^2 in a 100x100 pixel array with an interpixel resolution of 0.1 mm.

Activation times were assigned to the maximum rate of rise of an action potential as previously reported[15] using the Bayly et al. algorithm.[17] In short, activation time was determined from the maximum rate of optical action potential rise at each pixel, and a parabolic surface was fit to activation times in order to determine a CV vector at each pixel. Longitudinal and transverse CV (CV_L and CV_T), and anisotropic ratios (ratio of CV_L/CV_T, AR) were quantified.

Statistical Analysis: Equal variance and sample size, one/two-tailed student's t-tests were performed on paired and unpaired data to detect significance using Matlab. Specific statistical

analyses are indicated in Figure legends. Single factor ANOVA was performed to detect differences in perinexal width between solutions and WT/HZ mice, and t-tests were used as a post-hoc test to determine significance in perinexal width at specific distances. Bonferroni correction was applied for multiple comparisons.

All statistical tests were performed on absolute data values except for data in Figure 2.5 and 6. Values reported in these figures are relative to Control solutions ($[Na^+]_o$ = 155.2 mM and $[K^+]_o$ = 4.0 mM).

All data are reported as mean ± standard deviation unless stated otherwise. $p<0.05$ was reported as significant.

RESULTS

Interstitial Volume:

V_{IS} is the interstitial volume between myocytes in myocardial tissues excluding blood and lymph vessels. Previously, we provided evidence that altering V_{IS}, by varying the osmolarity of the perfusate,[15] modulated the CV-GJ relationship. In this study, differences in osmolarity correlated with $[Na^+]_o$ where increasing $[Na^+]_o$, on average, increased osmolarity by 5% (Table 2.1). We previously reported that increasing osmolarity by approximately 40% increased histologically assessed V_{IS} by 61%. A similar analysis was performed in the current study to determine whether the 5% increase in osmolarity resulting from increased $[Na^+]_o$ altered V_{IS}.

H&E stained ventricular sections of WT and HZ hearts perfused with solutions published by Morley et al. (Solution 1)[5] and Eloff et al. (Solution 2),[6] are shown in Figure 2.1a and b. V_{IS} was not significantly different as a result of perfusate in WT ventricles. In contrast, V_{IS} in HZ ventricles was greater when perfused with Solution 1 than 2 (Figure 2.1b). The $\%V_{IS}$ was significantly reduced in HZ hearts perfused with Solution 2 (Figure 2.1c) compared to hearts perfused with Solution 1. Thus, a 5% increase in osmolarity was associated with a significant increase in V_{IS} (70%) only in HZ hearts.

Perinexus:

The intercalated disc and specifically the perinexus - a specialized domain of cell membrane adjacent to gap junction (GJ) plaques, has been identified as a site of dense voltage-gated sodium channel ($Na_V1.5$) localization.[16,18-20] Representative electron micrographs of GJs and neighboring perinexi in Figure 2.2a and b demonstrate the effects of perfusate on perinexal width (W_P). W_P in both WT and HZ hearts was larger with Solution 1 than Solution 2 (Figure

2.2a Upper Panels versus Lower Panels). Solution 1 was then modified to contain the same $[Na^+]_o$ and $[K^+]_o$ as Solution 2 (Solution 1C) or vice versa (Solution 2C). Solution 1C also increased W_P relative to Solution 2C, as seen in representative Figure 2.2b. W_P, up to 105 nm from the edge of a gap junction for all experiments, is summarized in Figure 2.2c and d. For any given solution, W_P was not significantly different between WT and HZ hearts. Therefore, WT and HZ measurements were combined. Solution 1 and 1C increased W_P at all measured points relative to Solution 2 and 2C respectively. Additionally, Solution 1 was associated with a *larger* W_P and *higher* osmolarity relative to Solution 2. Interestingly, Solution 1C was also associated with a *larger* W_P but *lower* osmolarity relative to Solution 2C. This finding suggests that changes in perinexal width may not always correlate with osmolarity and that additional factors may be involved.

Interestingly, V_{IS} does not always correlate with W_P. Specifically, V_{IS} as quantified from gross histology in WT hearts was not different with Solution 1 or 2, but W_P was significantly larger in WT hearts perfused with Solution 1 than 2. On the other hand, V_{IS} correlated with W_P in HZ hearts.

Conduction Velocity:

In order to directly test the hypothesis that perfusate composition underlies the CV-GJ relationship in Gja1 heterozygous null hearts, Solutions 1 and 2 were serially perfused. Representative isochrones of epicardial conduction from optical maps are provided in Figure 2.3a, and CV is reported in Figures 2.3b and c. For all experiments in WT animals with the native complement of Cx43, CV_L, CV_T, and anisotropic ratio (AR) were not different during Solution 2 perfusion relative to Solution 1 (Figure 2.3b-d, Left Panels). In HZ hearts, Solution 2 preferentially slowed CV_T relative to Solution 1 without significantly altering CV_L or AR (Figure 2.3b-d, Right Panels). However, though we reproduce the Morley et al. results (no change in CV between WT and HZ hearts), CV slowing in HZ hearts relative to WT, as in the Eloff et al. study, was not statistically significant by comparison with a 2-tailed, unpaired t-test and Bonferonni correction.

Our previous studies suggested that *decreased* V_{IS}, and more specifically decreased W_P, is associated with *faster* conduction.[15,16] At first glance, the finding that Solution 1 is associated with *increased* W_P and *faster* conduction in HZ hearts appears inconsistent with these earlier findings. However, the concentrations of sodium and potassium in Solution 2 was also different

from Solution 1, leading us to hypothesize that $[Na^+]_o$ and $[K^+]_o$ may further modulate the CV-GJ relationship.

Conduction Velocity and Perinexal width:

We next compared conduction in the same hearts, with solutions containing similar $[Na^+]_o$ and $[K^+]_o$ but producing different perinexal spacing (Solutions 2 – Small W_P and 1C – Large W_P). While CV_L was not significantly different in WT or HZ hearts perfused with Solutions 2 and 1C (Figure 2.4a), CV_T was significantly slower in both WT and HZ hearts with wider perinexi (Solution 1C) than in hearts with narrower perinexi (Solution 2). The finding that increased W_P is associated with slower CV_T, but no change in AR, is summarized in Figures 2.4b and c. Importantly, Figure 2.4d demonstrates that increased W_P is associated with greater CV slowing in HZ animals relative to WT. This further supports our previous results that CV_T is more sensitive to GJ uncoupling when the perinexus is wide.[16] In summary, when we control for ionic composition, CV is inversely proportional to W_P, consistent with our previous study.[16]

Taken together, these data suggest that the CV-GJ relationship may be modulated by other factors such as $[Na^+]_o$ and $[K^+]_o$ in addition to perinexal spacing. Interestingly, the ionic compositions of Solutions 1 and 2 are significantly different, and the following experiments focus on the first two cationic differences (sodium and potassium, due to their plausible effect on excitability), W_P, and their combined effects on the CV-GJ relationship.

- Solution 1 - Increased Perinexal Width: Effects of $\Delta[Na^+]_o$ and $\Delta[K^+]_o$

In the following experiments, multiple solutions were perfused through the hearts. In order to reach a steady-state during each solution perfusion while limiting the entire experiment to 60 minutes, each heart was perfused with a maximum of 4 solutions in random order. Therefore, all data are normalized to a single solution that was constant in all experiments. Percent changes in CV by varying $[Na^+]_o$ and $[K^+]_o$ in Solution 1 to match those in Solution 2 are presented in Figure 2.5.

WT- In WT hearts, decreasing $[Na^+]_o$ (Solution 1A) did not vary CV_L, CV_T, or AR relative to control (Solution 1). However, increasing $[K^+]_o$ (Solution 1B) uniformly slowed CV_L and CV_T without significantly altering AR. Reducing $[Na^+]_o$ and increasing $[K^+]_o$ (Solution 1C) had an effect similar to increasing $[K^+]_o$ alone, where CV_L and CV_T were uniformly slowed compared to control, and no change in AR was observed.

HZ- Cardiac conduction in HZ hearts is summarized in Figure 2.5 (Right Panels). Notably, reducing $[Na^+]_o$ (Solution 1A) did not alter CV_L but significantly slowed CV_T relative to control Solution 1. Again, increasing $[K^+]_o$ (Solution 1B) did not significantly alter CV_L, but slowed CV_T and significantly increased AR . The combined effect of reducing $[Na^+]_o$ and increasing $[K^+]_o$ in Solution 1C reduced CV_T relative to Solution 1 without changing CV_L or AR .

Though some of the perfusate combinations slowed CV_T in both WT and HZ hearts, Solution 1A was the only solution to significantly slow CV_T in HZ hearts relative to WT as determined by unpaired comparison (#, Figure 2.5). These data demonstrate that perfusate composition can confound whether a 50% reduction of Cx43 is associated with conduction slowing.

- Solution 2 - Reduced Perinexal width: Effects of $\Delta[Na^+]_o$ and $\Delta [K^+]_o$

WT- To determine the relative effects of varying ionic composition in preparations with smaller W_P, Solution 2C was used as a control since it had similar $[Na^+]_o$ and $[K^+]_o$ to Solution 1. In WT hearts (Figure 2.6, Left Panels), decreasing $[Na^+]_o$ (Solutions 2B), increasing $[K^+]_o$ (Solution 2A) and both decreasing $[Na^+]_o$ and increasing $[K^+]_o$ (Solution 2) did not significantly change CV_L, CV_T, or AR relative to Solution 2C.

HZ- In HZ hearts (Figure 2.6, Right Panel), decreasing $[Na^+]_o$ alone (Solution 2B) or increasing $[K^+]_o$ alone (Solution 2A) did not affect CV_L, CV_T or AR relative to Solution 2C. However, the combined effect of decreasing $[Na^+]_o$ and increasing $[K^+]_o$ (Solution 2) reduced CV_T relative to Solution 2C without significantly altering CV_L or AR. In summary, altering $[Na^+]_o$ and/or $[K^+]_o$ does not significantly affect CV in WT hearts with narrow perinexi, but both decreasing $[Na^+]_o$ and increasing $[K^+]_o$ in HZ hearts with narrow perinexi can significantly slow CV.

DISCUSSION

The purpose of this study was to determine how varying extracellular sodium, potassium and W_P modulates the CV-GJ relationship in the Gja1 heterozygous null mouse. It has been previously demonstrated that all three factors can individually modulate CV.[15,16,21,22] Interestingly, we demonstrate that modest variations of these parameters, which individually might not produce a response, can in combination significantly affect conduction. Furthermore, the ionic concentrations in perfusates used in this study mostly lie within reported physiological values for mice. Specifically, mouse serum sodium level ranges from 140-160 mM and

potassium ranges from 5-7.5 mM.[23] Together, these results suggest that combinatorial and physiologic variations in ionic concentration and W_P can significantly modify the CV-GJ relationship.

Conduction and the Morley and Eloff et al. Solutions:

The results of the present study reproduce the CV-GJ relationship reported by Morley et al, where Solution 1 did not produce conduction slowing in Cx43 HZ hearts.[5] However, our results are only partially consistent with those of Eloff and co-workers. In brief, Eloff et al. reported significant CV_L and CV_T slowing in HZ animals relative to WT.[6] In our experiments, Solution 2 did not produce significant CV slowing in HZ hearts relative to WT. However, when comparing Solution 2 in WT and HZ hearts, we demonstrate that Solution 2 slowed CV_T more in HZ than in WT hearts. These data provide evidence that CV_T sensitivity to Cx43 level is greater with the Eloff et al. perfusate. Experimental differences such as multiple and serial perfusions in this study may underlie the lack of 1:1 agreement with the Eloff et al. study. Yet, the Eloff et al. perfusate was not the only solution to reveal decreased CV in the Cx43 HZ mouse. Specifically, the modified Morley Solution 1A, slowed CV_T significantly in HZ animals relative to WT animals, again demonstrating that differences between WT and HZ animals can be elicited by varying perfusate composition. Therefore, we provide further evidence that conduction slowing secondary to a 50% loss of Cx43 *can* be unmasked by perfusate composition.

Effect of perinexal width:

We have previously demonstrated that bulk V_{IS} confounds the CV-GJ relationship.[15,16] More recently, it was demonstrated that intercellular separation within the intercalated disc at the perinexus correlates well with CV changes.[16] With the support of computational modeling, we proposed that ephaptic coupling - the generation of electric fields in restricted spaces between myocytes - may mechanistically modulate the CV-GJ relationship. In the present study, it is demonstrated that Solutions 1 and 1C produced wider perinexi than Solutions 2 and 2C. When we controlled for similar $[Na^+]_o$ and $[K^+]_o$, WT and HZ preparations with wider perinexi exhibited greater transverse conduction slowing than preparations with narrower perinexi - consistent with our previous results.

One important ionic difference between the solutions that could underlie a change in perinexal spacing is $[Ca^{2+}]_o$. The intercalated disc is composed of many junctional proteins which require extracellular calcium to form and maintain cell-to-cell adhesion.[24,25] Solution 2, with the highest

$[Ca^{2+}]_o$ produced the narrowest W_P consistent with the hypothesis that W_P can be modulated by $[Ca^{2+}]_o$.

Effect of Extracellular Sodium ion concentration:

Hyponatremia has been associated with slowed conduction in the heart,[22] presumably by reducing cellular excitability.[26] Reducing cellular excitability could affect the rate of extracellular potential change in the perinexus and thereby weaken ephaptic coupling between myocytes. Despite the relatively small change in $[Na^+]_o$ (~5%) in this study, the finding that altered $[Na^+]_o$ can modulate CV in HZ hearts is consistent with a previous report.[22] Yet, the extent of CV modulation appears also to depend on $[K^+]_o$ and W_P. More specifically, CV modulation by varying $[Na^+]_o$ was evident in *hypo*kalemic-Cx43 HZ preparations with wide perinexi, and *hyper*kalemic-Cx43 HZ preparations with narrow perinexi. Under both conditions, GJ coupling is likely reduced in HZ hearts, presumably increasing conduction dependence on ephaptic coupling. However, ephaptic cell-to-cell transmission of action potential is probably reduced in the first instance by wider perinexi and in the second instance by reduced excitability.

Effect of Extracellular Potassium ion concentration:

The relationship between $[K^+]_o$ and CV is biphasic. Small increases in $[K^+]_o$ raise the resting membrane potential closer to the threshold of voltage gated sodium channel activation and could result in supernormal conduction.[21] Further increasing $[K^+]_o$ can slow conduction by inactivating voltage gated sodium channels and thereby reducing excitability.[27,28] Relative to Solution 1, Solution 2 had 34% more $[K^+]_o$, which would alter the potassium reversal potential by approximately 10.9 mV. In preparations with wide perinexi, this degree of increased $[K^+]_o$ slowed CV in both WT and HZ mice hearts perfused with Solution 1 combinations (Solution 1B and 1C), presumably due to reduced excitability. On the other hand, in hearts with narrower perinexi and a stronger ephaptic contribution to conduction, CV is less sensitive to $[K^+]_o$. These findings are consistent with previous data from our group demonstrating that CV is more sensitive to sodium channel availability during loss of gap junctional coupling and/or increased W_P. Based on computational models, the proposed mechanism for differential CV sensitivity to sodium channel availability is related to the rate and amplitude of extracellular potential change in the intercalated disc.[16,29] In short, GJ uncoupling may increase CV dependence on an ephaptic mechanism. It is important to note that while the Morley et al. solution produced the widest W_P, the higher $[Na^+]_o$ and lower $[K^+]_o$ masked the effects of increased W_P. Likewise, while the Eloff et

al. solution produced the narrowest W_P, the lower $[Na^+]_o$ and higher $[K^+]_o$ may have relatively reduced ephaptic coupling despite the narrow perinexal space.

A final important finding in this study is that the CV - $[K^+]_o$ relationship may be modulated by W_P. Specifically, hearts with smaller perinexi were the most resistant to changes in $[K^+]_o$ possibly due to compensation by stronger ephaptic coupling.

Perfusates and the CV-Cx43 Mouse:

The present study only analyzed the CV modulation by two ions, associated with cellular excitability, in detail from two different studies. However, other independent groups have analyzed the CV-Cx43 relationship with a variety of perfusates. When comparing the Tyrode solutions of only adult mouse studies with an approximate 50% Cx43 reduction, we find close agreement with our results. For example, the study by Van Rijen et al. also reported no change in CV in an inducible Cx43 knock-out mouse model.[10] Importantly, the Van Rijen et al. study utilized a solution with relatively low $[K^+]_o$ (4.5mM), low $[Na^+]_o$ (109.2 mM), and high $[Ca^{2+}]_o$. In short, our Solution 1 is closest to their perfusate composition, and this perfusate did not produce significant conduction slowing in WT or HZ hearts. In contrast to our results, a study by Guerrero et al.[7] reported that a solution identical to the Eloff et al. solution, and similar to Solution 2 used in this manuscript, slowed conduction by nearly 50 % in transgenic Cx43 HZ hearts.

LIMITATIONS:

The use of buffers for superfusion and perfusion is a foundational tool for studying biological processes *ex vivo*. Further, *in vivo* studies report a range of physiologic normal serum ionic composition. It is important to note that not all sodium, potassium, and particularly calcium quantifications are related to ionized concentrations in experimental buffers, plasma, or blood. Therefore, it may be difficult at this point to suggest that a superior perfusate exists which will maximally enhance the CV-GJ relationship.

With respect to calcium, previous studies have demonstrated that elevated intracellular calcium can slow CV by uncoupling gap junctions.[30,31] However, in this study, when we controlled for sodium and potassium (Solution 2 versus 1C), we found that higher extracellular calcium was associated with faster CV, arguing against calcium-induced inhibition of Cx43. This further

illustrates that the relationship between ionic concentrations, W_P, CV and Cx43 is complex and requires further study.

Perinexal width measurements were made in glutaraldehyde-fixed tissue. Although most fixation protocols have been associated with alterations in the tissue structure we previously demonstrated that glutaradehyde fixation is a relatively robust approach to measure extracellular volumes.[15] Furthermore, this and our previous study[16] demonstrate that significant trends in W_P due to solution composition are measurable after glutaraldehyde fixation. This being said, developing new approaches to dynamically measure microdomain structural changes is important given the emerging importance of ephaptic conduction.

Increasing perfusate osmolarity has been associated with larger V_{IS}, cell size reduction and slow CV.[15] In this study we measured V_{IS} and W_P, and determined that all changes in extracellular volumes did not correlate with osmolarity. Additionally, in contrast with our previous study, we report here that the relatively higher osmolarity perfusates are associated with increased CV (increasing $[Na^+]_o$). However, we did not quantify changes in cell size. It is important to note that the relationship between CV and cell size is controversial as well, with computational models predicting that either increasing or reducing cell size can slow CV.[15,32-35]. While the primary results here fit well with the theory that alterations in the CV-GJ relationship are modulated by W_P and perfusate composition, we cannot exclude the possible role of perfusates altering cell size and the CV-GJ relationship.

CONCLUSIONS:

The literature indicates that GJ uncoupling is a common factor associated with several cardiac diseases.[2-4] However, there is debate over the nature of the relationship with some studies suggesting a relatively close correlation, whereas others indicate a more non-linear relationship with a threshold in GJ coupling below which conduction slows or fails. The present study provides data that may go some way to resolving the controversy, indicating that perfusate composition *can* exacerbate GJ uncoupling leading to slowed conduction and increased arrhythmia susceptibility.

Further, dehiscence of the intercalated disc has also been observed under pro-arrhythmic cardiac conditions such as hypocalcemia[36,37] and sepsis.[4] Like GJ uncoupling, modest separation at the perinexus does not always correlate with conduction slowing, but there is now

mounting evidence that W_P can modulate the CV-GJ relationship under specific conditions by altering ephaptic coupling (EpC). Our new results suggest that physiologic ionic differences also modulate the CV-GJ-EpC relationship. In conclusion, future studies and therapies designed to address conduction slowing secondary to loss of functional gap junctions may consider extracellular ionic composition as a confounding modulator of arrhythmogenic conduction slowing.

REFERENCES:

1. Kleber AG, Rudy Y. Basic mechanisms of cardiac impulse propagation and associated arrhythmias. *Physiological Reviews.* 2004;84:431-488.

2. Poelzing S, Rosenbaum DS. Altered connexin43 expression produces arrhythmia substrate in heart failure. *American Journal of Physiology. Heart and Circulatory Physiology.* 2004;287:H1762-1770.

3. Cascio WE, Yang H, Muller-Borer BJ, et al. Ischemia-induced arrhythmia: the role of connexins, gap junctions, and attendant changes in impulse propagation. *Journal of Electrocardiology.* 2005;38:55-59.

4. Celes MR, Torres-Duenas D, Alves-Filho JC, et al. Reduction of gap and adherens junction proteins and intercalated disc structural remodeling in the hearts of mice submitted to severe cecal ligation and puncture sepsis. *Critical Care Medicine.* 2007;35:2176-2185.

5. Morley GE, Vaidya D, Samie FH, et al. Characterization of conduction in the ventricles of normal and heterozygous Cx43 knockout mice using optical mapping. *Journal of Cardiovascular Electrophysiology.* 1999;10:1361-1375.

6. Eloff BC, Lerner DL, Yamada KA, et al. High resolution optical mapping reveals conduction slowing in connexin43 deficient mice. *Cardiovascular Research.* 2001;51:681-690.

7. Guerrero PA, Schuessler RB, Davis LM, et al. Slow ventricular conduction in mice heterozygous for a connexin43 null mutation. *The Journal of Clinical Investigation.* 15 1997;99:1991-1998.

8. Thomas SA, Schuessler RB, Berul CI, et al. Disparate effects of deficient expression of connexin43 on atrial and ventricular conduction: evidence for chamber-specific molecular determinants of conduction. *Circulation.* 1998;97:686-691.

9. Vaidya D, Tamaddon HS, Lo CW, et al. Null mutation of connexin43 causes slow propagation of ventricular activation in the late stages of mouse embryonic development. *Circulation Research.* 2001;88:1196-1202.

10. van Rijen HV, Eckardt D, Degen J, et al. Slow conduction and enhanced anisotropy increase the propensity for ventricular tachyarrhythmias in adult mice with induced deletion of connexin43. *Circulation.* 2004;109:1048-1055.

11. Danik SB, Liu F, Zhang J, et al. Modulation of cardiac gap junction expression and arrhythmic susceptibility. *Circulation Research.* 2004;95:1035-1041.

12. Dhillon PS, Gray R, Kojodjojo P, et al. Relationship between gap-junctional conductance and conduction velocity in mammalian myocardium. *Circulation. Arrhythmia and Electrophysiology.* 2013;6:1208-1214.

13. Thomas SP, Kucera JP, Bircher-Lehmann L, et al. Impulse propagation in synthetic strands of neonatal cardiac myocytes with genetically reduced levels of connexin43. *Circulation Research.* 2003;92:1209-1216.

14. Beauchamp P, Choby C, Desplantez T, et al. Electrical propagation in synthetic ventricular myocyte strands from germline connexin43 knockout mice. *Circulation Research.* 2004;95:170-178.

15. Veeraraghavan R, Salama ME, Poelzing S. Interstitial volume modulates the conduction velocity-gap junction relationship. *American Journal of Physiology. Heart and Circulatory Physiology.* 2012;302:H278-286.

16. Veeraraghavan R, Lin J, Hoeker G, et al. Sodium channels in the Cx43 gap junction perinexus may constitute a cardiac ephapse: an experimental and modeling study. *Pflugers Archiv: European Journal of Physiology.* 2015; 467:2093-2105.

17. Bayly PV, KenKnight BH, Rogers JM, et al. Estimation of conduction velocity vector fields from epicardial mapping data. *Institute of Electrical and Electronic Engineers - Transactions on Bio-medical Engineering.* 1998;45:563-571.

18. Rhett JM, Ongstad EL, Jourdan J, et al. Cx43 associates with Na(v)1.5 in the cardiomyocyte perinexus. *The Journal of Membrane Biology.* 2012;245:411-422.

19. Sato PY, Musa H, Coombs W, et al. Loss of plakophilin-2 expression leads to decreased sodium current and slower conduction velocity in cultured cardiac myocytes. *Circulation Research.* 2009;105:523-526.

20. Agullo-Pascual E, Lin X, Leo-Macias A, et al. Super-resolution imaging reveals that loss of the C-terminus of connexin43 limits microtubule plus-end capture and NaV1.5 localization at the intercalated disc. *Cardiovascular Research.* 2014;104:371-381.

21. Nygren A, Giles WR. Mathematical simulation of slowing of cardiac conduction velocity by elevated extracellular. *Annals of Biomedical Engineering.* 2000;28:951-957.

22. Yanagi N, Maruyama T, Uehata S, et al. Electrical and mechanical abnormalities in the heart of a schizophrenic patient with hyponatremia derived from water intoxication. *Journal of Cardiology.* 1998;32:197-204.

23. Research Animals Resources UoM. Reference Values for Laboratory Animals. Normal Hematology Values. 2009; www.ahc.umn.edu/rar/refvalues.html, 2013.

24. Watt FM, Mattey DL, Garrod DR. Calcium-induced reorganization of desmosomal components in cultured human keratinocytes. *The Journal of Cell Biology.* 1984;99:2211-2215.

25. Chitaev NA, Troyanovsky SM. Adhesive but not lateral E-cadherin complexes require calcium and catenins for their formation. *The Journal of Cell Biology.* 1998;142:837-846.

26. Ballantyne F III, Davis LD, Reynolds EW Jr. Cellular basis for reversal of hyperkalemic electrocardiographic changes by sodium. *The American Journal of Physiology.* 1975;229:935-940.

27. Weidmann S. The effect of the cardiac membrane potential on the rapid availability of the sodium-carrying system. *The Journal of Physiology.* 1955;127:213-224.

28. Gettes LS, Reuter H. Slow recovery from inactivation of inward currents in mammalian myocardial fibres. *The Journal of Physiology.* 1974;240:703-724.

29. Lin J, Keener JP. Microdomain effects on transverse cardiac propagation. *Biophysical Journal.* 2014;106:925-931.

30. Lurtz MM, Louis CF. Intracellular calcium regulation of connexin43. *American Journal of Physiology. Cell Physiology.* 2007;293:C1806-1813.

31. Kagiyama Y, Hill JL, Gettes LS. Interaction of acidosis and increased extracellular potassium on action potential characteristics and conduction in guinea pig ventricular muscle. *Circulation Research.* 1982;51:614-623.

32. Spach MS, Heidlage JF, Dolber PC, et al. Electrophysiological effects of remodeling cardiac gap junctions and cell size: experimental and model studies of normal cardiac growth. *Circulation Research.* 2000;86:302-311.

33. Veeraraghavan R, Salama ME, Poelzing S. Interstitial volume modulates the conduction velocity-gap junction relationship. *American Journal of Physiology - Heart and Circulatory Physiology.* 2012;302:H278-H286.

34. Seidel T, Salameh A, Dhein S. A simulation study of cellular hypertrophy and connexin lateralization in cardiac tissue. *Biophysical Journal.* 2010;99:2821-2830.

35. Toure A, Cabo C. Effect of cell geometry on conduction velocity in a subcellular model of myocardium. *Institute of Electrical and Electronic Engineers - Transactions on Bio-medical Engineering.* 2010;57:2107-2114.

36. Greve G, Rotevatn S, Saetersdal T, et al. Ultrastructural studies of intercalated disc separations in the rat heart during the calcium paradox. *Research in Experimental Medicine. Zeitschrift ur die gesamte experimentelle Medizin einschliesslich experimenteller Chirurgie.* 1985;185:195-206.

37. Ganote CE, Grinwald PM, Nayler WG. 2,4-Dinitrophenol (DNP)-induced injury in calcium-free hearts. *Journal of Molecular and Cellular Cardiology.* 1984;16:547-557.

Table 2.1 Perfusate Composition

Solution 1 is the published Morley et al. solution [5] and Solution 2 is the published Eloff et al. solution [6]. Osmolarity values are reported as Mean ± SD.

Tyrode Composition (in mM)								
	1	**1A**	**1B**	**1C**	**2**	**2A**	**2B**	**2C**
NaCl	130	130	130	130	118.3	126.2	118.3	126.2
NaHCO3	24	17.3	24	17.3	29	29	29	29
NaH2PO4	1.2		1.2					
Total [Na^+]	**155.2**	**147.3**	**155.2**	**147.3**	**147.3**	**155.2**	**147.3**	**155.2**
KCl	4	4	4	4	4.7	4.7	3	3
KH2PO4			2.1	2.1	1.4	1.4	1	1
Total [K^+]	**4**	**4**	**6.1**	**6.1**	**6.1**	**6.1**	**4**	**4**
MgCl2	1	1	1	1				
MgSO4					1	1	1	1
Glucose	5.6	5.6	5.6	5.6	10	10	10	10
CaCl2	1.8	1.8	1.8	1.8	3.4	3.4	3.4	3.4
BDM	15	15	15	15	10	10	10	10
Osmolarity (mOsm)	318.8 ± 0.9	304.8 ± 1.1	318.4 ± 1.3	307.8 ± 0.7	310.4 ± 1.3	328 ± 0.8	308.2 ± 0.7	323.6 ± 0.8

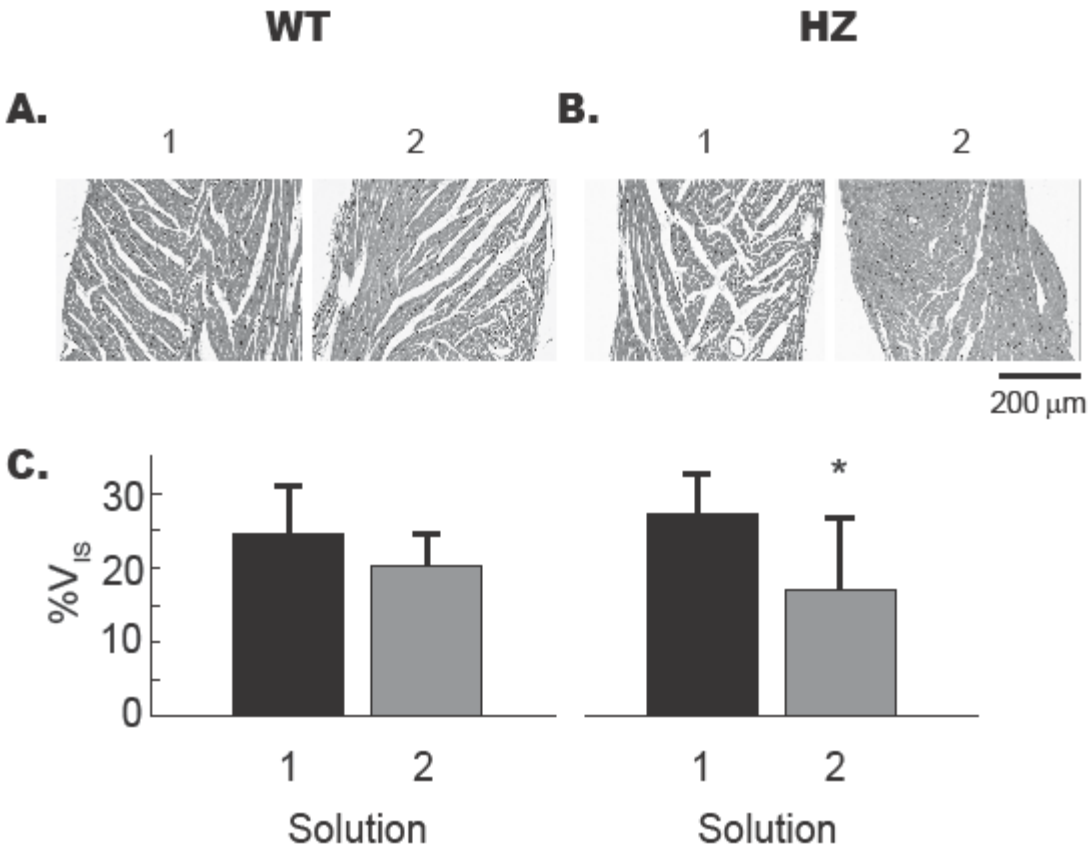

Fig. 2.1 Modulation of Interstitial Volume by Perfusates

Images of H&E stained tissue from WT (a) and HZ (b) hearts perfused with Solutions 1 and 2 show V_{IS} as white space, myocytes in gray and nuclei as black spots. Percent V_{IS} (c) is similar in WT hearts. In HZ hearts, a larger V_{IS} was observed during perfusion of Solution 1 relative to 2. **Statistics:** *Unpaired, two-tailed, equal variance and sample size Student's t-test with Bonferonni correction (2 comparisons/dataset). *, p<0.05*.

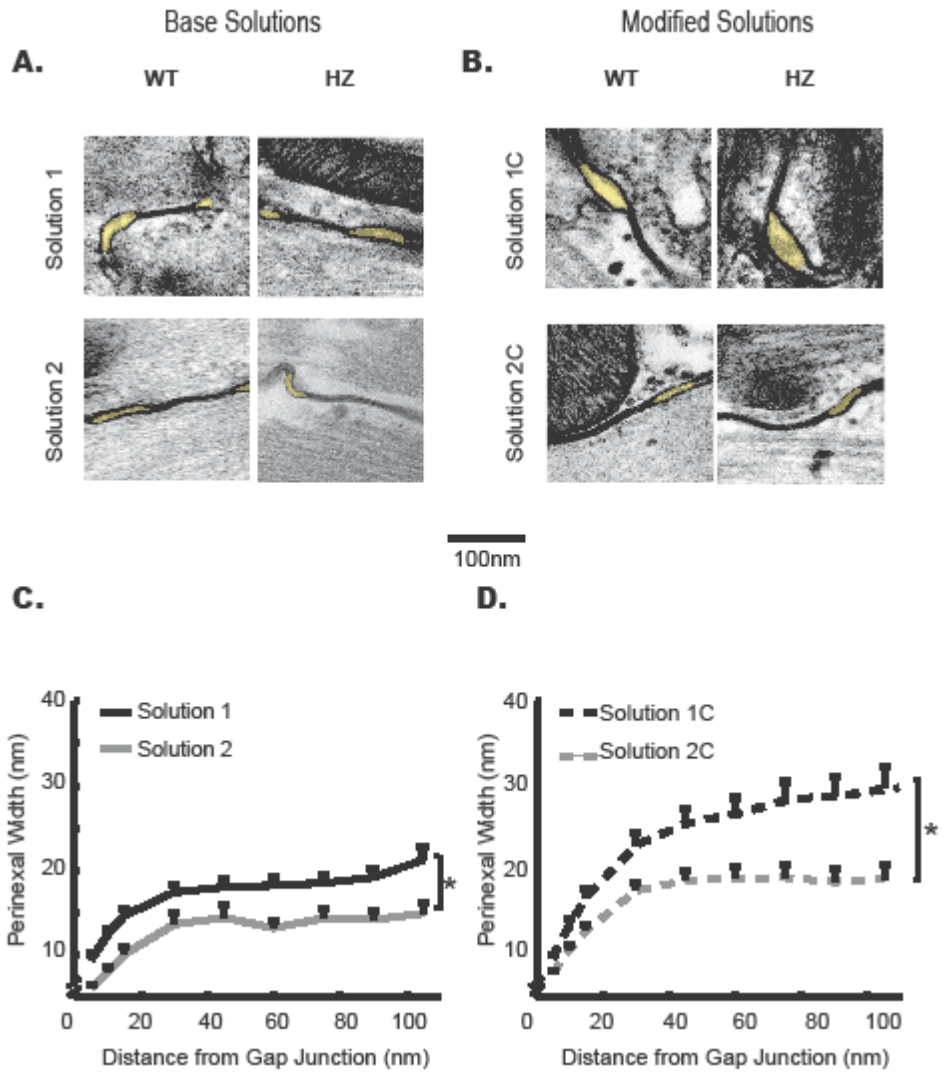

Fig. 2.2 Modulation of the Perinexus by Perfusates

The perinexus (highlighted in yellow) is modulated by the base solutions (1 and 2) and the modified solutions (1C and 2C). Solution 1 increases W_P in both WT and HZ hearts compared to Solution 2 (a) and Solution 1C has wider W_P compared to Solution 2C (b). Combined W_P for WT and HZ are summarized as a function of distance from edge of the GJ plaque (c). **Statistics:** *Single Factor ANOVA Post hoc test - Unpaired, two-tailed, equal variance and sample size Student's t-test*. *, $p<0.05$.

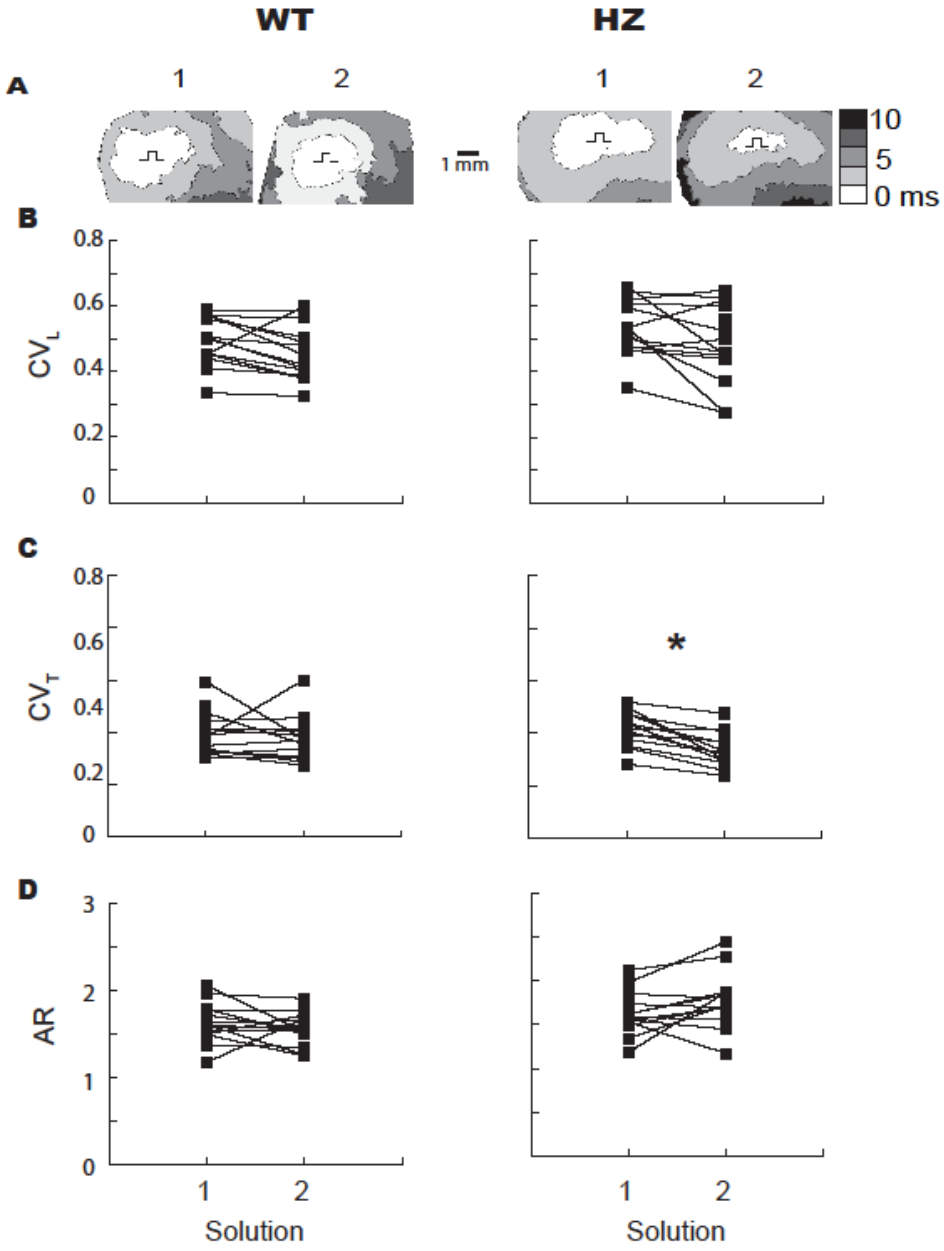

Fig. 2.3 Modulation of Conduction by Perfusates

Representative activation maps from WT and HZ mice hearts (a). Crowding of isochrones lines along with summary CV_L (b), CV_T (c) and Anisotropic Ratio (d) demonstrate that Solution 2 slows conduction in HZ hearts. ⊓ indicates pacing site. **Statistics:** *Paired, one-tailed, equal variance and sample size Student's t-tests with Bonferonni correction. *, p<0.05.*

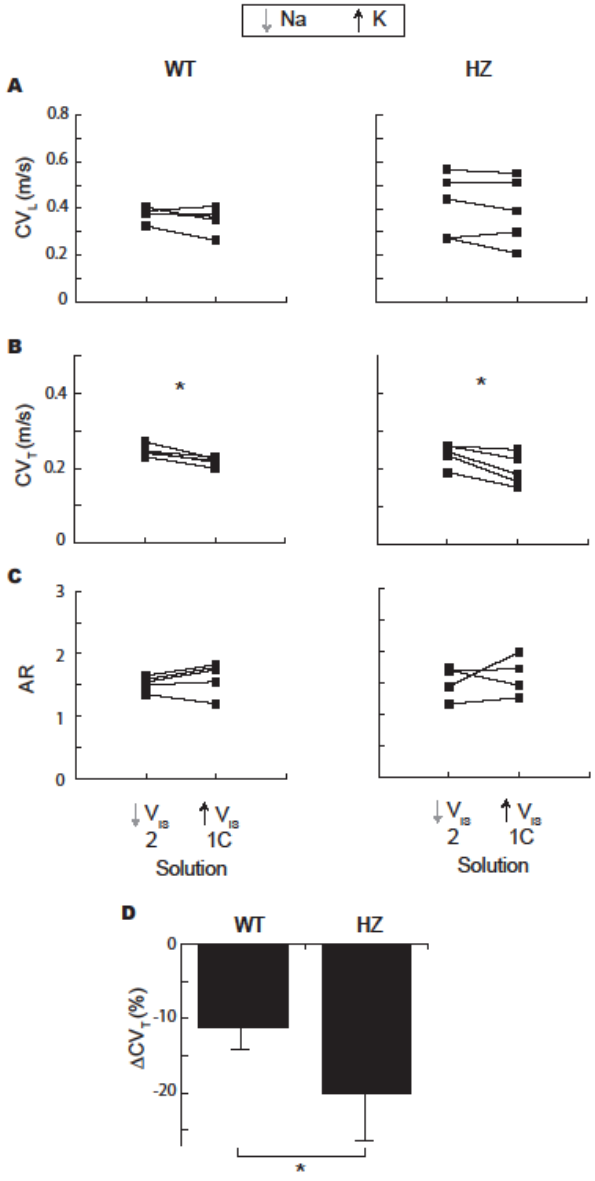

Fig. 2.4 Conduction Velocity – Perinexal width Relationship

Solution 2 and 1C have similar $[Na^+]_o$ and $[K^+]_o$ but produced different W_P (Solution 2 – Small W_P, Solution 1C – Large W_P) and different CV_T in the same heart. There was no change in CVL during either solution perfusion (a) but Solution 2 was associated with faster CV_T (b). No change in AR (c) was observed. CV_T slowing is greater in HZ hearts relative to WT during Solution 1C perfusion (d). **Statistics:** *Paired, one-tailed, equal variance and sample size Student's t-tests. *, p<0.05*.

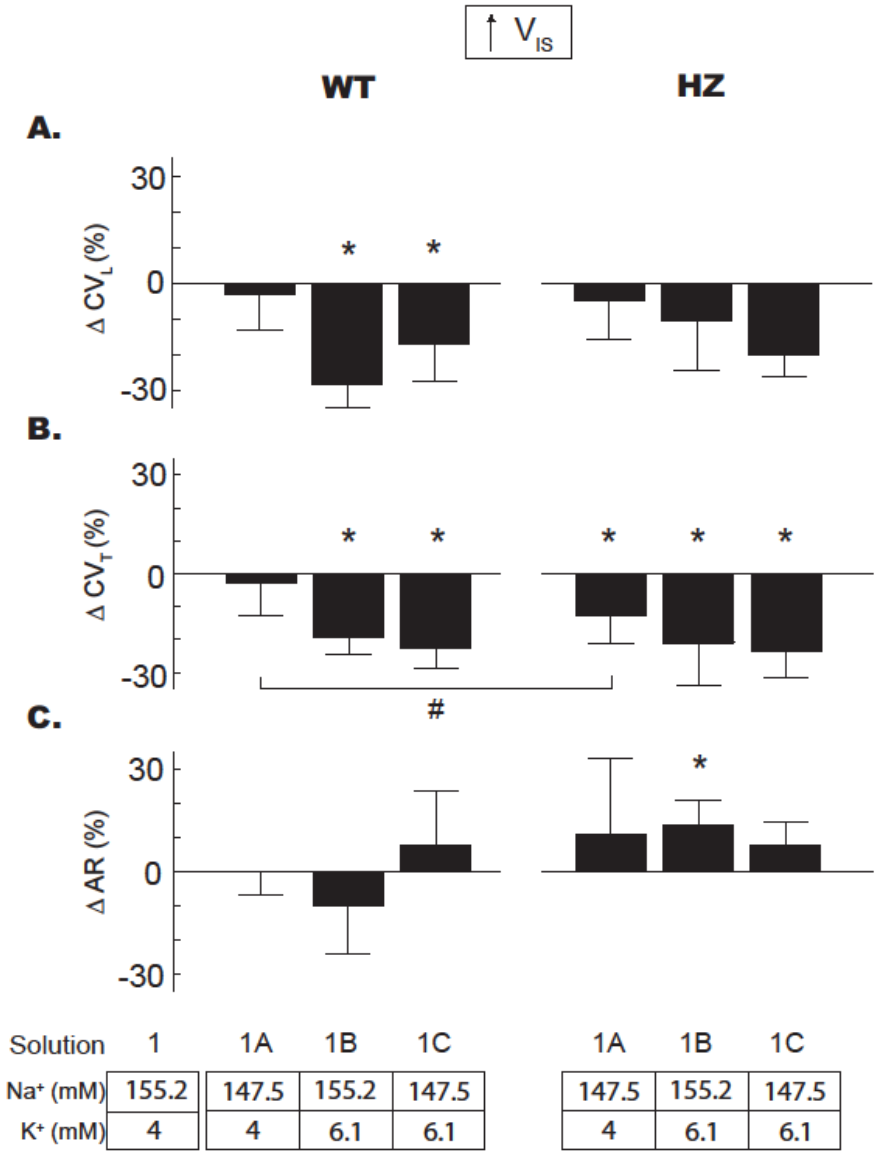

Solution	1	1A	1B	1C	1A	1B	1C
Na^+ (mM)	155.2	147.5	155.2	147.5	147.5	155.2	147.5
K^+ (mM)	4	4	6.1	6.1	4	6.1	6.1

Fig. 2.5 Modulation of Conduction Velocity by altering Ionic Composition of Solution 1

Relative change in longitudinal conduction velocity (a), Transverse conduction velocity (b) and anisotropic ratio with wide W_P (c). Varying sodium modulated CV_T only in HZ hearts, whereas varying potassium altered CV in WT and HZ hearts. **Statistics:** * *denotes p<0.05 detected by paired, two-tailed, equal variance and sample Student's t-tests with Bonferonni correction performed on percent changes relative to zero. # denotes p<0.05 between WT and HZ hearts determined by unpaired, two-tailed, equal variance and sample size Student's t-tests.*

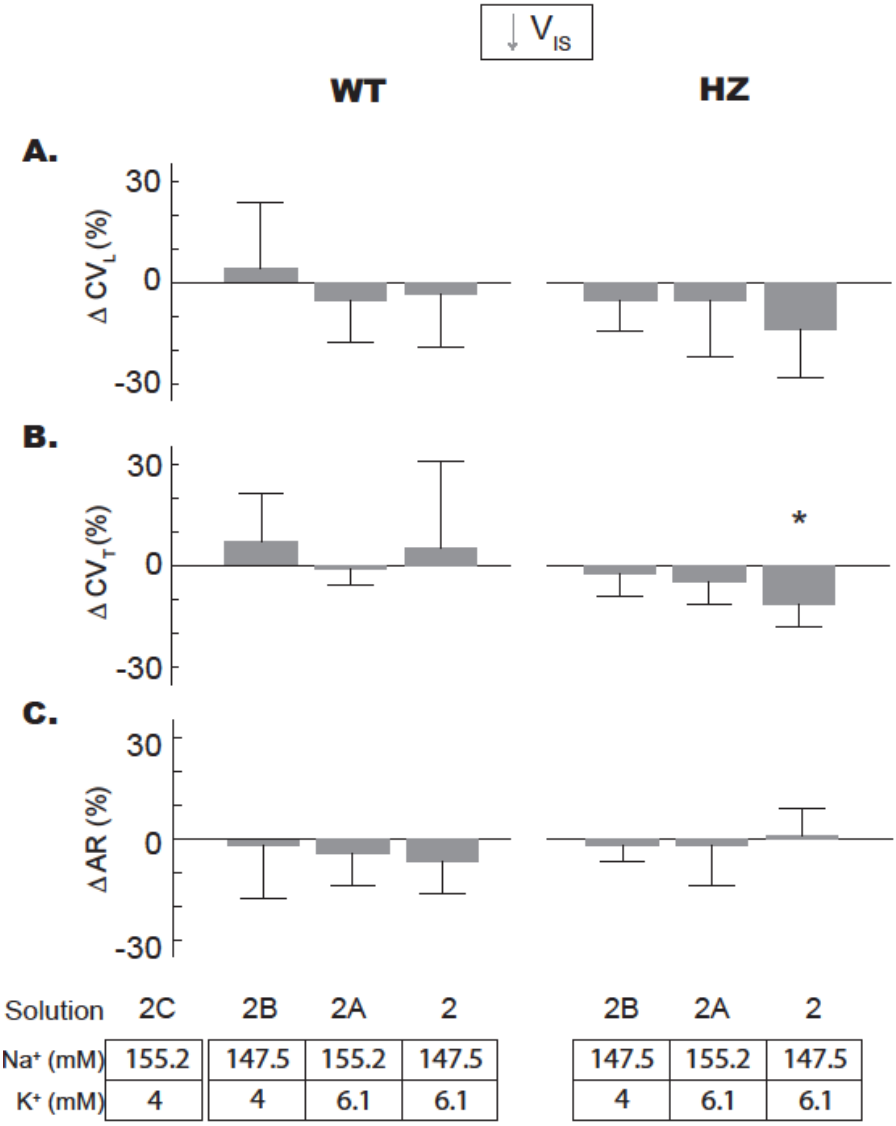

Solution	2C	2B	2A	2	2B	2A	2
Na^+ (mM)	155.2	147.5	155.2	147.5	147.5	155.2	147.5
K^+ (mM)	4	4	6.1	6.1	4	6.1	6.1

Fig. 2.6 Modulation of Conduction Velocity by altering Ionic Composition of Solution 2

Relative change in longitudinal conduction velocity (a), Transverse conduction velocity (b) and anisotropic ratio (c) with narrow W_P. Significant changes were observed only when both sodium was reduced and potassium was increased. **Statistics:** * *denotes p<0.05 detected by paired, two-tailed, equal variance and sample size Student's t-tests with Bonferonni correction performed on percent changes relative to zero.*

CHAPTER – 3

PERFUSATE CALCIUM ION CONCENTRATION AS A MODULATOR OF CONDUCTION VELOCITY DURING NORMAL AND DISEASE STATES

INTRODUCTION:

The synchronized spread of electrical activity is important for coordinating efficient cardiac contraction, and slowed conduction is a well-established substrate for lethal cardiac arrhythmias. Gap junctional coupling, tissue excitability, intercalated disc micro-architecture, and extracellular ion concentrations have been identified as important determinants of cardiac conduction.[1-5] Many studies have now demonstrated that simultaneously altering more than one determinant of cardiac conduction can synergistically modulate conduction velocity (CV) significantly more than even pathologic alterations of a single parameter.[6-9]

More interestingly, we recently determined that altering perfusate composition within concentration ranges consistent with murine plasma ionic concentrations, produces complex effects on CV that are interdependent on sodium, potassium, and functional expression of the principal ventricular gap junction protein connexin43 (Cx43).[5,6] In previous manuscripts, we suggested that the effects are consistent with the theory of ephaptic coupling (EpC) as well as gap junctional coupling. EpC, which can facilitate electrical coupling between myocytes through electric fields that develop in restricted extracellular spaces like the perinexus,[6,9] is dependent on the volume of intercalated disc microdomains as well as rate of charge depletion from these regions.[6,10] Specifically, we previously demonstrated that wider perinexi – increased intercellular separation – with low $[Na^+]_o$ and high $[K^+]_o$, both of which can reduce rate of charge depletion from the perinexus, was associated with slower impulse propagation through myocardium.[6]

The perinexus has been suggested to be a candidate structure of a cardiac ephapse and an important modulator of CV.[6,9] Specifically, previous studies demonstrated that changing tissue hydration in guinea pig with mannitol or albumin can alter bulk interstitial edema,[8] and in the case of mannitol also increase perinexal width (W_P) [9] to modulate cardiac conduction in a manner most consistent with the theoretical predictions of EpC. More recently, we found that perfusate ion composition can also modulate W_P and CV in mouse,[6] and we speculated that increasing extracellular calcium might decrease W_P, since intercellular adhesion is calcium sensitive. Therefore, in this study we hypothesize that extracellular calcium modulates W_P.

Mathematical models of EpC also predict a phenomenon termed self-attenuation, which is similarly dependent on intercellular separation within the intercalated disc and extracellular ion composition.[10-12] More specifically, the mechanism of self-attenuation has been described as the process by which sodium current (I_{Na}) attenuates itself by reducing driving force when the

cleft between myocytes is sufficiently narrow.[11] This delays myocyte activation and manifests as macroscopic conduction slowing. The driving force for I_{Na} is the difference between the transmembrane potential (V_m) and the Nernst potential for sodium (E_{Na}). Either increasing V_m or decreasing E_{Na} can reduce the driving force and thereby the sodium current. Therefore, two important components that are required to support self-attenuation are 1) reduced sodium driving force and 2) reduced width of intercalated disc spaces like the perinexus. Based on these predictions, we also hypothesize that decreasing W_P and reducing sodium driving force slows cardiac conduction by a mechanism consistent with ephaptic self-attenuation.

The results of this study demonstrate that increasing $[Ca^{2+}]_o$ decreases W_P. Furthermore, decreasing W_P during *normo*natremia increased CV consistent with our previous studies,[6,9] and decreasing W_P during *hypo*natremia decreased CV, consistent with computational predictions of ephaptic self-attenuation.

METHODS:

All protocols were approved by the Institutional Animal Care and Use Committee at Virginia Polytechnic Institute and State University and conform to the guidelines of the NIH Guide for the Care and Usage of Laboratory Animals.

Langendorff Preparations: Mice were anesthetized by inhalation of isoflurane vapors from an isoflurane soaked cotton gauze in a custom designed closed chamber. Cervical dislocation was performed upon cessation of respiration and was immediately followed by thoracotomy and excision of the heart. Wild type (WT, 100% Cx43) and heterozygous (HZ, ~ 50% Cx43) mice, 10-30 weeks old, on the C57BL/6 background were cannulated and Langendorff perfused as previously described[6] with solutions containing (in mM) NaCl 118.3, $NaHCO_3$ 29, KCl 4.7, KH_2PO_4 1.4, $MgSO_4$ 1, Glucose 10 at pH 7.4. $CaCl_2$ concentration was varied from 1 to 3.4 mM. The perfusate and the bath solution was the same at any given time.The perfusion pressure was maintained at ~70 mmHg and the heart was suspended in a bath maintained at ~37°C along with the perfusates. The process was repeated during hyponatremia (NaCl 91mM). The osmolarities of the various perfusates were measured using a Wescor VAPRO5520 Vapor Pressure Osmometer and are reported in Table 1.

Optical Mapping: Hearts (8 solutions X 2 mouse types X 5/7 replicates, N=96) were perfused with the voltage sensitive dye, Di-4-ANEPPS at a concentration of 4μM and excess dye was

washed out. Each heart was serially perfused with four solutions of either increasing or decreasing calcium concentration. Hearts were perfused with each solution for approximately 8 mins before being optically mapped. Motion was reduced by 2,3-butanedionemonoxime (10 mM) and the heart was stabilized against the front glass of the bath by applying slight pressure to the posterior surface. Hearts were paced using a unipolar silver wire placed on the anterior surface and a reference wire at the back of the bath. Stimuli of 1V amplitude and 1ms duration at a BCL of 150ms were applied. Conduction velocity – longitudinal (CV_L) and transverse (CV_T) and anisotropic ratio (AR) – and action potential duration (APD) were quantified as previously described.[6] Briefly, the heart was excited by 510nm light and the excited light passed through a 610nm filter and then was recorded using the MiCam Ultima CMOS L-camera at a sampling rate of 1000 frames/s. The maximum rate of rise of the optical action potentials were assigned as activation times and conduction velocity vectors were determined by fitting the activation times at every pixel to a parabolic surface. Vectors upto 5 pixels away from a user defined line indicating the direction of propagation, that fell within ~3 or 5 mm (CV_T and CV_L, respectively) from the pacing site, not including the first 2 rows, and whose direction was not more than 7.5° from the direction of propagation were included in the analysis. This region is roughly illustrated by the orange and green boxes in the isochrones maps. APD was calculated as the time interval between activation and 90% repolarization.

Transmission Electron Microscopy: Hearts (7 solutions X 2 mouse types X 3 replicates X 15 images, N=630) were perfused with the respective solution for 30 minutes and $1mm^3$ cubes were then fixed overnight in 2.5% glutaraldehyde at 4°C. Samples were washed in PBS and processed for TEM as previously described.[6] The samples were then sectioned onto copper grids and the sections were imaged at 150,000X magnification using a JEOL JEM 1400 transmission electron microscope. Perinexal images were then analyzed in a blinded manner by ImageJ to determine W_P. It has to be noted here that the W_P measurements in this study refer to the intermembrane separation adjacent to the GJ plaque as we previously reported in mice[6] and guinea pigs[9] and not the spatial extent (distance from the gap junction edge) of the perinexus as reported by Rhett et al.[13] Additionally, based on our previous studies, W_P changes in the plateau portion of this nanodomain (30 – 105nm away from the edge of the gap junction) best correlated with conduction velocity, and therefore values reported here are averages of 6 measurements at 15nm intervals from within this region.

Western Immunoblotting: Hearts (4 solutions X 2 mouse types X triplicates run twice, N=48), perfused with the respective solutions for 30 minutes, were snap frozen. Tissue was homogenized in a lysis buffer containing (in mM) HEPES 50, KCl 150, EDTA 1, EGTA 1, DTT 1, NaF 1, Na_3VO_4 0.1 and 0.5% Triton X-100. Protein concentration was normalized following quantification with the BioRad DC protein assay. SDS-PAGE electrophoresis was performed as previously described[14] using 4-20% NuPage Bis-Tris gels which were then transferred to a PVDF membrane and blocked with 5% BSA in TNT buffer (0.1% Tween 20, 150 mM NaCl, 50 mM Tris pH 8.0) at room temperature for one hour. Membranes were then incubated with rabbit anti-phospho-Cx43^{Ser368} (1:1000 in 5% BSA TNT, #3511 Cell Signaling Technology) primary antibody overnight at 4°C. Membranes were washed and incubated with goat anti-rabbit HRP secondary antibody (1:5000, abcam) for 1 h at room temperature, washed, and bound antibody detected using Clarity Western ECL Substrate (BioRad) and imaged using the BioRad Chemidoc MP system. To detect total Cx43, membranes were first stripped with Re-Blot Plus Strong (Millipore) according to manufacturer's instructions. Following blocking for 1 h at room temperature in 5% milk in TNT buffer, membranes were incubated with primary antibodies against Cx43 (1:4000, C6219 rabbit, Sigma Aldrich), and mouse antiGAPDH (1:4000 RDI-TRK5G4-6C5, mouse, Research Diagnostics Inc.) overnight at 4°C diluted in 5% milk TNT. Membranes were then washed and incubated with the secondary antibodies goat anti-mouse AlexaFluor555 and goat anti-rabbit AlexaFluor647 (both 1:1000 in milk TNT, Life Technologies) for 1 hour at RT. Following several washes in TNT, membranes were imaged using the Biorad Chemidoc MP System and protein expression was quantified by densitometry using ImageLab software (BioRad). For quantification, all samples were run together on 26-well gels. Cx43 expression levels were normalized to GAPDH and pCx43 to total Cx43 to compare between samples.

Impedance Spectroscopy: GJ resistance was estimated using the four-point electrode technique as previously described in cardiac tissue. [15-20] The electrical impedance spectra in the mice hearts (4 solutions X 2 mouse types X 5/3 replicates for WT/HZ, N=64) were measured during perfusion with different solutions. The four point measurement technique was implemented to reduce the effect of electrode polarization and facilitate the measurement at low frequencies. Due to the small size of the heart, a custom-made electrode array with inter-electrode distance of approximately 200μm was used. For each measurement, the electrodes penetrated to a depth of 500μm from the heart surface in an orientation approximately parallel to the epicardial fiber orientation. The rest of the electrode length was insulated to minimize the

parasitic conductivity path induced by the perfusion fluid on the heart exterior. The Gamry Instruments Interface1000 was used in the galvanostatic mode to introduce a 500μA AC between the two outer electrodes, and the two inner electrodes measured the change in voltage, over a range of 1Hz-1MHz.

The resistance-reactance curves between 1-100kHz, obtained from these recordings, were fitted with a circle to determine gap junctional resistance (R_{GJ}) as previously described.[16,21-23] The x-intercepts of the circle were determined, as they correspond to the intracellular resistance (right intercept) and the cytoplasmic resistance (left intercept). The difference between the two is reported as R_{GJ} below. All resistance values are reported as percent change from control (solution containing, 147.3mM $[Na^+]_o$ and 1mM $[Ca^{2+}]_o$), except for the comparison between WT and HZ R_{GJ}, where absolute values were used.

Due to potential inconsistencies associated with anisotropic nature of the tissue and different fiber orientations between animals, data are compared in a paired fashion within hearts to determine whether impedance spectroscopy can detect changes in gap junctional resistance due to perfusate composition. Unpaired comparisons between WT and HZ heart were used to determine whether the measurement could detect a 50% reduction in connexin43 protein. Finally, positive control impedance estimates were made in hearts treated with 50μM Carbenoxolone (CBX) or subjected to 30 minutes of no-flow ischemia (ISC).

Statistical Analysis: All data are reported as mean ± standard deviation unless stated otherwise. Single factor ANOVA was used to detect differences between WT and HZ W_P. Two-tailed, equal sample size and variance, paired/unpaired Student's t-test was performed to determine significant difference in W_P, CV, protein expression as well as GJ resistance data. Bonferonni correction was applied for multiple comparisons.

RESULTS:

Normonatremia - Perinexal width:

In order to investigate whether $[Ca^{2+}]_o$ alters intercellular separations within the intercalated disc, perfusate $[Ca^{2+}]_o$ was increased from 1 to 3.4mM, and W_P was quantified from transmission electron micrographs (TEM, Figure 3.1A) in hearts perfused with normonatremic solutions. W_P was not significantly different between WT and Cx43 HZ hearts at any $[Ca^{2+}]_o$ as revealed by a

single factor ANOVA (p=0.45) and all reported data and comparisons include both WT and HZ W_P values.

Summary data demonstrates that W_P was inversely correlated to $[Ca^{2+}]_o$ in the range of 1 to 3.4 mM (Figure 3.1B). A single factor ANOVA reveals a significant relationship between $[Ca^{2+}]_o$ and W_P ($p<0.001$). Post hoc comparison between 1 and 3.4 mM $[Ca^{2+}]_o$ reveals that W_P is significantly narrower at the higher calcium concentration (17.8±0.8 and 13.8±0.9nm, respectively). Additionally, increasing $[Ca^{2+}]_o$ from 1 to 1.8 mM, visually appears to increase in W_P, however, this was not significant (p=0.252). Importantly, the W_P values reported here are consistent with those observed in our previous study in mouse hearts exposed to a similar range of $[Ca^{2+}]_o$.[6]

Normonatremia – Conduction velocity

We previously demonstrated under conditions of physiologic $[Na^+]_o$ in mice as well as guinea pig hearts that W_P and CV are inversely correlated. [6,9] Specifically, decreasing W_P was associated with faster CV. Representative conduction isochrones in Figure 3.2A demonstrate the response of CV to increasing $[Ca^{2+}]_o$ – decreasing W_P. CV_L and CV_T vectors were averaged from two regions each that are indicated by green and orange boxes respectively.

The relationship between CV, $[Ca^{2+}]_o$, and Cx43 expression is complex as illustrated in Figure 3.2B. Increasing $[Ca^{2+}]_o$ over the range of 1 to 3.4mM did not significantly alter CV_L in either WT or HZ hearts. On the other hand, increasing $[Ca^{2+}]_o$ over the same range appears to sigmoidally modify CV_T in WT hearts. Specifically, increasing $[Ca^{2+}]_o$ from 1 to 1.8mM did not significantly alter CV_T. However, increasing $[Ca^{2+}]_o$ to 2.6 or 3.4 mM significantly increased CV_T (0.22±0.03 to 0.28±0.04 or 0.31±0.03 m/s respectively) relative to 1mM $[Ca^{2+}]_o$.

In HZ hearts, increasing $[Ca^{2+}]_o$ over the range of 1 to 3.4 mM only increased CV_T for very low $[Ca^{2+}]_o$. Specifically, CV_T significantly increased for $[Ca^{2+}]_o$ raised from 1 to 1.8 mM (0.21±0.03 and 0.27±0.03, respectively), but CV_T was not different between $[Ca^{2+}]_o$ of 1.8 and 3.4 mM (0.27±0.03, 0.28±0.02, and 0.27±0.03 m/s). While summary data of AR visually suggests that AR may decrease in both WT and HZ hearts with increasing $[Ca^{2+}]_o$, this relationship was not significant.

Our previous studies have suggested that loss of functional gap junctions increases CV sensitivity to cardiac hydration. To explore the unique responses of CV_T to $[Ca^{2+}]_o$, the relative change in CV_T for WT and HZ hearts are compared for $[Ca^{2+}]_o$ between 1 - 1.8, and 1 - 3.4 mM (Figure 3.2C). The data reveals that CV_T increases more in HZ hearts for $[Ca^{2+}]_o$ between 1 and 1.8. Interestingly, the difference is attenuated when comparing CV_T for $[Ca^{2+}]_o$ between 1 and 3.4 mM suggesting that CV is more sensitive to W_P changes during reduced Cx43 GJ coupling.[6,9] The sensitivity of Cx43 HZ hearts to $[Ca^{2+}]_o$ appears to be limited by a mechanism preventing further CV increases even as W_P decreases.

Hyponatremia – Perinexal Width:

Interestingly, computational models of EpC predict that the relationship between CV and intercalated disc separation may be biphasic, particularly when GJ coupling is reduced.[11,12] In short, for very narrow intercellular separations, conduction can also slow by a process termed "self-attenuation." To probe whether ephaptic self-attenuation can occur, W_P was reduced in the setting of reduced sodium reversal potential and driving force (hyponatremia).

First, the structural relationship between W_P - $[Ca^{2+}]_o$ was quantified in hearts perfused with a hyponatremic solution ($[Na^+]_o$ = 120mM), and representative micrographs are presented in Figure 3.3A. Once again, a single factor ANOVA reported significant differences in W_P between solutions ($p<0.05$) and $[Ca^{2+}]_o$ (1 to 3.4 mM, Figure 3.3B). Further post-hoc analysis revealed significantly wider W_P at the lowest relative to highest $[Ca^{2+}]_o$ (19.4±0.6 versus 17.2±0.6 nm). Additionally, W_P was not different between WT and HZ hearts ($p=0.83$) during hyponatremia as well.

Hyponatremia – Conduction Velocity

First, it is important to note that hyponatremia was associated with significantly slower CV_T relative to normonatremia in both WT and HZ hearts at all $[Ca^{2+}]_o$. Furthermore, representative isochrones maps in Figure 3.4A suggest that increasing $[Ca^{2+}]_o$ during hyponatremia now decreases CV, and this relationship is different from the normonatremic cases presented in Figure 3.2. Lastly, the isochrones suggest increased likelihood of conduction block into the left ventricle in both WT and HZ hearts particularly at the highest $[Ca^{2+}]_o$. Under these conditions, CV was measured from the RV. The number of hearts in which conduction block was observed is indicated above the isochrones in Panel A and in these hearts, CV_L and CV_T were averaged only in one direction each as indicated by the green and orange box in Figure 3.4A.

In WT hearts, increasing $[Ca^{2+}]_o$ from 1 to 1.8 or 2.6mM did not significantly alter CV_L, CV_T or AR. However, increasing $[Ca^{2+}]_o$ from 1 to 3.4mM slowed CV_T (0.17±0.03 to 0.12±0.03 m/s) and increased AR (1.6±0.2 vs 2.0±0.5) without measurably changing CV_L. The finding that increasing $[Ca^{2+}]_o$ during hyponatremia has the opposite effect on CV relative to normonatremia is consistent with theoretical predictions of ephaptic self-attenuation. Specifically, CV increased in hearts with narrow perinexi and high E_{Na}, but decreased in hearts with narrow perinexi and low E_{Na}.

CV slowing was also observed in HZ hearts in response to increasing $[Ca^{2+}]_o$ during hyponatremia. Increasing $[Ca^{2+}]_o$ slowed CV_T (0.17±0.02 to 0.11±0.03, 0.12±0.03 or 0.12±0.03m/s respectively) without measurably altering CV_L or AR. Interestingly, hyponatremia did not produce a significantly greater CV_T response in HZ relative to WT hearts at the lowest $[Ca^{2+}]_o$ of 1 and 1.8 mM (Figure 3.4C). This finding is consistent with the predictions of mathematical models that in the self-attenuation range, the effect of GJ coupling on CV is reduced.[10-12]

Extracellular Calcium and Gap junctional coupling:

i) Cx43 expression and phosphorylation:

Calcium ions are an important component of several cell signaling pathways and can modulate the functional states of proteins like Cx43.[24-26] The effect of varying $[Ca^{2+}]_o$ and $[Na^+]_o$ on total Cx43 and phosphorylated Cx43 at Ser368 (pCx43) were quantified in this study to determine whether $[Ca^{2+}]_o$ might alter gap junction expression levels after 30 minutes of perfusion. Representative and summary data are illustrated in Figure 3.5.

Perfusion with the extremes of the $[Ca^{2+}]_o$ and $[Na^+]_o$ used in this study (Figure 3.5A) did not alter the expression of total Cx43 or pCx43 (Figure 3.5B and C). However, it must be noted that in the HZ hearts, increasing $[Ca^{2+}]_o$ to 3.4mM trended to decrease total Cx43 expression at both high and low $[Na^+]_o$ ($p=0.080$ and 0.094 respectively), but these changes did not reach statistical significance after correction for multiple comparisons. As expected, HZ hearts expressed significantly less total Cx43 expression (Figure 3.5D, data normalized to GAPDH), but the ratio of pCx43 to total Cx43 ratio was similar to WT hearts (Figure 3.5E, data normalized to total Cx43).

ii) Gap Junctional Resistance:

Since protein levels do not necessarily correlate to its function, gap junctional coupling was estimated by tissue impedance spectroscopy. Figure 3.6A shows a representative resistance-reactance curve with the best circle fit. In Figure 3.6B, the percent change in R_{GJ} relative to control, during perfusion of 50μM CBX and after 30 minutes of no-flow ischemia are reported as positive controls. As expected, both CBX and ischemia (ISC) significantly increased R_{GJ} relative to control. Furthermore, the increase in R_{GJ} during inhibition of Cx43 by CBX is consistent with a previous study with guinea pig that reported a similar increase in R_{GJ} in the presence of CBX. [16] The percent change in R_{GJ} relative to control, during perfusion of different solutions in WT and HZ hearts are presented in Figure 3.6C. Varying $[Na^+]_o$ and $[Ca^{2+}]_o$ in the range used in this study did not significantly change R_{GJ}. As an additional positive control for demonstrating that impedance spectroscopy can detect loss of functional Cx43 as previously demonstrated,[21] R_{GJ} was compared between WT and HZ hearts . Summary data in Figure 3.6D demonstrates that R_{GJ} in WT hearts was significantly lower relative to HZ, as expected.

The impedance data coupled with the immunoblotting suggest that the perfusates used in this study either did not alter Cx43 functional expression, or altered it below the resolution for detection. Taken together, the data suggests that varying $[Ca^{2+}]_o$ and $[Na^+]_o$ in the specified range may not change GJ coupling, while these interventions did produce measureable changes in cardiac conduction.

Action Potential Duration:

Altering calcium concentration has been demonstrated to modify the functioning of several ion channels like $Na_v1.5$[27,28] and the small-conductance calcium activated potassium channels (SK).[29] Modulation of these ion channels can then manifest as changes in action potential duration and morphology, and also alter CV. However, alterations in these proteins have been reported for much larger $[Ca^{2+}]_o$, and the effect of small variations as used in this study has not been explored. Therefore, we quantified APD in WT and HZ hearts perfused with 1 and 3.4mM $[Ca^{2+}]_o$ solutions.

Representative action potentials signal averaged over approximately 10 beats, from the same heart perfused with 1 and 3.4 mM $[Ca^{2+}]_o$, and 120mM $[Na^+]_o$ are presented in Figure 3.7A and the summary of APD in Figure 3.7B. Importantly, APD did not significantly change in response to $[Ca^{2+}]_o$ or $[Na^+]_o$ as determined from a single factor ANOVA (p=0.9 and 0.2 for WT and HZ,

respectively). Additionally, Figure 3.7B also demonstrates that Cx43 expression levels do not significantly alter APD for any concentration of $[Ca^{2+}]_o$ or $[Na^+]_o$. Taken together, the data suggests that the CV-$[Ca^{2+}]_o$ response reported above is not measurably affected by the ionic currents underlying the action potential.

DISCUSSION:

The results of this study demonstrate that $[Ca^{2+}]_o$ can modulate W_P and CV as hypothesized. More specifically, increasing $[Ca^{2+}]_o$ from 1 to 3.4 mM reduces W_P during both normonatremia as well as hyponatremia. However, the relationship between $[Ca^{2+}]_o$ and CV is more complex and dependent on $[Na^+]_o$. Specifically, increasing $[Ca^{2+}]_o$ can increase CV during normonatremia and decrease CV during hyponatremia. Taken together, these findings suggest that $[Ca^{2+}]_o$ modulates W_P, which modulates CV differently during normonatremia and hyponatremia by a mechanism that is not gap junction dependent.

Extracellular calcium and perinexal width:

At several points along the intercalated disc, transmembrane proteins that form gap junctions, desmosomes, or adherens junctions bind to their counterparts on the apposing cell membrane, structurally holding the two membranes together.[30] Several proteins that compose these junctions like N-Cadherins, desmocollin and desmoglein, among others have calcium-dependent adhesion properties.[31-33] In the absence of calcium or during hypocalcemia, the binding affinity of these proteins could be reduced, making these junctions looser points of contact, which in turn results in greater separation between the membranes at the intercalated disc.[34,35]

Varying $[Ca^{2+}]_o$ in this study resulted in W_P modulation. Specifically, increasing calcium ion concentration was associated with narrower perinexi or, in other words, W_P and $[Ca^{2+}]_o$ were inversely correlated. However, this correlation was weaker during hyponatremia.

Ephaptic coupling:

Cellular excitation of cardiac myocytes occurs when transmembrane potential (V_m), which is the difference between the intracellular and extracellular potentials ($V_m = \Phi_i - \Phi_o$), depolarizes the cell sufficiently to activate voltage gated sodium channel. The post-junctional cell V_m can rise by either decreasing Φ_o or increasing Φ_I. The most commonly accepted method for raising post junctional V_m is by electrotonically increasing Φ_i via gap junctions. On the other hand, Φ_o can be

altered by the depletion or accumulation of charge in the extracellular space caused by, for example, withdrawal of sodium or increased potassium in intercellular clefts during the activation of the pre- junctional cell. Such a non-gap junctional, non-synaptic form of electrical coupling between myocytes is what is termed as EpC, and several more mechanisms for EpC have been mathematically proposed.[36]

One important requirement for EpC is the presence of micro-domains with closely abutting cell membranes. Several such intercalated disc structures like the perinexus[9] and connexome[37] have been proposed as possible cardiac ephapses with volumes that can be modulated. The study by Veeraraghavan et al[9] also identified the consequences that perinexal width modulation has on conduction velocity by pharmacological as well as mathematical methods. Specifically, narrower perinexi promotes faster transmission of electrical impulses from the pre- to the post-junctional cell due to the closer spacing of the two membranes. Thus increasing $[Ca^{2+}]_o$, as we did in this study, could increase CV in normonatremic hearts by narrowing perinexi and improving EpC between cells consistent with our previous works.[6,9]

In this study, transverse CV was more sensitive to experimental interventions that altered W_P and sodium driving force. To understand this finding, it is important to consider that gap junction uncoupling preferentially alters transverse CV, because the propagating wavefront in the transverse direction encounters more GJs per unit length relative to the longitudinal direction. Parallel to this concept, perinexi, which are theoretical EpC junctions, are also localized to the intercalated disc. Therefore, a wavefront propagating transverse to fibers will encounter more gap and ephaptic junctions relative to the longitudinal direction of propagation. In short, inhibiting EpC is expected to likewise preferentially affect transverse CV.

Self-attenuation:

Self-attenuation was previously suggested in mathematical models of cardiac conduction incorporating extracellular field effects as well as a polarized voltage-gated sodium ion channel distribution to the intercalated disc, both of which are essential to support EpC.[11,12] Self-attenuation was described as the process by which peak I_{Na} attenuates itself due to reduced cleft width and sodium current driving force. The sodium current driving force, as described above, can be reduced by either increasing V_m or decreasing E_{Na}. While two models[10,11] predict self-attenuation solely based on changes in V_m, the Peskin[12] model additionally tracks ion concentrations and Nernst potentials. Therefore, the models that incorporate both V_m overshoot

and changes in E_{Na} within the intercalated disc may be more sensitive to ephaptic self-attenuation.[12]

In the present study, cleft width was reduced by increasing $[Ca^{2+}]_o$ and sodium driving force was reduced by reducing $[Na^+]_o$. In the case of the high $[Na^+]_o$ solutions, where sodium driving force was relatively larger, altering W_P alone increased CV consistent with our previous work in guinea pigs and mice possibly due to modulation of EpC outside of the self-attenuation range reported by mathematical models. Importantly, this study for the first time identifies that in the setting of reduced sodium driving force (low $[Na^+]_o$ solutions), the relationship between $[Ca^{2+}]_o$, W_P and CV is consistent with self-attenuation. Specifically, our data is consistent with the hypothesis that reducing W_P during reduced $[Na^+]_o$ further reduces available $[Na^+]_o$ in the perinexus during sodium mediated depolarization. Under these conditions, depolarization of the pre-junctional cell withdraws a large number of available sodium ions from the intercalated disc microdomain. This charge withdrawal greatly reduces the sodium current driving force for the post-junctional cell. The reduced driving force then delays propagation of the electrical impulse from the pre- to the post-junctional myocyte resulting in CV slowing.

It is difficult to compare the results of this work with previous studies investigating the relationship between CV and $[Ca^{2+}]_o$ due to significant experimental differences. For example, elevating $[Ca^{2+}]_o$ from 1 to 2 mM did not alter CV while raising $[Ca^{2+}]_o$ from 2 to 8 mM significantly slowed CV in false tendons isolated from dog ventricles.[38] Another study reported non-significant changes in longitudinal and transverse CV in dog papillary muscle when $[Ca^{2+}]_o$ was varied similar to concentrations used in our study.[39] Therefore, while previous studies in different animal models, tissue preparations, and with different perfusate compositions demonstrated that raising $[Ca^{2+}]_o$ within some narrow window can decrease or not change CV, to our knowledge this is the first study to demonstrate that CV and $[Ca^{2+}]_o$ can positively or negatively correlate depending on $[Na^+]_o$ in a manner consistent with the mathematical predictions of ephaptic self-attenuation.[10-12]

Gap Junctional coupling:

Calcium ions are involved in the regulation of several physiological functions and play a key role in various signaling pathways.[40] Intracellular calcium homeostasis is tightly regulated by a highly developed system that involves several intracellular calcium stores.[41,42] However, during certain pathophysiological states, intracellular calcium increases which then results in modulation of

several factors that can then alter CV.[43] For example, intracellular calcium concentration has been shown to modulate gap junctional coupling.[24-26] Elevated $[Ca^{2+}]_i$ alters Cx43 gating by a Ca^{2+}/Calmodulin dependent pathway and reduces intercellular coupling.[44] Cx43 uncoupling has been associated with slow CV when the extracellular ionic composition is altered to weaken EpC.[1,6,45,46] However, this study demonstrates that modulating $[Ca^{2+}]_o$ (1 – 3.4mM) does not change either total or phosphorylated Cx43 expression during normonatremia as well as hyponatremia. Additionally, varying $[Ca^{2+}]_o$ did not alter gap junctional resistance, and increasing $[Ca^{2+}]_o$ was also associated with faster CV during normonatremia. Furthermore, the changes in electrophysiology were measured at a much earlier time point (8 mins) compared to Cx43 expression measurements (30 mins). These findings suggest that gap junctional coupling may not be the mechanism by which $[Ca^{2+}]_o$ modulates CV in this study.

LIMITATIONS:

Modulating $[Ca^{2+}]_o$ could have several physiological implications in the heart which includes altered contraction, calcium handling, cell signaling pathways and apoptosis.[40] $[Ca^{2+}]_o$ was varied from 1 – 3.4 mM in this study, which is a range wider than the normal physiological $[Ca^{2+}]_o$ which typically falls between 1.7 and 2.5 mM in mice.[47] However, previous studies investigating the effects of hypercalcemia have reported significant changes in GJ coupling at much higher $[Ca^{2+}]_o$ (greater than 5mM).[24,48]

The perinexus has been identified as the site of dense localization of several ion channels, and it is possible that downregulation of Cx43 in HZ mice could affect the structure of the perinexus. First, this study demonstrates that intercellular separation within the perinexus (W_P) is not different between WT and HZ hearts for any intervention. This does not exclude the possibility that the spatial extent of the perinexus – distance from the GJ edge – is altered in HZ animals, and this requires further investigation. Furthermore, it has been previously demonstrated in the same mouse model that the structure of GJ plaques in HZ mice was not different compared to WT, though the number of GJ plaques was reduced.[49] This suggests that at least the GJ plaque and intercellular separation are conserved even when GJs are genetically reduced.

CONCLUSIONS:

Extracellular ion concentration is a crucial component in modulating cardiac conduction. This study identifies that extracellular sodium and calcium composition could differently modulate CV during health and conditions like hyponatremia commonly associated with several diseases

which include congestive heart failure,[50] kidney[51] and liver[52] disorders. Specifically, while reducing W_P by increasing $[Ca^{2+}]_o$ was beneficial and increased CV during normonatremia, it slowed CV during hyponatremia. Furthermore, the changes in CV reported in this study were independent of Cx43 protein expression, phosphorylation or GJ resistance suggesting the role of a non-GJ mediated mechanism for CV modulation like EpC.

These data reinforce the importance of regulating serum ion concentration during health and more importantly during disease. Furthermore, there is now mounting evidence that modulating parameters predicted to alter EpC can be used as a tool in the treatment of conduction based disorders in the heart.

REFERENCES:

1. Kleber AG, Rudy Y. Basic mechanisms of cardiac impulse propagation and associated arrhythmias. *Physiological Reviews.* 2004;84:431-488.

2. Nygren A, Giles WR. Mathematical simulation of slowing of cardiac conduction velocity by elevated extracellular. *Annals of Biomedical Engineering.* 2000;28:951-957.

3. Ballantyne F III, Davis LD, Reynolds EW Jr. Cellular basis for reversal of hyperkalemic electrocardiographic changes by sodium. *The American Journal of Physiology.* 1975;229:935-940.

4. Veeraraghavan R, Gourdie RG, Poelzing S. Mechanisms of cardiac conduction: a history of revisions. *American Journal of Physiology. Heart and Circulatory Physiology.* 2014;306:H619-627.

5. George SA, Poelzing S. Cardiac conduction in isolated hearts of genetically modified mice - Connexin43 and salts. *Progress in Biophysics and Molecular Biology.* 2015.

6. George SA, Sciuto KJ, Lin J, et al. Extracellular sodium and potassium levels modulate cardiac conduction in mice heterozygous null for the Connexin43 gene. *Pflugers Archiv : European Journal of Physiology.* 2015;467:2287-2297.

7. Stein M, van Veen TA, Remme CA, et al. Combined reduction of intercellular coupling and membrane excitability differentially affects transverse and longitudinal cardiac conduction. *Cardiovascular Research.* 2009;83:52-60.

8. Veeraraghavan R, Salama ME, Poelzing S. Interstitial volume modulates the conduction velocity-gap junction relationship. *American Journal of Physiology. Heart and Circulatory Physiology.* 2012;302:H278-286.

9. Veeraraghavan R, Lin J, Hoeker G, et al. Sodium channels in the Cx43 gap junction perinexus may constitute a cardiac ephapse: an experimental and modeling study. *Pflugers Archiv: European Journal of Physiology.* 2015; 467:2093-2105.

10. Lin J, Keener JP. Microdomain effects on transverse cardiac propagation. *Biophysical Journal.* 2014;106:925-931.

11. Kucera JP, Rohr S, Rudy Y. Localization of sodium channels in intercalated disks modulates cardiac conduction. *Circulation Research.* 2002;91:1176-1182.

12. Mori Y, Fishman GI, Peskin CS. Ephaptic conduction in a cardiac strand model with 3D electrodiffusion. *Proceedings of the National Academy of Sciences of the United States of America.* 2008;105:6463-6468.

13. Rhett JM, Ongstad EL, Jourdan J, et al. Cx43 associates with Na(v)1.5 in the cardiomyocyte perinexus. *The Journal of Membrane Biology.* 2012;245:411-422.

14. Smyth JW, Hong TT, Gao D, et al. Limited forward trafficking of connexin 43 reduces cell-cell coupling in stressed human and mouse myocardium. *The Journal of Clinical Investigation.* 2010;120:266-279.

15. Stiles DK, Oakley BA. Four-point electrode measurement of impedance in the vicinity of bovine aorta for quasi-static frequencies. *Bioelectromagnetics.* 2005;26:54-58.

16. Dhillon PS, Chowdhury RA, Patel PM, et al. Relationship between connexin expression and gap-junction resistivity in human atrial myocardium. *Circulation. Arrhythmia and Electrophysiology.* 2014;7:321-329.

17. Sanchez JA, Rodriguez-Sinovas A, Fernandez-Sanz C, et al. Effects of a reduction in the number of gap junction channels or in their conductance on ischemia-reperfusion arrhythmias in isolated mouse hearts. *American Journal of Physiology. Heart and Circulatory Physiology.* 2011;301:H2442-2453.

18. Padilla F, Garcia-Dorado D, Rodriguez-Sinovas A, et al. Protection afforded by ischemic preconditioning is not mediated by effects on cell-to-cell electrical coupling during myocardial ischemia-reperfusion. *American Journal of Physiology. Heart and Circulatory Physiology.* 2003;285:H1909-1916.

19. Jain SK, Schuessler RB, Saffitz JE. Mechanisms of delayed electrical uncoupling induced by ischemic preconditioning. *Circulation Research.* 2003;92:1138-1144.

20. Smith WTt, Fleet WF, Johnson TA, et al. The Ib phase of ventricular arrhythmias in ischemic in situ porcine heart is related to changes in cell-to-cell electrical coupling. *Circulation.* 15 1995;92(10):3051-3060.

21. Dhillon PS, Gray R, Kojodjojo P, et al. Relationship between gap-junctional conductance and conduction velocity in mammalian myocardium. *Circulation. Arrhythmia and Electrophysiology.* 2013;6:1208-1214.

22. Chapman RA, Fry CH. An analysis of the cable properties of frog ventricular myocardium. *The Journal of Physiology.* 1978;283:263-282.

23. Cooklin M, Wallis WR, Sheridan DJ, et al. Changes in cell-to-cell electrical coupling associated with left ventricular hypertrophy. *Circulation Research.* 1997;80:765-771.

24. Maurer P, Weingart R. Cell pairs isolated from adult guinea pig and rat hearts: effects of [Ca2+]i on nexal membrane resistance. *Pflugers Archiv : European Journal of Physiology.* 1987;409:394-402.

25. Rudisuli A, Weingart R. Electrical properties of gap junction channels in guinea-pig ventricular cell pairs revealed by exposure to heptanol. *Pflugers Archiv : European journal of physiology.* 1989;415:12-21.

26. Kagiyama Y, Hill JL, Gettes LS. Interaction of acidosis and increased extracellular potassium on action potential characteristics and conduction in guinea pig ventricular muscle. *Circulation Research.* 1982;51:614-623.

27. Tan HL, Kupershmidt S, Zhang R, et al. A calcium sensor in the sodium channel modulates cardiac excitability. *Nature.* 2002;415:442-447.

28. Koval OM, Snyder JS, Wolf RM, et al. Ca2+/calmodulin-dependent protein kinase II-based regulation of voltage-gated Na+ channel in cardiac disease. *Circulation.* 2012;126:2084-2094.

29. Wang H, Li T, Zhang L, et al. [Effects of intracellular calcium alteration on SK currents in atrial cardiomyocytes from patients with atrial fibrillation]. *Zhongguo ying yong sheng li xue za zhi = Zhongguo yingyong shenglixue zazhi = Chinese Journal of Applied Physiology.* 2014;30:296-300, 305.

30. Li J, Radice GL. A new perspective on intercalated disc organization: implications for heart disease. *Dermatology Research and Practice.* 2010;2010:207835.

31. Vleminckx K, Kemler R. Cadherins and tissue formation: integrating adhesion and signaling. *BioEssays : News and Reviews in Molecular, Cellular and Developmental Biology.* 1999;21:211-220.

32. Wallis S, Lloyd S, Wise I, et al. The alpha isoform of protein kinase C is involved in signaling the response of desmosomes to wounding in cultured epithelial cells. *Molecular Biology of the Cell.* 2000;11:1077-1092.

33. Chitaev NA, Troyanovsky SM. Direct Ca2+-dependent heterophilic interaction between desmosomal cadherins, desmoglein and desmocollin, contributes to cell-cell adhesion. *The Journal of Cell Biology.* 1997;138:193-201.

34. Greve G, Rotevatn S, Saetersdal T, et al. Ultrastructural studies of intercalated disc separations in the rat heart during the calcium paradox. *Research in Experimental Medicine. Zeitschrift fur die gesamte experimentelle Medizin einschliesslich experimenteller Chirurgie.* 1985;185:195-206.

35. Ganote CE, Grinwald PM, Nayler WG. 2,4-Dinitrophenol (DNP)-induced injury in calcium-free hearts. *Journal of Molecular and Cellular Cardiology.* 1984;16:547-557.

36. Sperelakis N. An electric field mechanism for transmission of excitation between myocardial cells. *Circulation Research.* 2002;91:985-987.

37. Leo-Macias A, Liang FX, Delmar M. Ultrastructure of the intercellular space in adult murine ventricle revealed by quantitative tomographic electron microscopy. *Cardiovascular Research.* 2015;107:442-452.

38. Pressler ML, Elharrar V, Bailey JC. Effects of extracellular calcium ions, verapamil, and lanthanum on active and passive properties of canine cardiac purkinje fibers. *Circulation Research.* 1982;51:637-651.

39. Veenstra RD, Joyner RW, Rawling DA. Purkinje and ventricular activation sequences of canine papillary muscle. Effects of quinidine and calcium on the Purkinje-ventricular conduction delay. *Circulation Research.* 1984;54:500-515.

40. Zarain-Herzberg A, Fragoso-Medina J, Estrada-Aviles R. Calcium-regulated transcriptional pathways in the normal and pathologic heart. *International Union of Biochemistry and Molecular Biology Life.* 2011;63:847-855.

41. Fearnley CJ, Roderick HL, Bootman MD. Calcium signaling in cardiac myocytes. *Cold Spring Harbor Perspectives in Biology.* 2011;3:a004242.

42. Kohlhaas M, Maack C. Calcium release microdomains and mitochondria. *Cardiovascular Research.* 2013;98:259-268.

43. Di Diego JM, Antzelevitch C. High [Ca2+]o-induced electrical heterogeneity and extrasystolic activity in isolated canine ventricular epicardium. Phase 2 reentry. *Circulation.* 1994;89:1839-1850.

44. Xu Q, Kopp RF, Chen Y, et al. Gating of connexin 43 gap junctions by a cytoplasmic loop calmodulin binding domain. *American Journal of Physiology. Cell Physiology.* 2012;302:C1548-1556.

45. Eloff BC, Lerner DL, Yamada KA, et al. High resolution optical mapping reveals conduction slowing in connexin43 deficient mice. *Cardiovascular Research.* 2001;51:681-690.

46. Guerrero PA, Schuessler RB, Davis LM, et al. Slow ventricular conduction in mice heterozygous for a connexin43 null mutation. *The Journal of Clinical Investigation.* 1997;99:1991-1998.

47. Research Animals Resources UoM. Reference Values for Laboratory Animals. Normal Hematology Values. 2009; www.ahc.umn.edu/rar/refvalues.html, 2013.

48. Weingart R. The actions of ouabain on intercellular coupling and conduction velocity in mammalian ventricular muscle. *The Journal of Physiology.* 1977;264:341-365.

49. Saffitz JE, Green KG, Kraft WJ, et al. Effects of diminished expression of connexin43 on gap junction number and size in ventricular myocardium. *American Journal of Physiology. Heart and Circulatory Physiology.* 2000;278:H1662-1670.

50. Oren RM. Hyponatremia in congestive heart failure. *The American Journal of Cardiology.* 2005;95:2B-7B.

51. Lin CS, Cheng CJ, Shih KC, et al. Recurrent hyponatremia in a patient with chronic kidney disease. *Journal of Nephrology.* 2006;19:394-398.

52. Gines P, Guevara M. Hyponatremia in cirrhosis: pathogenesis, clinical significance, and management. *Hepatology.* 2008;48:1002-1010.

Table 3.1. Perfusate Osmolarity. The osmolarity of the perfusates with varying $[Na^+]_o$ and $[Ca^{2+}]_o$ are listed in mOsm.

$[Na^+]_o$ (mM)	$[Ca^{2+}]_o$ (mM)	Osmolarity (mOsm)
147.3	1.0	304.3
147.3	1.8	303.0
147.3	2.6	301.3
147.3	3.4	301.3
120	1.0	250.3
120	1.8	253.0
120	2.6	250.3
120	3.4	246.3

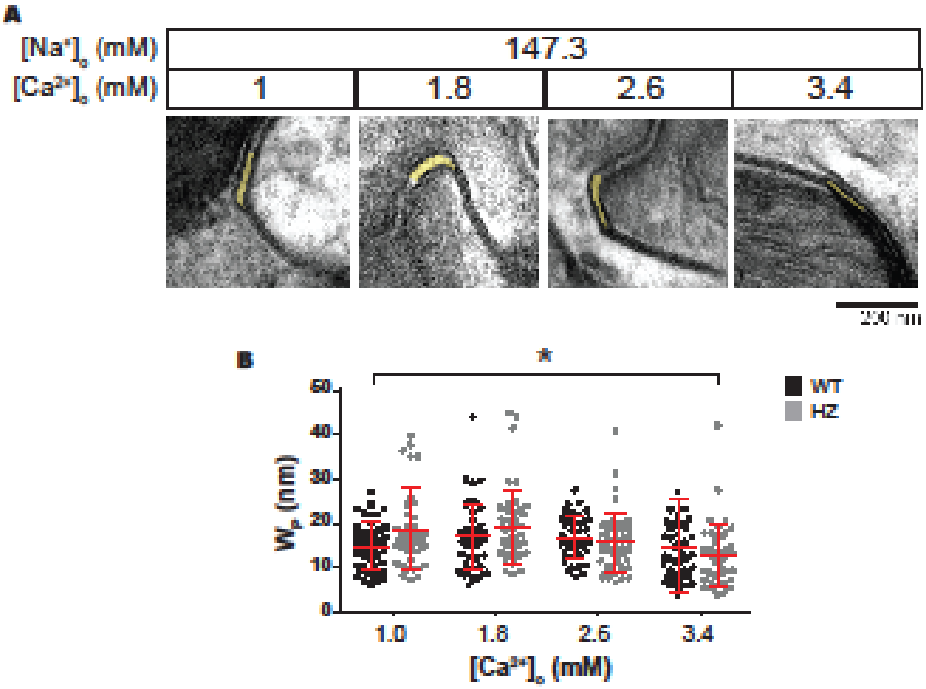

Figure 3.1. Extracellular Calcium – Perinexal Width Relationship during Normonatremia. **A.** Representative electron micrographs of hearts perfused with varying $[Ca^{2+}]_o$. Perinexi are highlighted in yellow. **B.** Summary data of W_P as a function of $[Ca^{2+}]_o$ from WT (Black) and HZ hearts (Grey). Mean and standard deviation are indicated by red lines. n=3X15 images. * indicates $p<0.05$ between $[Ca^{2+}]_o$ = 1 and 3.4 mM by unpaired Student's t-test. Error bars represent standard error.

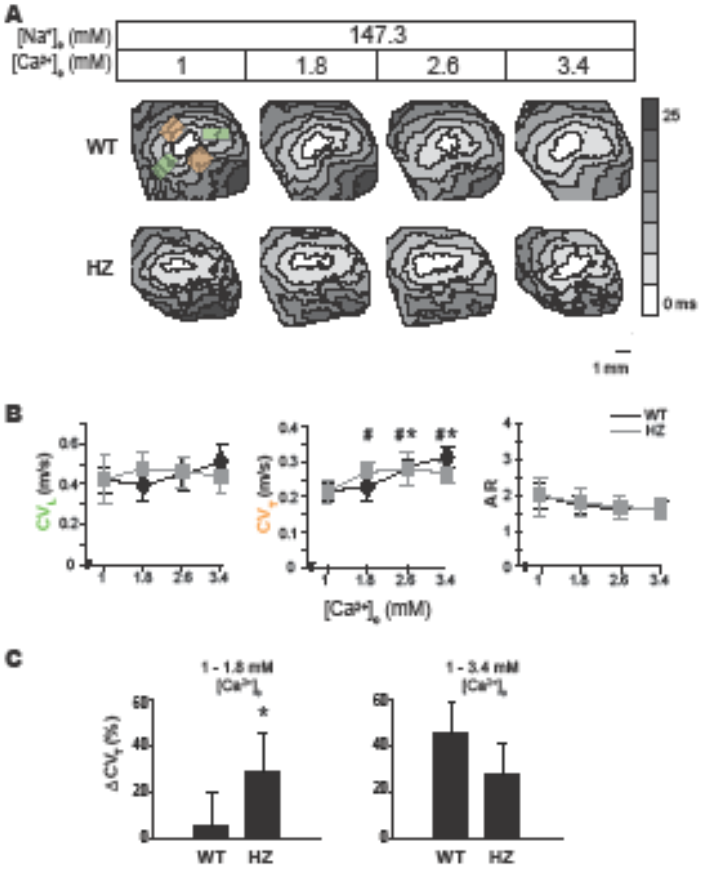

Figure 3.2. Extracellular calcium modulates Conduction Velocity during Normonatremia. **A**. Representative activation maps obtained by optically mapping a single heart during the serial perfusion of solutions with increasing $[Ca^{2+}]_o$. Orange boxes to the top and bottom of the pacing site indicate the regions from which CV_T was averaged and green boxes to the left and right indicate regions from which CV_L was averaged. **B**. Average CV_T, CV_L and AR (Anisotropic Ratio) from WT (Black line) and HZ (Gray line) hearts. **C.** Percent change in CV_T between $[Ca^{2+}]_o$ = 1 -1.8 mM and 1 – 3.4 mM in WT and HZ hearts demonstrates increased sensitivity of HZ hearts to W_P in the former and not the latter range. n=5. * and # indicates $p<0.05$ relative to $[Ca^{2+}]_o$ = 1mM in WT and HZ, respectively by paired Student's t-test.

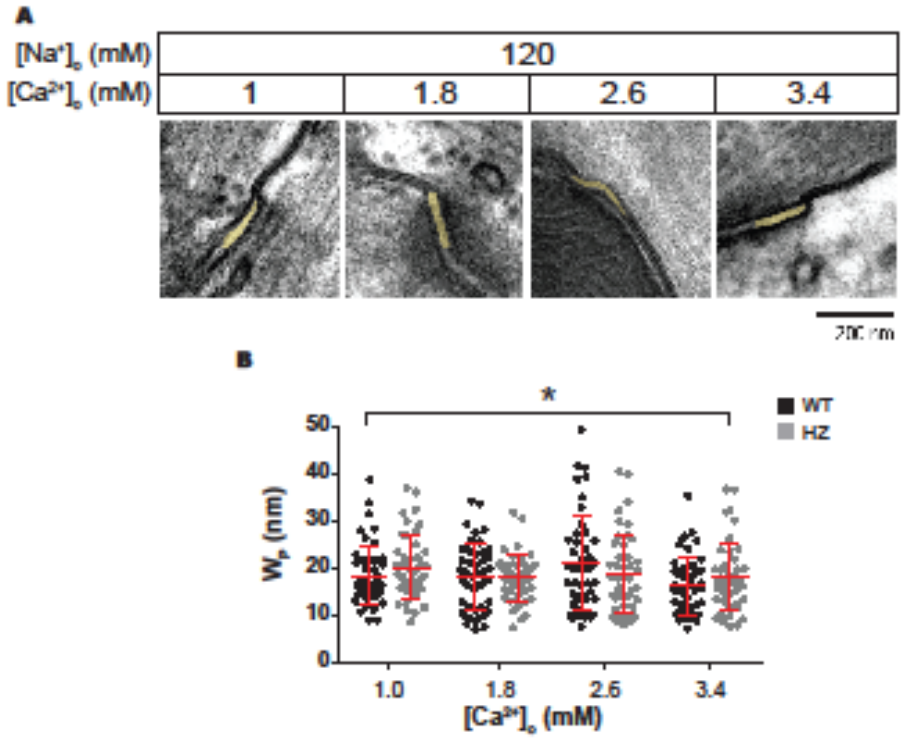

Figure 3.3. Extracellular Calcium – Perinexal Width Relationship during Hyponatremia. A. Representative electron micrographs of hearts perfused with varying $[Ca^{2+}]_o$ during hyponatremia. Perinexi are highlighted in yellow. **B.** Summary data of W_P as a function of $[Ca^{2+}]_o$ from WT (Black) and HZ hearts (Grey). Mean and standard deviation are indicated by red lines. n=3X15 images. * indicates $p<0.05$ between $[Ca^{2+}]_o$ = 1 and 3.4 mM by unpaired Student's t-test.Error bars represent standard error.

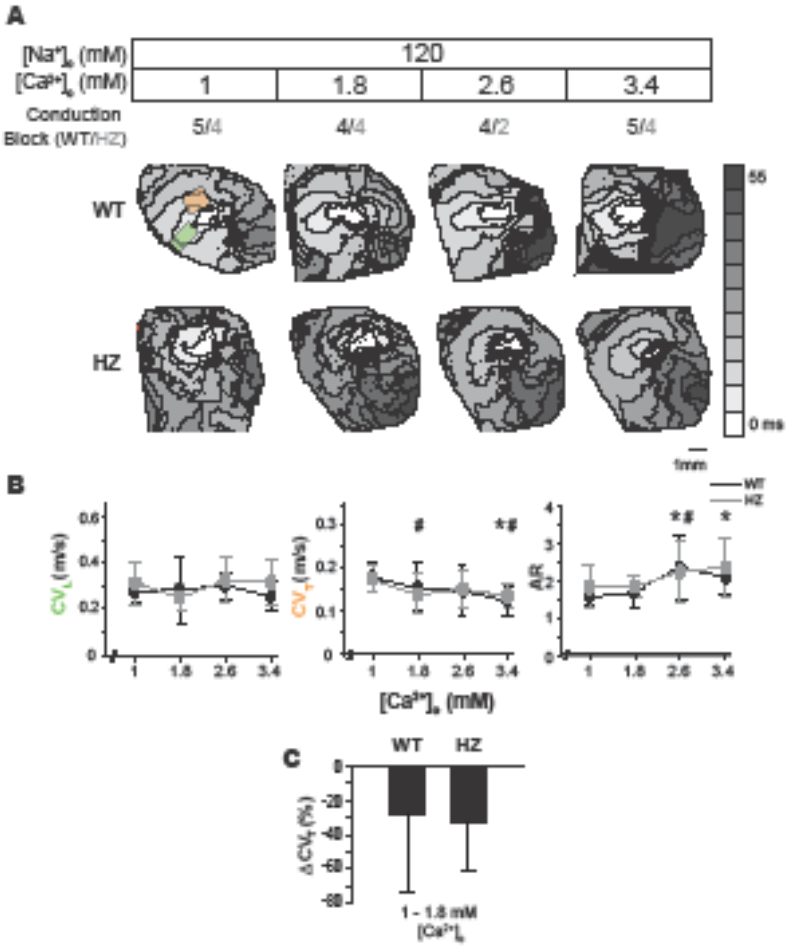

Figure 3.4. Extracellular calcium modulates Conduction Velocity during Hyponatremia. A. Representative activation maps obtained by optically mapping a single heart during the serial perfusion of solutions with increasing $[Ca^{2+}]_o$ during hyponatremia. The orange box to the top of the pacing site indicates the region from which CV_T was averaged and the green box to the left indicates the region from which CV_L was averaged in hearts with CV block over the left ventricle. **B.** Average CV_T, CV_L and AR (Anisotropic Ratio) from WT (Black line) and HZ hearts (Gray line). **C.** Percent change in CV_T between $[Ca^{2+}]_o$ = 1 and 1.8mM in WT and HZ hearts. n=5. * and # indicates $p<0.05$ relative to $[Ca^{2+}]_o$ = 1mM in WT and HZ, respectively by paired Student's t-test.

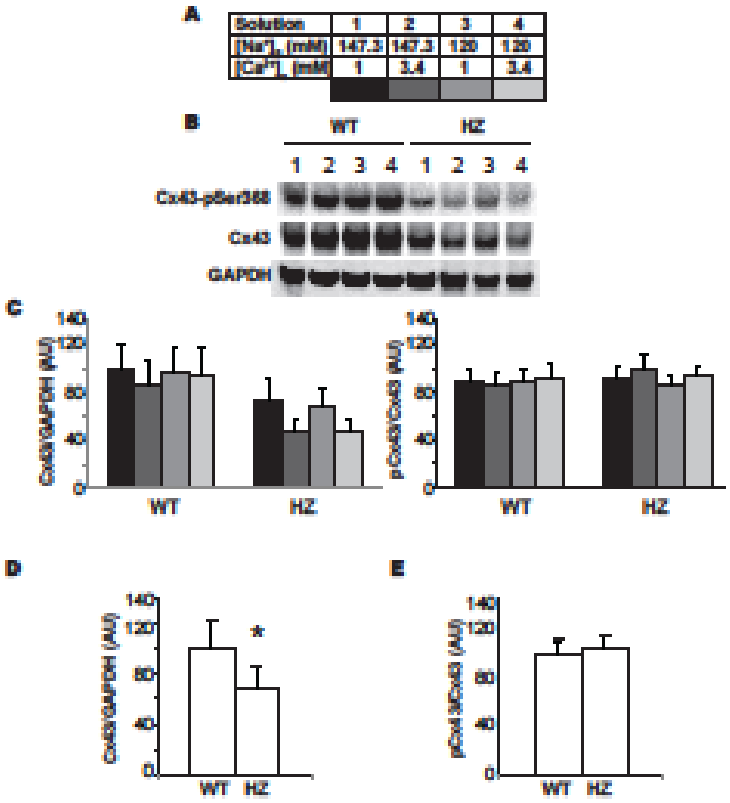

Figure 3.5. Cx43 expression during variation in extracellular sodium and calcium ion concentration. A. Upper and lower limits of the range over which $[Na^+]_o$ and $[Ca^{2+}]_o$ were varied in this study and the color code for the panels below. Representative Western immunoblots of total and pSer368 Cx43 (**B.**) Total Cx43 normalized to GAPDH (left) and pCx43 normalized to total Cx43 in **C.** illustrates that varying $[Na^+]_o$ and $[Ca^{2+}]_o$ do not significantly alter Cx43 expression. **D.** Total Cx43 is significantly reduced in HZ hearts relative to WT. **E.** The ratio of pCx43 to total Cx43 is not different between WT and HZ hearts. n=3. * indicates $p<0.05$ by unpaired Student's t-test.

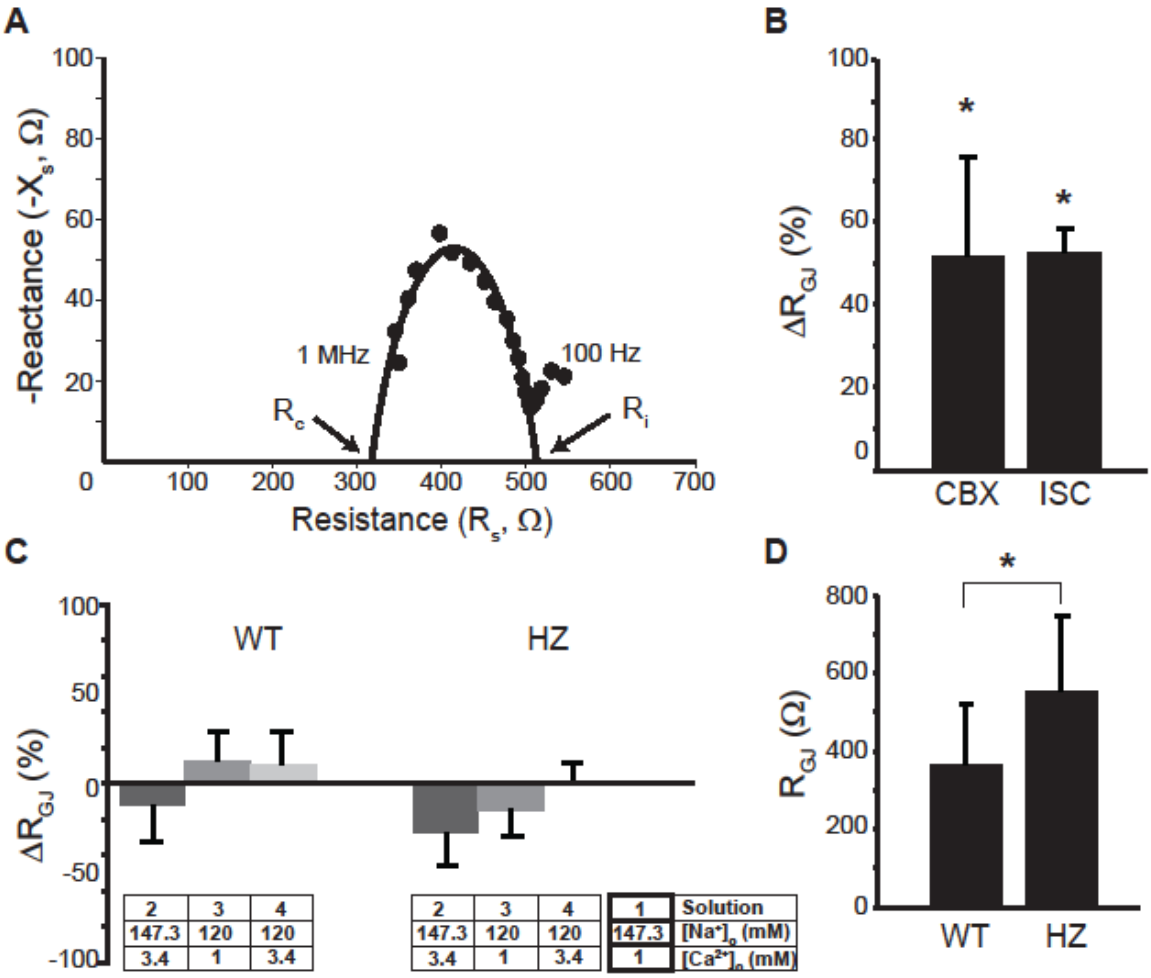

Figure 3.6. Tissue impedance during variation in extracellular sodium and calcium ion concentration. A. Representative resistance-reactance curve with circle fit. **B.** Percent change in gap junctional resistance after treatment with 50μM carbenoxolone (CBX) and 30 minutes of ischemia (ISC). **C.** Average gap junctional resistance values determined during perfusion of solutions with various $[Na^+]_o$ and $[Ca^{2+}]_o$. **D.** GJ resistance is significantly increased in HZ hearts relative to WT. n=5 for WT and n=3 for HZ. * indicates $p<0.05$ by paired Student's t-test in Panels B and C, and unpaired Student's t-test in Panel D.

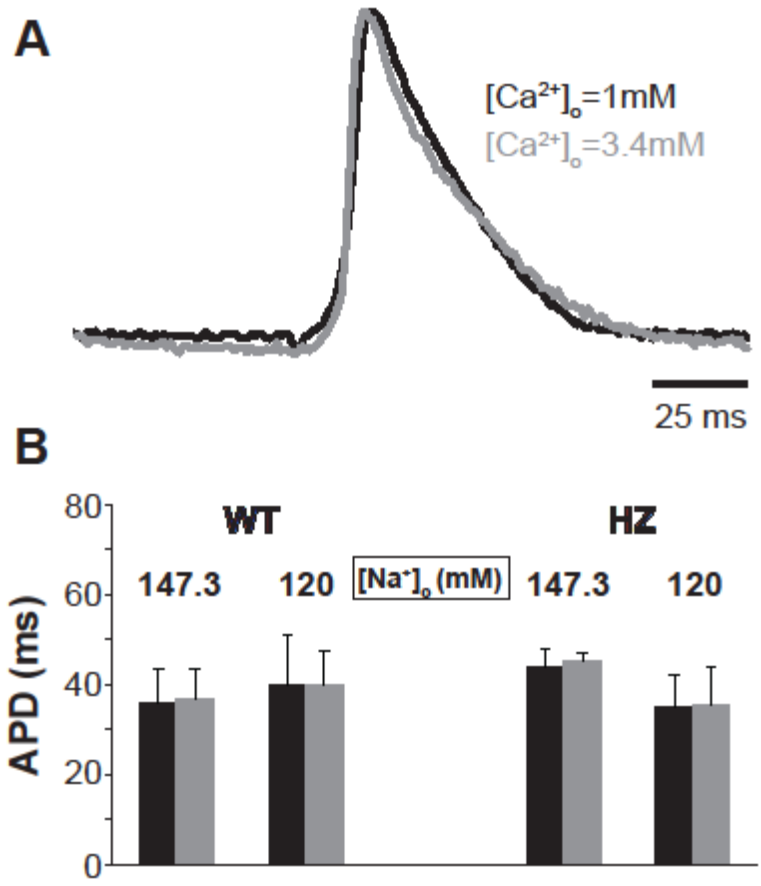

Figure 3.7. Action potential duration not affected by $[Na^+]_o$, $[Ca^{2+}]_o$ or Cx43 expression. A. Representative action potentials signal averaged over approximately 10 beats from the same heart perfused with $[Ca^{2+}]_o$ = 1mM (Black) and 3.4 mM (Gray). **B.** Neither $[Na^+]_o$, $[Ca^{2+}]_o$, nor Cx43 expression alter mean epicardial APD.

CHAPTER – 4

PERFUSATE COMPOSITION MODULATION DURING ACUTE TNFα EXPOSURE

INTRODUCTION:

Inflammation is the body's protective response to counteract pathogens or other external stimuli. It is associated with the modulation of several factors, including the up- and downregulation of many cytokines, which are cell signaling molecules.[1] Cytokines modulate numerous cellular processes in the body, some beneficially and others detrimentally during inflammation. Myocardial inflammation has previously been associated with many cardiac diseases[2,3] and modulates several determinants of cardiac functioning, both mechanical and electrical. In terms of the mechanical aspects of cardiac functioning, myocardial inflammation has been demonstrated to cause cardiac dysfunction and reduced ejection fraction.[4,5] Myocardial inflammation has also been demonstrated to modulate key factors that can affect propagation of electrical impulses like gap junctional (GJ) coupling,[6,7] ionic currents, which manifest as changes in action potential (AP) parameters,[2,8] and tissue hydration state among others.[9]

Tumor Necrosis Factor α (TNFα) is a pro-inflammatory cytokine that is upregulated during the inflammatory response and is a key marker of the acute inflammatory phase in several pathophysiologic states including ischemia, myocarditis and cardiomyopathies.[10,11] TNFα upregulation modulates other cytokine expression and has a cascading effect on the inflammatory process. The effect of TNFα on various cellular functions has been extensively studied in various tissue types. For example, some studies demonstrate that exposure to TNFα reduces [12,13] total Connexin43 (Cx43), the principle gap junctional protein in cardiac ventricles, while others report no change.[14] Another set of studies have also identified that TNFα can modulate Cx43 phosphorylation states in anterior pituitary cells.[16] However, the acute TNFα exposure-induced changes in GJ coupling in ventricular cardiomyocytes are not fully understood. In addition to its effect on GJ coupling, TNFα has also been demonstrated to modulate vascular permeability which can alter tissue hydration state.[17,18] However, it is not known how this translates to the level of intercellular separation at nanodomains along the intercalated disc, such as the perinexus. Additionally, TNFα has also been reported to reduce the expression of structural proteins along the intercalated disc (ID) and cause ID dehiscence.[13] Both these factors can cause perinexal widening which has been associated with CV slowing possibly due to weaker ephaptic coupling (EpC) between myocytes.[19,20] Therefore, TNFα alone can modulate various determinants of CV similar to previously reported models of myocardial inflammation. In this study, we use pathophysiologic TNFα upregulation as a model for myocardial inflammation and focus on the effect and mechanism of action of acute TNFα

exposure on ventricular conduction. We hypothesized, that TNFα modulates CV by reducing electrical coupling in the heart – EpC and/or GJC.

In this study, we determined the ventricular conduction velocity (CV) response to TNFα exposure, at a pathophysiological concentration (100pg/ml), over 90 minutes. Our results suggest that CV slows with TNFα exposure relative to control. This CV slowing is associated with reduction in EpC with no significant modulation of GJC. Finally, elevating extracellular calcium ion concentration ($[Ca^{2+}]_o$) in the presence of TNFα, improved both forms of electrical coupling, which could have contributed to increasing CV to control values.

METHODS:

All experimental protocols have been approved by the Institutional Animal Care and Use Committee at Virginia Polytechnic Institute and State University and are in accordance with the NIH Guide for Care and Usage of Laboratory Animals.

Landgendorff Preparation: Male Hartley Guinea Pigs (13-15months old, 1000 – 1300g) were anesthetized by exposure to isoflurane and hearts were excised following thoracotomy as previously described.[20] The heart was then attached to a Langendorff perfusion system and perfused with a solution containing, in mM, 1.25 CaCl2, 140 NaCl, 5.5 NaOH, 4.5 KCl, 5.5 Dextrose, 0.7 MgCl2, 9.9 HEPES, pH 7.4 at 37°C. The atria were removed and the heart was suspended in a bath containing the same perfusate at 37°C. Pressure was kept constant at approximately 50 mmHg.

Optical Mapping: After a 30 minute stabilization period, hearts (n=6 X 3 treatment – Control, TNFα, TNFα+High Calcium) were perfused with 7.5 μM Di-4-ANEPPS for approximately 10 minutes and excess dye was washed out. The electromechanical uncoupler, 2,3-butanedionemonoxime was added to the perfusate to reduce motion. A silver pacing wire was placed on the anterior surface of the heart and a reference wire was introduced at the back of the bath to stimulate the heart with 1V, 1ms stimuli at a BCL of 300ms. The dye was then excited by light at 510 nm and the emitted light was filtered by a 610 nm filter and captured by a Micam Ultima CMOS L-camera as previously described.[19]

Optical data thus collected were analyzed to measure CV – both longitudinal (CV_L) and transverse (CV_T), anisotropic ratio ($AR = CV_L/CV_T$), action potential duration (APD) and rise time

(RT). Briefly, activation times were assigned at the maximum rate of rise of the action potential, which were then fitted to a parabolic surface to determine CV. APD was defined as the time interval between activation time and 90% repolarization. RT was calculated as the time interval between 20 – 80% of the upstroke of the action potential.

After the first recording at t=0, the hearts were either continued to be perfused with normal Tyrode solution (Control) or Tyrode + 100pg/ml TNFα (TNFα treatment). Optical recordings were acquired at 15 minute intervals. Among the TNFα treated hearts, after acquiring the optical recording at t=30 minutes, half the samples were either perfused with solution containing 2.5mM $[Ca^{2+}]_o$ (High Calcium Treatment) in addition to TNFα or continued with 1.25mM $[Ca^{2+}]_o$ as before (TNFα treatment).

Electrocardiography: Volume conducted ECGs from n=6 hearts (X 3 treatments) were recorded by silver chloride electrodes placed in the bath. The signals were sampled at 1000 Hz and filtered to remove noise. Paced QRS duration and QT intervals were measured at every 15 minutes during all three conditions – Control, TNFα and high calcium.

Transmission Electron Microscopy: Tissue was collected from hearts (n=3 X 3 treatment X 15 images per heart) at t=0 minutes and after 90 minutes of Control, TNFα and high calcium treatment, sliced into $1mm^3$ sections, fixed in 2.5% glutaraldehyde overnight at 4°C and then washed and stored in PBS also at 4°C. Samples were then processed for TEM as previously described[19] and imaged using a JEM JEOL1400 Electron Microscope at X150,000 magnification. Fifteen images were acquired per sample, which were then analyzed using ImageJ to measure perinexal width. The average of 6 intermembrane distances between 30 – 105nm away from the edge of the GJ plaque, 15nm apart, are reported as W_P. Data are reported at mean ± standard error.

Western Blotting: Samples (n=3 X 3 treatment) were snap frozen at t=0 or after 90 minutes of Control, TNFα or high calcium treatment and immunoblotting was performed as previously described[21] to determine Cx43 and pCx43 – Ser368 expression. Briefly, samples were homogenized in RIPA lysis buffer (50mM Tris pH 7.4, 150mM NaCl, 1mM EDTA, 1% Triton X-100, 1% sodium deoxycholate, 2mM NaF, 200μM Na2VO34) and electrophoresis was performed to separate proteins which were then transferred onto a PVDF membrane. This was then blocked with 5% BSA for 2 hours at room temperature, followed by incubation with pCx43-

Ser368 primary antibody (1:1000, #3511, Cell Signalling Technologies) overnight at 4°C and secondary antibody (1:5000, Goat Anti-Rabbit HRP, abcam) for 2 hours at room temperature. Protein expression was then quantified by ECL assay using a BioRad Chemidoc MP system. The membranes were then stripped with ReBlot Plus Strong (Millipore) as per manufacture instructions and blocked with 5% milk for 2 hours at room temperature. Membranes were then incubated with primary anitbodies against Cx43 (1:4000, C2619 rabbit, Signma Aldrich) and GAPDH (1:4000, T6199 mouse, Sigma Aldrich) overnight at 4°C, followed by the corresponding secondary anitbodies (both 1:1000, goat anti-mouse AlexaGluor555 and goat anti-rabbit AlexaFluor647) for 2 hours at room temperature. Finally, total Cx43 and GAPDH protein expression was quantified using the BioRad Chemidoc MP system. Total Cx43 was normalized to GAPDH and pCx43 was normalized to total Cx43.

Confocal Immunofluorescence: Ventricular sections (n=3 X 3 treatment) were snap frozen in OCT at t=0 minutes and after 90 minutes of Control, TNFα or high calcium treatment. Samples were sectioned at 5μm thickness onto glass slides and fixed with 2% paraformaldehyde for 5 minutes on a rotator. Slides were then washed and samples were blocked with a solution containing 1% BSA and 1% Triton X-100 in PBS for 1 hour at room temperature. Samples were then incubated with primary antibody against Cx43 (1:4000, C2619 rabbit, Signma Aldrich) and N-Cadherin (1:100, 610920, mouse, BD Biosciences) overnight at 4°C. Slides were then washed and samples were incubated with the corresponding secondary antibodies (1:4000, Goat Anti-Rabbit AlexaFluor 488 and Goat Anti-Mouse AlexaFluor 633) for 2 hours at room temperature. Prolong Gold Antifade (Life Technologies) was then applied to the slides and slide covers were inserted. Slides were cured for approximately 48 hours. Cx43 and N-Cadherin distribution were imaged using a TCS SP8 laser scanning confocal microscope using a X63 oil immersion lens. Images acquired were then analyzed similar to previously described methods.[22,23] Briefly, images were converted to a binary format after thresholding and difference between the Cx43 and N-Cadherin image was determined to identify percent Cx43 that is not colocalized with N-Cadherin. The percent Cx43 colocalized with N-Cadherin was then calculated and normalized to total Cx43.

Statistical Analysis: Single factor or two way ANOVA tests were performed to detect significant differences in the data and Student's t-test was applied as a post hoc analysis. Bonferroni correction was performed as necessary with multiple comparisons. All data are

reported as mean ± standard deviation unless stated otherwise. $p<0.05$ was reported as significant.

RESULTS:

Conduction Velocity - Control vs TNFα:

Hearts were optically mapped during perfusion of tyrode with and without TNFα over a 90 minute period, and representative isochrones maps are illustrated in Figure 4.1A. CV_L, CV_T and AR were calculated and are reported in Figure 4.1B.

In hearts perfused with control tyrode solution, both CV_L and CV_T isotropically increased at 90 minutes with no change in AR. However, in TNFα perfused hearts, CV_L alone increased over time with no change in CV_T which resulted in increased AR. Additionally, CV_T was significantly slower in TNFα perfused hearts relative to control at t=90 minutes. Therefore, the presence of TNFα in the perfusate is associated with anisotropic CV, specifically CV slowing preferentially in the transverse direction and CV speeding preferentially in the longitudinal direction, both of which contributes to increased anisotropy of conduction.

Conduction Velocity - Control vs TNFα + High Calcium:

Next TNFα treated hearts were perfused with a high calcium solution after t=30 minutes to determine if elevating extracellular calcium can rescue CV slowing due to TNFα alone. Percent changes in CV_L, CV_T and AR are reported in Figure 4.2 to compare the effects of TNFα + high calcium to control tyrode perfused hearts.

Once again, percent change in CV_L was significantly larger at t=90 minutes relative to t=0 minutes and was similar between control and hearts with TNFα + high calcium. This suggests that neither TNFα nor high calcium have a significant impact on CV_L. On the other hand, the CV_T curve, illustrated in Figure 4.2B, appeared to separate from control during the initial 30 minutes of just TNFα perfusion. However, elevating calcium restored CV_T back to control values at t=90 minutes and also significantly increased CV_T from t=0 minutes, based on paired comparison. AR changes in control and TNFα + high calcium perfused hearts were not significantly different. Taken together, these data suggest that hearts treated with high calcium in the presence of TNFα behave similar to control hearts.

Action Potential:

TNFα has previously been demonstrated to modulate several ionic currents in the heart.[24-26] In order to determine if the observed CV changes due to TNFα and increased calcium were due to modulation of ionic currents, action potential parameters like RT and APD were calculated. RT is roughly the time taken for the cell to depolarize and an increase in this parameter would correspond to either changes in the excitatory phase of the AP or changes in sodium current. APD changes, on the other hand, are most likely a result of altered calcium currents that maintain the AP plateau or the repolarizing potassium currents.

RT was not significantly different between t=0 and 90 minutes during control or TNFα perfusion. However, increasing calcium was associated with increased RT. This is illustrated in Figure 4.3A and is summarized in Figure 4.3B, left panel.

APD, on the other hand, significantly prolonged over time during control tyrode perfusion but this effect was not observed in the presence of TNFα with normal or high calcium (Figure 4.3B, Right Panel) suggesting that TNFα may be modulating ionic currents that can modulate APD. The optically mapped region on the anterior epicardial surface was then divided into 4 quadrants and APD was compared (Figure 4.3C) to determine if the effects of TNFα and TNFα + high calcium were homogenous. No significant quadrant-based changes in APD were determined.

ECG:

Optical maps were obtained from a roughly 16X16 mm region on the anterior epicardial surface of the heart and the CV and AP parameters reported above are based on changes in this specific region. However, ion channel heterogeneity in the myocardium has been identified to differentially modulate APD and CV which then increases risk for arrhythmias.[27-29] In order to determine, if the reported AP and CV changes were observed at the whole-heart level, ECG parameters were quantified. Specifically, QRS duration and QT interval were measured, which would indicate if the above effect of TNFα on CV and APD, respectively, was globally observed throughout the entire heart. Representative ECGs recorded from control, TNFα and TNFα+ high calcium treated hearts are in Figure 4.4A.

QRS duration is generally used as a surrogate for CV and shorter QRS duration corresponds to faster CV. Changes in QRS duration over time was not significantly different with any of the

treatments. However, QRS duration was significantly prolonged in TNFα perfused hearts relative to control, consistent with CV slowing reported above.

QT interval in control hearts increased over time, consistent with APD prolongation reported above. Interestingly, QT interval was also prolonged in TNFα perfused hearts even though this did not correspond to the lack of difference in anterior epicardial (optical mapping region) APDs reported above. Finally, increasing calcium in the presence of TNFα was associated with reduced QT interval. In short, at the whole heart level, control and TNFα perfused hearts had different QRS durations but similar QT intervals. This is consistent with CV slowing, however, repolarization differences probably do not significantly contribute to this effect.

Perinexus:

Next, the effect of TNFα on proposed modulators of ephaptic coupling like W_P was determined. Specifically, we aimed to determine if TNFα-induced edema also appeared at the perinexal level. No change was observed in W_P over 90 minutes in control tyrode perfused hearts but TNFα significantly increased W_P (Figure 4.5). Addition of high calcium in the presence of TNFα reduced W_P and restored it back to control values. This is consistent with our previous study, where we demonstrated that increasing extracellular calcium decreases perinexal width[19] and suggests that W_P could be an important factor that can account for TNFα induced CV slowing and its rescue by elevated calcium.

Connexin43 expression, phosphorylation and distribution:

Finally, the effect of TNFα perfusion on gap junctional coupling was also tested to determine if TNFα alters Cx43 protein expression, phosphorylation or distribution.

Representative western blots in Figure 4.6A and the summary data in Figure 4.6B illustrate that the expression of total Cx43 and the ratio of pCx43/Cx43 was not significantly altered over 90 minutes with either control tyrode or TNFα perfusion. Interestingly, elevating extracellular calcium significantly increased total Cx43 expression relative to TNFα alone with no change in the ratio of pCx43/Cx43. Therefore, though Cx43 modulation may not contribute to CV slowing by TNFα, improving GJ coupling may be a mechanism that contributes to CV preservation with high calcium.

Next, the distribution of Cx43 was also determined to identify if TNFα causes Cx43 lateralization (Figure 4.7). Although Cx43 expression was not significantly modulated over time with control tyrode perfusion, a significant percent of Cx43 was not colocalized with the intercalated disc protein, N-Cadherin. This suggests that Cx43 relocalizes to the lateral membranes over 90 minutes with control tyrode perfusion. Cx43 distribution in TNFα perfused hearts was more complex. Although, the percent of Cx43 colocalized with N-Cadherin was non-significantly reduced similar to control values at 90 minutes there was a significant regional heterogeneity even within the anterior epicardial (optical mapping region) sample we analyzed. This is evidenced by the large standard deviation bar in the TNFα group. Finally, in TNFα + high calcium perfused hearts, not only was Cx43 expression preserved but so was distribution preserved around the myocyte. Cx43 colocalization with N-Cadherin in TNFα+ high calcium perfused hearts was similar to control at t=0 minutes. Lastly, hearts exposed to 1 hour of no flow ischemia was used as a positive control and in these hearts again, Cx43 colocalization with N-Cadherin was significantly reduced relative to control.

DISCUSSION:

This study focused on the effects of TNFα, a pro-inflammatory cytokine, on CV and determined if acute TNFα exposure was associated with modulation of determinants of CV like ephaptic and gap junctional coupling. Briefly, CV slowing was observed in TNFα perfused hearts relative to control and this was associated with wide W_P but no change in Cx43 expression or phosphorylation. Additionally, Cx43 was heterogeneously remodeled in the area investigated. Elevating extracellular calcium in the presence of TNFα rescued CV by restoring W_P to control values and improving GJ expression, phosphorylation and distribution.

TNFα and Ephaptic Coupling:

TNFα is one of the markers of acute inflammation and has been associated with numerous effects in the body. One major effect of TNFα that affects several regions of the body is vascular leakiness. Elevated levels of TNFα have been demonstrated to increase vascular permeability.[17,18] Increased vascular permeability can then lead to edema formation in tissue.[9] In the heart, edema has been demonstrated to slow CV and increase arrhythmogenesis.[19,20,30]

In addition to interstitial edema, the results of this study indicate that TNFα can increase extracellular volumes in restricted nanodomains along the intercalated discs, like the perinexus. Fluid retention in the bulk interstitial space could be one causative factor that contributes to

TNFα-induced perinexal edema. Another explanation could be the effect of TNFα on structural junction proteins along the intercalated disc. For example, TNFα has been demonstrated to reduce the expression of N-Cadherin[13] and plakoglobin[31] in the heart, which are essential components of the structural junctions that hold the two adjacent membranes together. Loosening of these structures could also be contributing to perinexal edema.

Finally, the same structural proteins have also been demonstrated to have calcium sensitive domains that determine its binding affinity.[32-34] Elevating extracellular calcium could rescue the loss of tight adhesion at these junctions during TNFα exposure, thereby restoring W_P to control values.

TNFα and Gap Junctional Coupling:

The effect of TNFα on Cx43 expression has been extensively studied and the results are numerous and varied, such as no change, Cx43 reduction or increase based on tissue types, concentration of TNFα, period of exposure and other experimental differences between these studies.[12-15] TNFα has also been demonstrated to reduce Cx43 phosphorylation at serine 368 in anterior pituitary cells,[16] which is important in determining Cx43 GJ channel conductance. Cx43 remodeling and lateralization has also been reported in the atria of TNFα overexpressing mice.[14]

In this study, the effect of acute TNFα exposure on Cx43 expression, phosphorylation and distribution were studied. Though total Cx43 expression was reduced in response to 90 minutes of 100pg/ml TNFα, this reduction was not significant and neither was the change in ratio of phosphorylated to total Cx43. Interestingly, the distribution of Cx43 around the myocyte was heterogeneously altered even within the region analyzed here. This finding is similar to that observed in the atria of TNFα overexpressing mice where Cx43 expression was not altered but Cx43 was redistributed all around the myocyte.[14] Heterogeneous Cx43 expression has been previously associated with increased risk of arrhythmias.[27,29]

The interesting finding that elevating extracellular calcium to 2.5mM, as described in this study, increases Cx43 expression in the presence of TNFα is novel and was an unexpected beneficial effect of high calcium. Furthermore, this increase in expression was also associated by increased localization at the intercalated disc. These results suggest that increasing calcium in

the range specified here is improving gap junctional coupling and its specific mechanism requires further investigation.

TNFα and Ionic Currents:

Interventricular heterogeneities in ion channel expression and function in the myocardium is well-established[35-37] and TNFα modulates a variety of these ionic currents.[24-26] In this study, TNFα was associated with local APD prolongation at the anterior epicardium, which did not translate to QT interval widening at the whole heart level. This could be suggesting that TNFα may be heterogeneously modulating ionic currents that can alter APD duration and is consistent with other disease conditions that increase APD heterogeneity in the heart, which can act as a substrate for arrhythmogenesis.[27,38,39] Another interesting finding of this study is that the QT interval shortening induced by elevating calcium was not associated with any changes in APD. This could be further suggesting that TNFα, even in the presence of increased extracellular calcium, differentially modulates APD in various regions of the heart. Taken together, the discrepancy between the APD and QT interval data reported here could be due to ion channel heterogeneity in the myocardium and possibly its differential modulation by TNFα.

Lastly, elevating calcium was also associated with prolonged RT. As mentioned above, an increase in RT could have been the effect of 1) modulating excitatory currents that initially raise the transmembrane potential to threshold for activation of sodium ion channels or 2) modulation of sodium currents which would manifest as changes in the maximum rate of rise of the action potential (dV/dt_{max}). Qualitatively assessing the morphology of the action potential suggests that increased RT could be the effect of slower initial excitation rather than changes in dV/dtmax. It is possible that the increased GJ coupling in these hearts provides a greater sink to the excitatory current, thereby increasing RT. However, this theory requires further investigation.

LIMITATIONS:

Most of the analysis described above involves only the anterior epicardial region of the heart and as evidenced by the differences between local parameters like CV and APD and whole heart parameters like QRS duration and QT interval, TNFα could be having differential effects on cellular functioning in different regions of the heart. Transmural and interventricular differences in several parameters like protein expression and APD have been previously described[24-26] and amplification of these differences by factors like TNFα needs to be completely understood in order to identify therapeutic options. Nevertheless, this study is the first to

highlight that acute TNFα exposure detrimentally affects CV in ventricles and identifies its contributing mechanisms.

Finally, TNFα is one of the many cytokines that is involved in the inflammatory process. Several others like IL-6, IFNγ and IL-8 have all been associated with modulation of several functions in the body. In this study, we focus on understanding the effects of individually modulating a key cytokine like TNFα, which is a crucial step before identifying the cumulative effects of inflammatory factors and unfolding this complex process of myocardial inflammation. Furthermore, TNFα inhibition has also developed as a therapy for diseases associated with inflammation,[40-42] which also amplifies the significance of understanding how TNFα and its inhibitors may affect cardiac functioning.

CONCLUSIONS:

TNFα upregulation during inflammation can have significant effects on cardiac electrophysiology which includes anisotropic conduction slowing. Altering the perfusate calcium composition has been identified as a means to conceal the effects of TNFα on cardiac conduction. Interestingly, increasing extracellular calcium concentration in guinea pig hearts improves both proposed forms of electrical coupling between cardiac myocytes – Ephaptic and Gap junctional coupling. This study provides evidence for the potential role of perfusate ion modulation as a therapy in cardiac diseases.

REFERENCES:

1. Zhang JM, An J. Cytokines, inflammation, and pain. *International Anesthesiology Clinics.* 2007;45:27-37.

2. De Jesus NM, Wang L, Herren AW, et al. Atherosclerosis exacerbates arrhythmia following myocardial infarction: Role of myocardial inflammation. *Heart Rhythm.* 2015;12:169-178.

3. Marchant DJ, Boyd JH, Lin DC, et al. Inflammation in myocardial diseases. *Circulation Research.* 2012;110:126-144.

4. Banka P, Robinson JD, Uppu SC, et al. Cardiovascular magnetic resonance techniques and findings in children with myocarditis: a multicenter retrospective study. *Journal of Cardiovascular Magnetic Resonance.* 2015;17:96.

5. Lurz P, Eitel I, Adam J, et al. Diagnostic performance of CMR imaging compared with EMB in patients with suspected myocarditis. *Journal of American College of Cardiology. Cardiovascular Imaging.* 2012;5:513-524.

6. Zhu Y, Mao Z, Lou D, et al. [The expression of connexin 43 and desmin in viral myocarditis]. *Zhonghua bing li xue za zhi Chinese Journal of Pathology.* 2000;29:288-290.

7. Xu HF, Ding YJ, Shen YW, et al. MicroRNA- 1 represses Cx43 expression in viral myocarditis. *Molecular and Cellular Biochemistry.* 2012;362:141-148.

8. Tang Q, Huang J, Qian H, et al. Antiarrhythmic effect of atorvastatin on autoimmune myocarditis is mediated by improving myocardial repolarization. *Life Sciences.* 2007;80:601-608.

9. Logstrup BB, Nielsen JM, Kim WY, et al. Myocardial oedema in acute myocarditis detected by echocardiographic 2D myocardial deformation analysis. *European Heart Journal Cardiovascular Imaging.* 2015.

10. Matsumori A, Yamada T, Suzuki H, et al. Increased circulating cytokines in patients with myocarditis and cardiomyopathy. *British Heart Journal.* 1994;72:561-566.

11. Intiso D, Zarrelli MM, Lagioia G, et al. Tumor necrosis factor alpha serum levels and inflammatory response in acute ischemic stroke patients. *Neurological Sciences.* 2004;24:390-396.

12. Kimura K, Nishida T. Role of the ubiquitin-proteasome pathway in downregulation of the gap-junction protein Connexin43 by TNF-{alpha} in human corneal fibroblasts. *Investigative Ophthalmology and Visual Science.* 2010;51:1943-1947.

13. Celes MR, Torres-Duenas D, Alves-Filho JC, et al. Reduction of gap and adherens junction proteins and intercalated disc structural remodeling in the hearts of mice submitted to severe cecal ligation and puncture sepsis. *Critical Care Medicine.* 2007;35:2176-2185.

14. Sawaya SE, Rajawat YS, Rami TG, et al. Downregulation of connexin40 and increased prevalence of atrial arrhythmias in transgenic mice with cardiac-restricted overexpression of tumor necrosis factor. *American Journal of Physiology. Heart and Circulatory Physiology.* 2007;292:H1561-1567.

15. Liu L, Gao Z, Zhang L, et al. Temporal dynamic changes of connexin 43 expression in C6 cells following lipopolysaccharide stimulation. *Neural Regeneration Research.* 2012;7:1947-1953.

16. Meilleur MA, Akpovi CD, Pelletier RM, et al. Tumor necrosis factor-alpha-induced anterior pituitary folliculostellate TtT/GF cell uncoupling is mediated by connexin 43 dephosphorylation. *Endocrinology.* 2007;148:5913-5924.

17. Chappell D, Hofmann-Kiefer K, Jacob M, et al. TNF-alpha induced shedding of the endothelial glycocalyx is prevented by hydrocortisone and antithrombin. *Basic Research in Cardiology.* 2009;104:78-89.

18. Hansen PR, Svendsen JH, Hoyer S, et al. Tumor necrosis factor-alpha increases myocardial microvascular transport in vivo. *The American Journal of Physiology.* 1994;266:H60-67.

19. George SA, Sciuto KJ, Lin J, et al. Extracellular sodium and potassium levels modulate cardiac conduction in mice heterozygous null for the Connexin43 gene. *Pflugers Archiv : European Journal of Physiology.* 2015;467:2287-2297.

20. Veeraraghavan R, Lin J, Hoeker GS, et al. Sodium channels in the Cx43 gap junction perinexus may constitute a cardiac ephapse: an experimental and modeling study. *Pflugers Archiv : European Journal of Physiology.* 2015;467:2093-2105.

21. Smyth JW, Hong TT, Gao D, et al. Limited forward trafficking of connexin 43 reduces cell-cell coupling in stressed human and mouse myocardium. *The Journal of Clinical Investigation.* 2010;120:266-279.

22. Smyth JW, Zhang SS, Sanchez JM, et al. A 14-3-3 mode-1 binding motif initiates gap junction internalization during acute cardiac ischemia. *Traffic.* 2014;15:684-699.

23. Yan J, Thomson JK, Wu X, et al. Novel methods of automated quantification of gap junction distribution and interstitial collagen quantity from animal and human atrial tissue sections. *PloS One.* 2014;9:e104357.

24. Guillouet M, Gueret G, Rannou F, et al. Tumor necrosis factor-alpha downregulates sodium current in skeletal muscle by protein kinase C activation: involvement in critical illness polyneuromyopathy. *American Journal of Physiology. Cell Physiology.* 2011;301:C1057-1063.

25. Grandy SA, Fiset C. Ventricular K+ currents are reduced in mice with elevated levels of serum TNFalpha. *Journal of Molecular and Cellular Cardiology.* 2009;47:238-246.

26. Fernandez-Velasco M, Ruiz-Hurtado G, Hurtado O, et al. TNF-alpha downregulates transient outward potassium current in rat ventricular myocytes through iNOS overexpression and oxidant species generation. *American Journal of Physiology. Heart and Circulatory Physiology.* 2007;293:H238-245.

27. Poelzing S, Rosenbaum DS. Altered connexin43 expression produces arrhythmia substrate in heart failure. *American Journal of Physiology. Heart and Circulatory Physiology.* 2004;287:H1762-1770.

28. Kitamura H, Ohnishi Y, Yoshida A, et al. Heterogeneous loss of connexin43 protein in nonischemic dilated cardiomyopathy with ventricular tachycardia. *Journal of Cardiovascular Electrophysiology.* 2002;13:865-870.

29. Gutstein DE, Morley GE, Vaidya D, et al. Heterogeneous expression of Gap junction channels in the heart leads to conduction defects and ventricular dysfunction. *Circulation.* 2001;104:1194-1199.

30. Veeraraghavan R, Salama ME, Poelzing S. Interstitial volume modulates the conduction velocity-gap junction relationship. *American Journal of Physiology. Heart and Circulatory Physiology.* 2012;302:H278-286.

31. Asimaki A, Tandri H, Duffy ER, et al. Altered desmosomal proteins in granulomatous myocarditis and potential pathogenic links to arrhythmogenic right ventricular cardiomyopathy. *Circulation. Arrhythmia and Electrophysiology.* 2011;4:743-752.

32. Vleminckx K, Kemler R. Cadherins and tissue formation: integrating adhesion and signaling. *BioEssays : News and Reviews in Molecular, Cellular and Developmental Biology.* 1999;21:211-220.

33. Wallis S, Lloyd S, Wise I, et al. The alpha isoform of protein kinase C is involved in signaling the response of desmosomes to wounding in cultured epithelial cells. *Molecular Biology of the Cell.* 2000;11:1077-1092.

34. Chitaev NA, Troyanovsky SM. Direct Ca2+-dependent heterophilic interaction between desmosomal cadherins, desmoglein and desmocollin, contributes to cell-cell adhesion. *The Journal of Cell Biology.* 1997;138:193-201.

35. Veeraraghavan R, Poelzing S. Mechanisms underlying increased right ventricular conduction sensitivity to flecainide challenge. *Cardiovascular Research.* 2008;77:749-756.

36. Volders PG, Sipido KR, Carmeliet E, et al. Repolarizing K+ currents ITO1 and IKs are larger in right than left canine ventricular midmyocardium. *Circulation.* 1999;99:206-210.

37. Di Diego JM, Sun ZQ, Antzelevitch C. I(to) and action potential notch are smaller in left vs. right canine ventricular epicardium. *The American Journal of Physiology.* 1996;271:H548-561.

38. Campbell K, Calvo CJ, Mironov S, et al. Spatial gradients in action potential duration created by regional magnetofection of hERG are a substrate for wavebreak and turbulent propagation in cardiomyocyte monolayers. *The Journal of Physiology.* 2012;590:6363-6379.

39. Winter J, Brack KE, Coote JH, et al. Cardiac contractility modulation increases action potential duration dispersion and decreases ventricular fibrillation threshold via beta1-adrenoceptor activation in the crystalloid perfused normal rabbit heart. *International Journal of Cardiology.* 2014;172:144-154.

40. Buyukakilli B, Atici A, Ozkan A, et al. The effect of tumor necrosis factor-alpha inhibitor soon after hypoxia-ischemia on heart in neonatal rats. *Life Sciences.* 2012;90:838-845.

41. Jobe LJ, Melendez GC, Levick SP, et al. TNF-alpha inhibition attenuates adverse myocardial remodeling in a rat model of volume overload. *American Journal of Physiology. Heart and Circulatory Physiology.* 2009;297:H1462-1468.

42. Moe GW, Marin-Garcia J, Konig A, et al. In vivo TNF-alpha inhibition ameliorates cardiac mitochondrial dysfunction, oxidative stress, and apoptosis in experimental heart failure. *American Journal of Physiology. Heart and Circulatory Physiology.* 2004;287:H1813-1820.

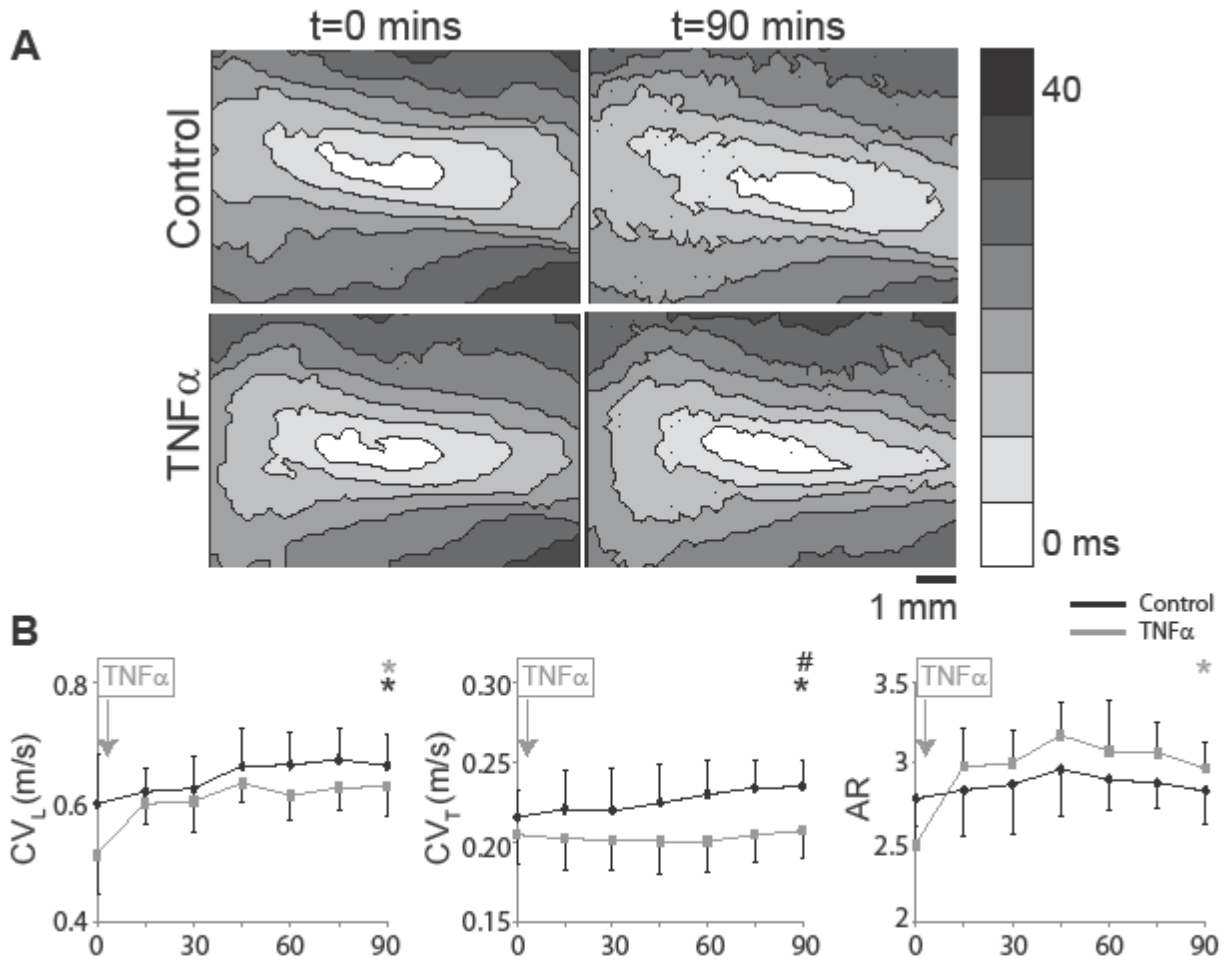

Figure 4.1: Conduction velocity modulation by TNFα A) Representative isochrones maps from control and TNFα perfused hearts at t=0 and 90 minutes. **B)** Summary of CV_L, CV_T and AR values calculated from the optical recordings are graphed. Black and gray * indicates $p< 0.05$ between t=0 and 90 minutes in control and TNFα perfused hearts respectively. # indicates $p<0.05$ between control and TNFα.

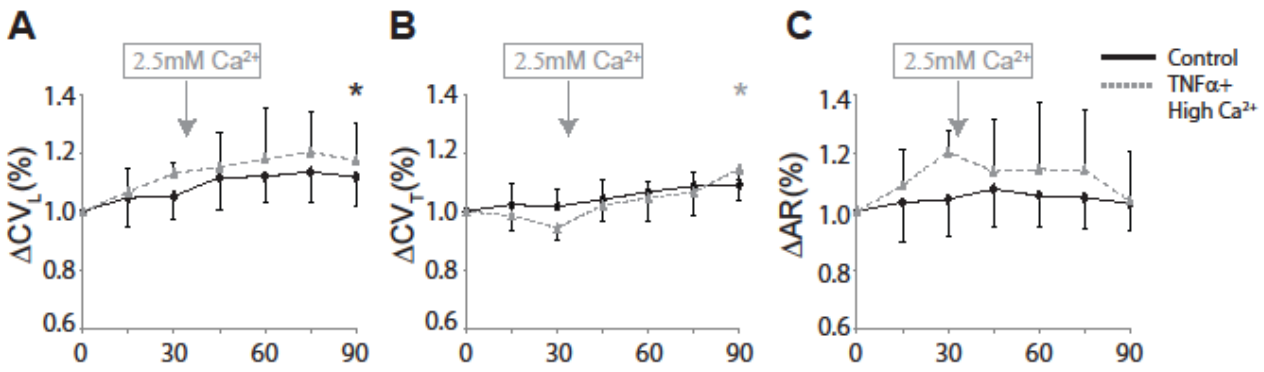

Figure 4.2: Conduction rescue by high calcium A, B, C) Percent change in CV_L, CV_T and AR over time induced by control tyrode perfusion and hearts treated with TNFα + high calcium at t>30 minutes is reported. Black and gray * indicates p< 0.05 between t=0 and 90 minutes in control and TNFα perfused hearts respectively.

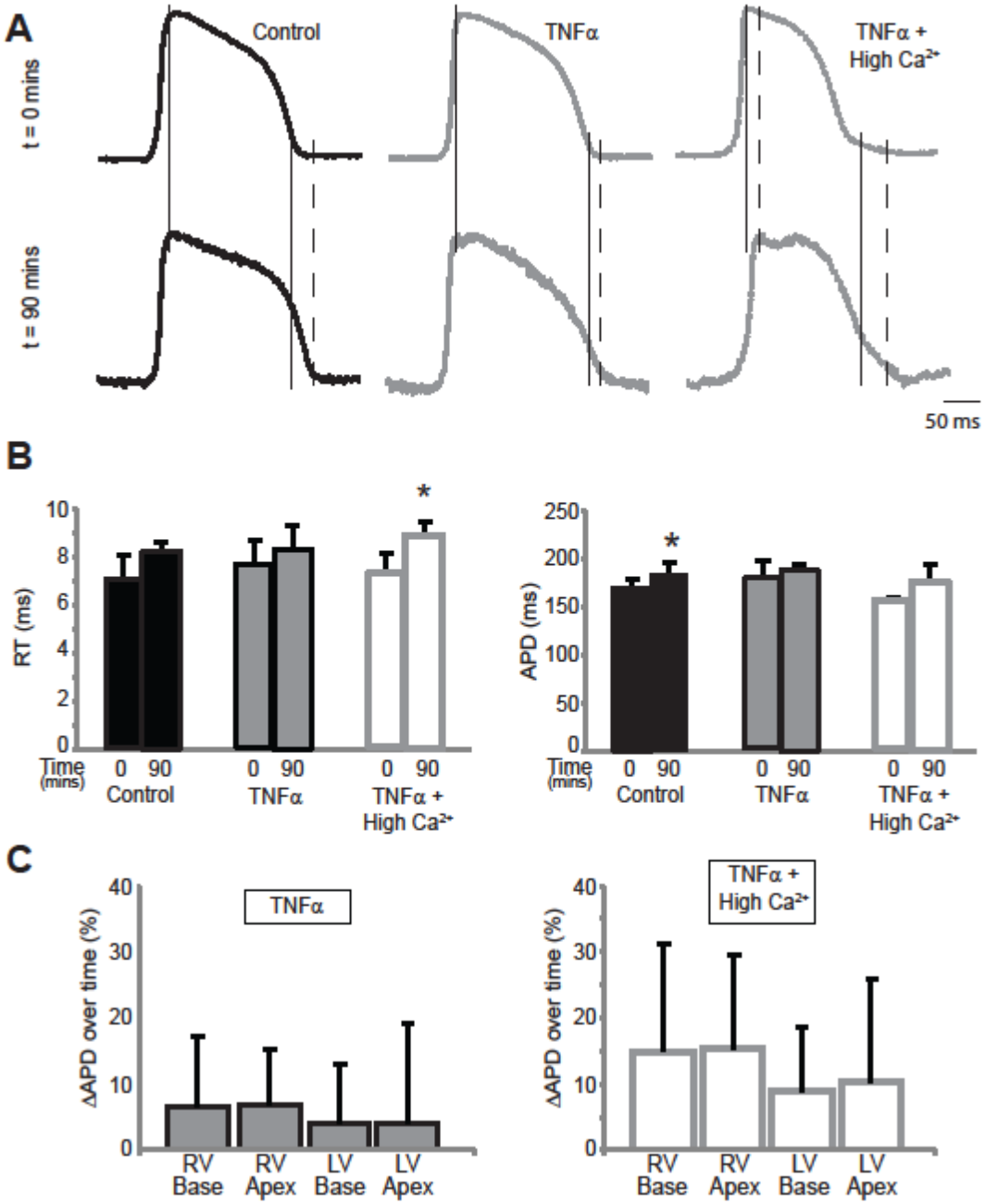

Figure 4.3: Action potential parameters A) Representative action potentials recorded from the anterior epicardium and signal averaged over ~5 beats of control, TNFα and TNFα + high calcium perfused hearts. **B)** Summary of RT (left) and APD (right) calculated from these hearts at t=0 and 90 minutes. **C)** Percent changes in APD from the fours quadrants of the optical mapping region are not significantly different. * indicates $p<0.05$ relative to t=0 minutes.

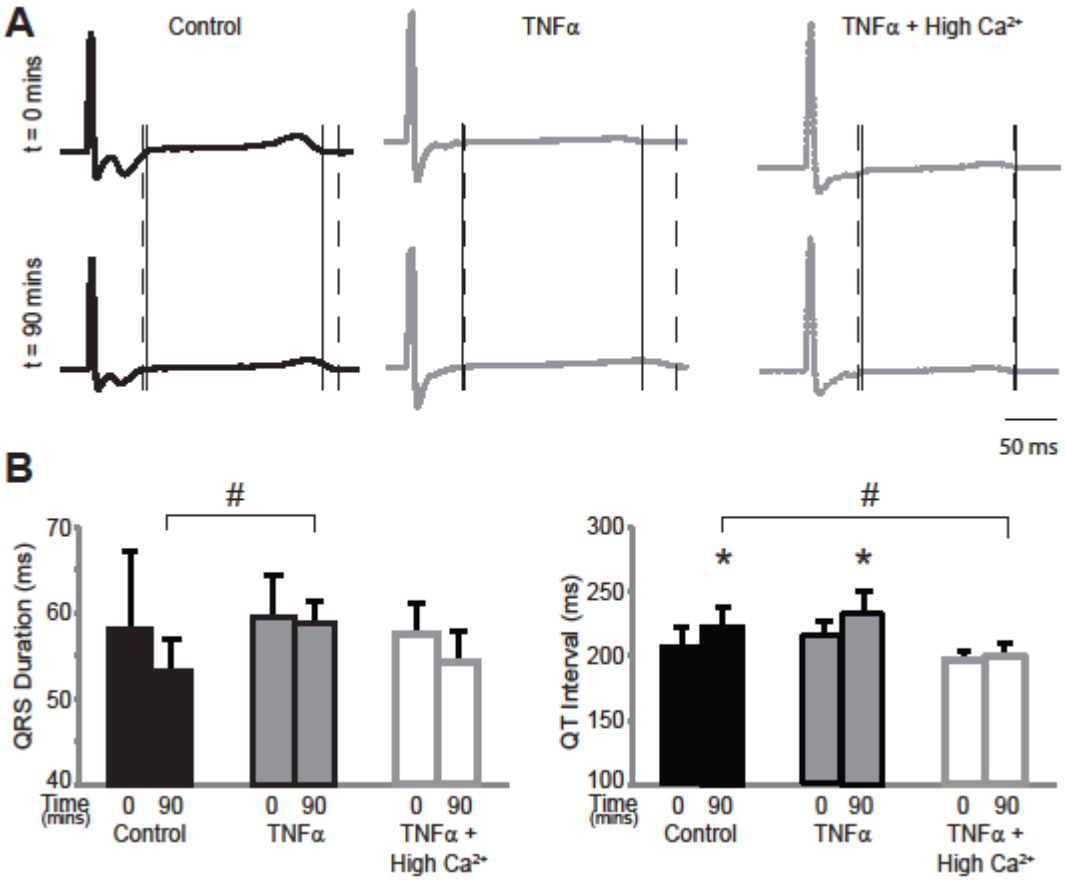

Figure 4.4: ECG parameters A) Representative volume-conducted ECG traces recorded from control, TNFα and TNFα + high calcium perfused hearts. Dashed vertical lines indicate end of QRS and T waves of ECGs from t=0 minutes and Solid vertical lines indicate end of QRS and T waves of ECGs from t=90 minutes. **B)** Summary of QRS duration and QT intervals measuremed from these hearts. * indicates $p<0.05$ relative to t= 0 minutes. # indicates $p<0.05$ relative to control.

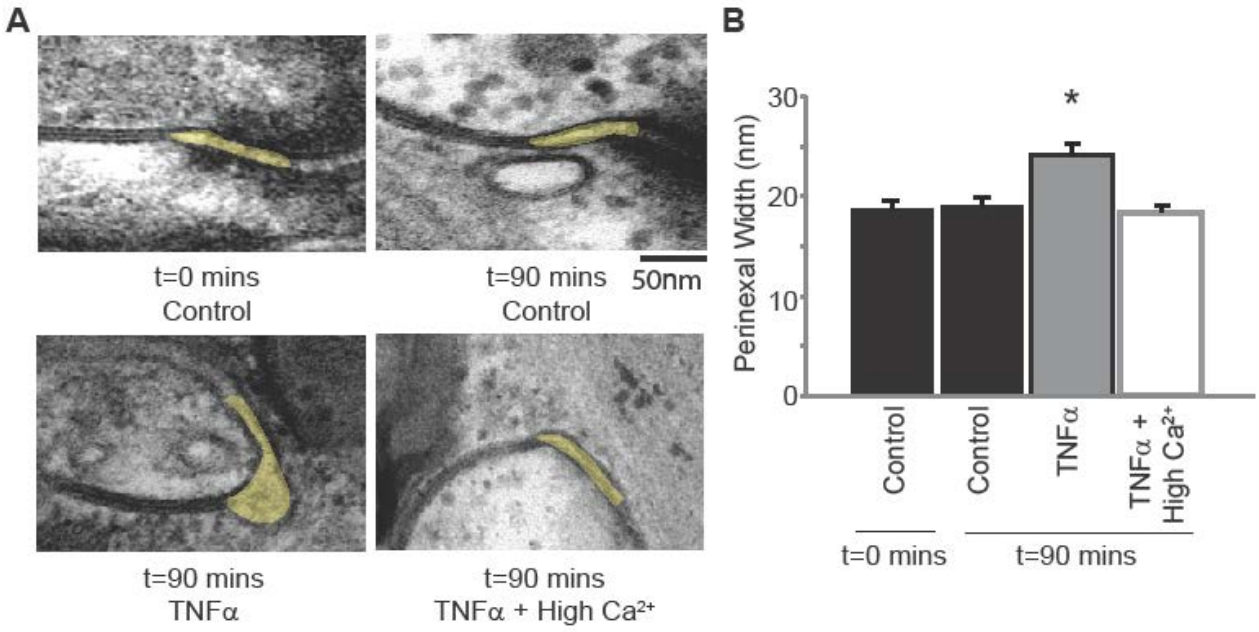

Figure 4.5: Modulation of perinexal width by TNFα A) Electron micrographs of representative perinexi (highlighted in yellow) from hearts treated with control, TNFα or TNFα + high calcium over 90 minutes. **B)** Average perinexal width measured from these hearts. * indicates $p<0.05$ relative to t=0.

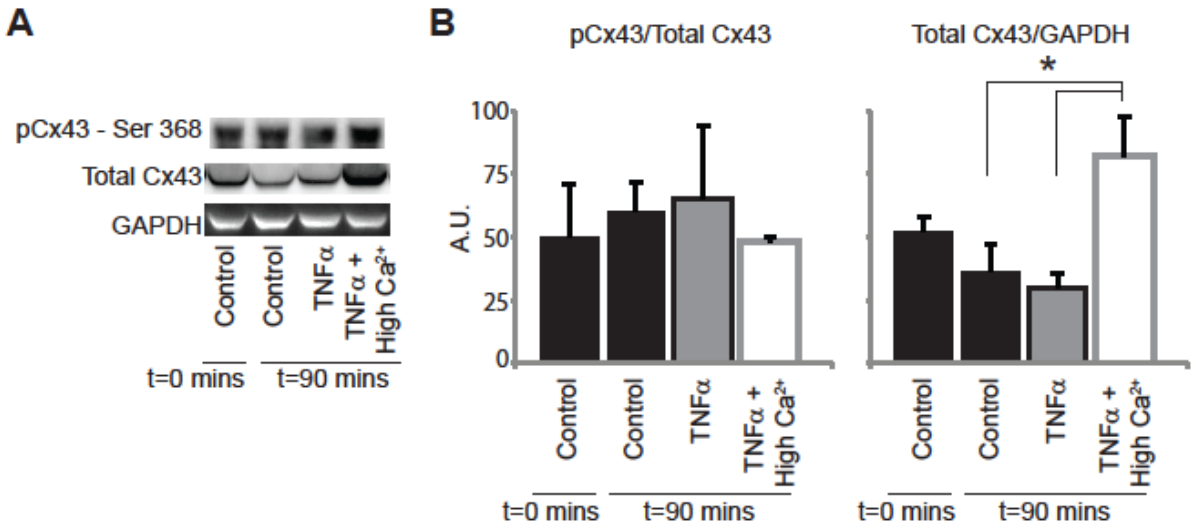

Figure 4.6: Cx43 expression and phosphorylation modulation by TNFα A) Representative images of membranes blotted for total Cx43, Cx43 phosphorylated at Ser368 and GAPDH as a loading control. **B)** Protein expression in hearts treated with control, TNFα and TNFα + high calcium at t=0 and 90 minutes was quantified and is reported.* indicates $p<0.05$.

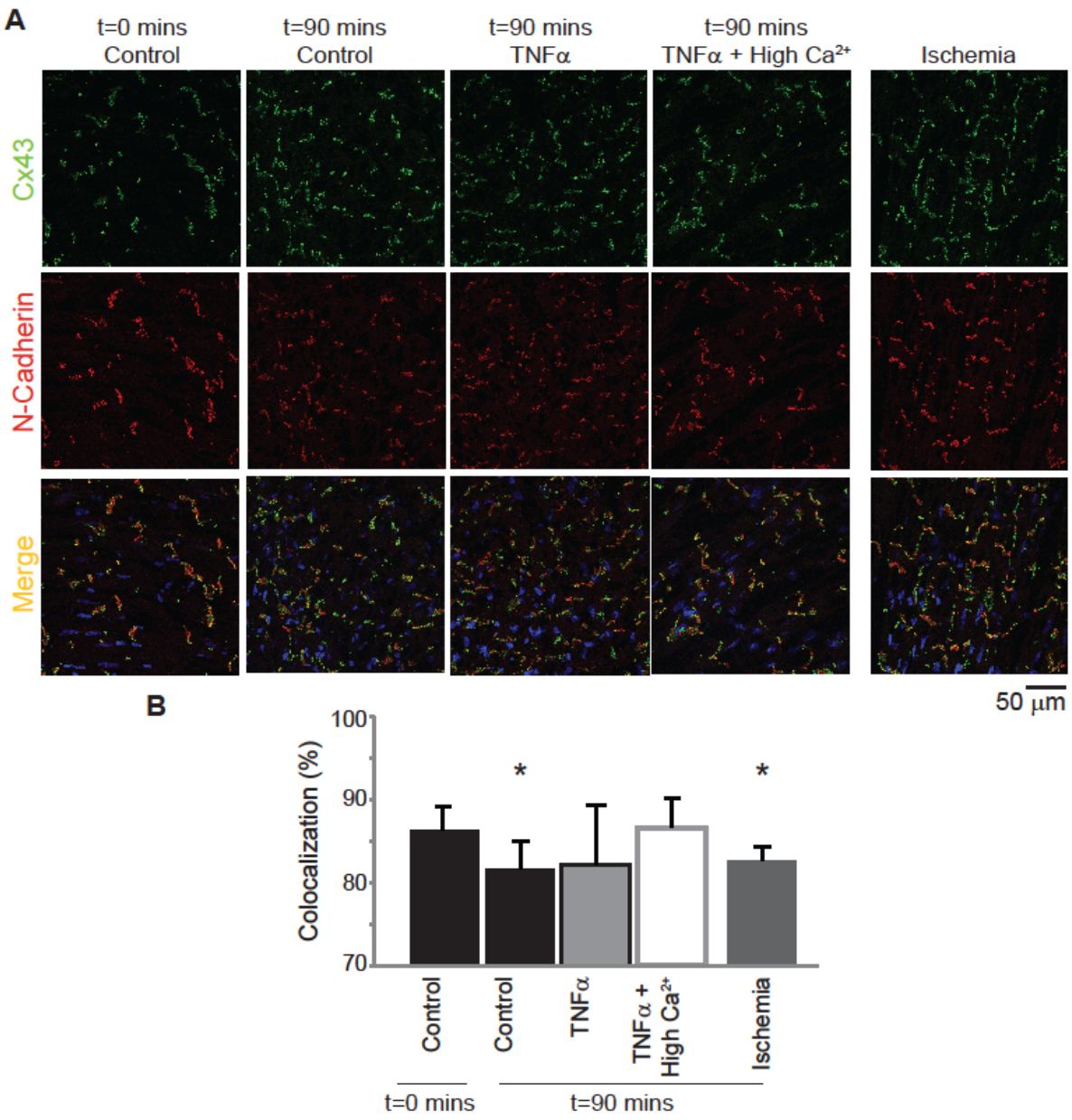

Figure 4.7: Cx43 distribution modulation by TNFα A) Representative samples stained for Cx43 (green) and N-Cadherin (red, to mark the intercalated disc). The colocalization of the two signals is indicated in yellow. Samples from control, TNFα and TNFα + high calcium were compared and 1 hour of no flow ischemia was used as a positive control. **B)** Quantification of percent Cx43 colocalized with N-Cadherin in the various groups listed above. * indicates $p<0.05$ relative to t=0 minutes.

CHAPTER – 5

PERFUSATE COMPOSITION MODULATION DURING METABOLIC ISCHEMIA

INTRODUCTION:

Myocardial ischemia is one of the leading causes of cardiovascular death in the United States and is caused by the lack of sufficient blood supply to cardiac tissue.[1] Complete cessation of blood flow results in death of the tissue and this condition called infarction has been estimated to occur once every 43 seconds in the US.[1] Inability to support the demands of the working myocardium results in several acute changes like gap junctional uncoupling[2,3] and ion channel remodeling[4,5] which can have detrimental functional consequences like slow and aberrant conduction leading to fatal arrhythmias.[6,7]

Modulating gap junctional coupling during ischemia has previously been suggested as a therapeutic option, and several drugs that modulate Cx43 coupling between ventricular myocytes have been proposed to treat cardiac diseases.[8,9] Of these, the peptide - rotigaptide, has been demonstrated to attenuate conduction slowing and prevent arrhythmias during ischemia by preventing Cx43 dephosphorylation.[9-11] However, dephosphorylation is only one method of Cx43 modification during ischemia, which also causes downregulation and lateralization of this protein as well.[12,13] Therefore, though GJ targeting compounds such as rotigaptide may promote Cx43 phosphorylation and theoretically preserve GJ coupling, if total Cx43 is still reduced during ischemia the net effect on GJ coupling is unknown. Additionally, the mechanism of action of rotigaptide is not fully understood as evidenced by its effect on infarct size contrary to what is hypothesized of GJ coupling enhancers.[14,15] Therefore, the effectiveness of such GJ targeting agents for preventing arrhythmias due to ischemia has been questioned.

We hypothesized that modulating an alternate form of electrical coupling between myocytes – ephaptic Coupling (EpC) – can similarly attenuate CV slowing during ischemia. Our previous studies demonstrated that modulators of ephaptic coupling like extracellular ion concentrations in nanodomains like the perinexi within the intercalated disc, as well as the width of this cleft (perinexal width – W_P) can modulate CV.[16,17] Specifically, modulating sodium and potassium concentration was proposed to change the positive charge available in perinexal domains and the rate of depletion of this charge,[16] respectively, while modulating calcium was demonstrated to alter W_P. In this study, EpC was modulated by varying the extracellular sodium ion concentration ($[Na^+]_o$) and extracellular calcium ion concentration ($[Ca^{2+}]_o$). The effects of these physiological variations in ionic composition on conduction and arrhythmogenesis in the heart during ischemia were determined.

Our findings indicate that varying perfusate ion composition has a significant effect on CV and arrhythmogenesis during ischemia without any observable effects during control or reperfusion. Specifically, during ischemia, ***increasing*** $[Na^+]_o$ was associated with faster CV. Elevating $[Na^+]_o$ has been hypothesized to improve EpC in the heart. Additionally, ***wider*** W_P also improved CV during ischemia and prevented arrhythmias. W_P was modulated by lowering $[Ca^{2+}]_o$ as well as by the addition of mannitol, both of which widen the perinexus by different proposed mechanisms. Regardless, both produced similar beneficial conduction effects during ischemia. Taken together, this study provides the first evidence for EpC as a therapeutic target during metabolic ischemia.

METHODS:

All protocols were approved by the Institutional Animal Care and Use Committee at Virginia Tech and are in accordance with the NIH Guide for the Care and Usage of Laboratory Animals.

Langendorff Heart Preparation*:* Male Hartley guinea pigs (13-15 months old) were anesthetized with isoflurane. Hearts were excised following thoracotomy, cannulated to a Langendorff system as previously described[18] and perfused with the various solutions listed in Table 5.1 at 37°C. For description within the text below, low, mid and high $[Ca^{2+}]_o$ refer to 1.25, 1.63 and 2mM $[Ca^{2+}]_o$ in the perfusate and low and high $[Na^+]_o$ refer to 147 and 153mM $[Na^+]_o$ in the perfusate. Hearts were immersed in a bath containing the same solution as it is perfused with, also maintained at 37°C. Perfusion pressure was maintained at 40-50 mmHg.

Ischemia Protocol: The experimental protocol included a 15 min control period followed by 30 mins of ischemia and finally 20 mins of reperfusion. To simulate metabolic ischemia, the solutions described in Table 5.1 were slightly modified; where they were bubbled with an N_2/CO_2 mixture for atleast 1 hour (hypoxia), pH was reduced (acidosis) and no glucose was added (aglycemia). During reperfusion, hearts were perfused with the same perfusate as during control. The ionic composition of the solutions were maintained the same throughout the experiment.

Optical Mapping: After a 30 min stabilization period, hearts were perfused with Di-4-ANEPPS at a concentration of 7.5μM for approximately 10 mins followed by a 10 min washout period. An electromechanical uncoupler 2,3-butanedionemonoxime was used to reduce motion artifacts. The heart was paced by a silver wire placed on the anterior surface of the heart. A reference

wire was placed at the back of the bath. At specific time points, the dye was excited by light passed through a 510 nm filter and the emission light was collected through a 610 nm filter by the Ultima L-type CMOS camera at a sampling rate of 1000 frames/s.

This data was then analyzed as previously described[16] to determine CV, APD and RT. Briefly, a parabolic surface was fit to activation times, defined as the maximum rate of rise of action potential, to determine CV. Action potential duration (APD) was defined as the time interval between activation time and 90% repolarization and rise time (RT) was defined as the time interval between 20 to 80% increase of the upstroke of the action potential.

Transmission Electron Microscopy: Tissue was fixed at various time points in the protocol, in 2.5% glutaraldehyde at 4°C overnight and then transferred to PBS at 4°C. The samples were then processed and sectioned onto copper grids as previously described[16] and imaged using a JEOL JEM1400 electron microscope at 150,000X magnification. Images of the perinexi were then analyzed using ImageJ and perinexal width (W_P) was determined. W_P values at 15nm intervals between 30 – 105nm away from the edge of the GJ plaque were averaged and are reported during control, ischemia and reperfusion. Data are reported as mean ± standard error.

Electrocardiography: Volume conducted ECGs were obtained by silver chloride electrodes placed in the bath. Signals were sampled at 1000Hz and filtered to remove noise.[18]

Western Blotting: Left ventricular tissue were snap frozen at specific time points in the protocol and western blotting was performed as previously described.[19] Briefly, the samples were then homogenized in RIPA lysis buffer (containing 50mM Tris pH 7.4, 150mM NaCl, 1mM EDTA, 1% Triton X-100, 1% sodium deoxycholate, 2mM NaF, 200μM Na2VO34) and protein concentration was normalized by a BCA assay. Electrophoresis was performed to separate proteins which were then transferred to a PVDF membrane, blocked with 5% bovine serum albumin for 2 hrs at room temperature and incubated overnight with primary antibodies against Cx43 phosphorylated at Ser368 (1:1000, #3511, Cell Signalling Technologies), at 4°C. The membranes were then washed and incubated with secondary antibody (1:5000, Goat Anti-Rabbit HRP, abcam) at room temperature for 1 hour. After washing, protein concentration was determined by ECL assay using a BioRad Chemidoc MP system. Membranes were stripped with ReBlot Plus according to manufacturer instructions and was blocked in 5% milk at room temperature for 2 hrs, incubated with primary anitbodies against Cx43 (1:4000, C2619 rabbit,

Signma Aldrich) and N-Cadherin (1:1000, 610920 mouse, BD Biosciences). Membranes were then washed and incubated with secondary antibodies (both 1:1000, goat anti-mouse AlexaGluor555 and goat anti-rabbit AlexaFluor647) and washed again. Membranes were again imaged using the BioRad Chemidoc MP system to determine protein concentration. Total Cx43 was normalized to GAPDH and pCx43 was normalized to total Cx43. Additionally, all values of pCx43/Cx43 and Cx43/N-Cadherin reported are normalized to Control hearts perfused with Solution A to compare between gels.

Statistics: All data are reported as mean ± standard deviation unless stated otherwise. Student's t-tests were performed to determine statistically significant differences between data points and Bonferroni correction was applied to compensate for multiple comparisons. Log Rank tests were performed to determine significant differences in the Kaplan Meier curves.

RESULTS:

Conduction Velocity: Varying $[Na^+]_o$ and $[Ca^{2+}]_o$ in the perfusate did not significantly modulate CV during control or reperfusion phases. However, irrespective of the perfusate used, both CV_L and CV_T significantly slowed during ischemia relative to control. Importantly, the percent change in CV_T during ischemia significantly varied by solutions. Representative isochrones maps of hearts with different CV responses during ischemia are provided in Figure 5.1A and the percent change in CV_T, CV_L and AR from hearts perfused with various solutions are summarized in Figure 5.1B, C and D respectively.

Solution A – high $[Ca^{2+}]_o$ and low $[Na^+]_o$ is used as the reference solution in this study, and all other solutions are reported as changes with respect to this solution. Solution A significantly reduced CV_L and CV_T (0.53±0.04 to 0.43±0.05 and 0.21±0.04 to 0.15±0.03 m/s respectively) during ischemia and increased AR (2.53±0.37 to 2.89±0.37). During reperfusion, both CV_L and CV_T returned to control values.

Solution B – high $[Ca^{2+}]_o$ and high $[Na^+]_o$. We then increased $[Na^+]_o$ to create Solution B and theoretically improve EpC based on our previous study.[16] Interestingly, this solution was highly arrhythmogenic during ischemia and produced ventricular fibrillation (VF) with pacing. Therefore, CV_L and CV_T could not be measured during ischemia. However, conduction returned to pre-ischemic values upon reperfusion.

Solution C – mid $[Ca^{2+}]_o$ and high $[Na^+]_o$. Our previous research suggests that the relationship between conduction and $[Ca^{2+}]_o$ may be biphasic under certain conditions. Therefore we next decreased $[Ca^{2+}]_o$ by 18.5% to create Solution C. To reflect the fact that we decreased $[Ca^{2+}]_o$ later in the study to 1.25mM, we note that Solution C contained mid $[Ca^{2+}]_o$ and high $[Na^+]_o$. This solution slowed CV_L and CV_T (0.55±0.05 to 0.46±0.08 and 0.20±0.03 to 0.15±0.03 m/s respectively) only after prolonged ischemia (20 mins) with no change in AR. Importantly, relative to reference Solution A, CV_T slowing was significantly attenuated only during the early phase of ischemia (-16±6% versus -29±5% of control). However by 30 mins of ischemia, CV slowed to the same extent as Solution A (-27±7% versus -31±5% of control). To summarize, during the early phase of ischemia, decreasing $[Ca^{2+}]_o$ and increasing $[Na^+]_o$ attenuates CV slowing and preserves conduction.

Solution D – low $[Ca^{2+}]_o$ and high $[Na^+]_o$. Since, electrophysiology assessed by cardiac conduction was improved with a solution containing lower $[Ca^{2+}]_o$, we further reduced $[Ca^{2+}]_o$ by 37.5% to create Solution D. Like all solutions, this slowed both CV_L and CV_T (0.59±0.04 to 0.52±0.06 and 0.23±0.02 to 0.19±0.01 m/s respectively) during ischemia without altering AR. However, relative to the reference Solution A, CV slowing during ischemia was significantly attenuated (-20±6% versus -31±5% of control) throughout all 30 minutes of the ischemic protocol. Upon reperfusion, CV_L and CV_T returned to control values. In other words, though Solution D perfused hearts maintained slow CV throughout the ischemic protocol, CV never deteriorated to the extent observed with the other solutions compared here.

Solution E – high $[Ca^{2+}]_o$ and high $[Na^+]_o$ + Mannitol. Finally, to determine if the beneficial effect of reducing $[Ca^{2+}]_o$ was due to its effect on W_P or due to its role in any of the other cellular functions, W_P was increased by the addition of mannitol while maintaining the highest $[Ca^{2+}]_o$. Thus Solution E was simply Solution B (high $[Ca^{2+}]_o$ and high $[Na^+]_o$) + mannitol. Unlike Solution B, which was highly arrhythmogenic, Solution E supported conduction during ischemia, but CV_L and CV_T were still significantly reduced. However, mannitol was incapable of continuously suppressing arrhythmias as preparations became arrhythmogenic after 30 minutes of ischemia. Consequently CV could not be measured at this time point. Despite this, CV slowing trended to attenuate at 20 mins of ischemia relative to Solution A (-20±4% versus -31±5 of control, $p<0.06$). Upon reperfusion, CV_L and CV_T returned to control values. Therefore, prolonged ischemia (30 mins) was associated with slow but still arrhythmogenic conduction during Solution E perfusion, similar to Solution C.

In summary, all solutions were associated with CV slowing during ischemia which then returned to control values during reperfusion. Comparing between solutions, no significant differences were observed during control and reperfusion phases. However, during ischemia, various solutions slowed CV to different extents. Of the solutions compared here, CV slowed most and arrhythmias increased with solutions containing high $[Ca^{2+}]_o$ (Solution A and B). On the other hand, lowering $[Ca^{2+}]_o$ or adding mannitol improved CV. Finally, Solution D with low $[Ca^{2+}]_o$ and high $[Na^{+}]_{o,}$ performed best with the least CV slowing observed during ischemia.

Action Potential: As mentioned above, ischemia has been associated with alterations in the expression and function of several important ion channels. These changes often manifest as alterations in action potential duration (APD) and morphology.[20] For example, ischemia is associated with opening of the ATP sensitive potassium channels (I_{KATP}) which can shorten APD.[21] However, previous studies have demonstrated that ischemia can produce either no change or APD shortening depending on the model of ischemia.[21,22] Additionally, ischemia has also been associated with decreased excitability which manifests as reduced maximum rate of rise of action potential (dV/dtmax).[21,23] Reduced dV/dtmax could in turn result in prolonged rise time (RT) during the upstroke of the action potential. This could be due to the contribution of numerous factors including elevated extracellular potassium ion concentration. In this section, we not only characterize the effects ischemia on the action potential, but we also determine how altering ionic composition, can further modify the action potential.

Action potential duration was measured during control and ischemia from hearts perfused with Solutions A through E as detailed above (Figure 5.2). Representative action potentials are illustrated in Figure 5.2A. In summary, action potential duration was not significantly different when comparing between solutions during the control period or after 30 mins of ischemia (Figure 5.2B, Left Panel). However, when comparing 30 minutes of ischemia to the control period for individual solutions, only one Solution significantly altered action potential duration during ischemia. Specifically, in hearts perfused with Solution A – high $[Ca^{2+}]_o$ and low $[Na^{+}]_o$ – APD prolonged during ischemia relative to control (133.9±15.2 to 154.5±11.6 ms, Figure 5.2C, Left Panel).

Similarly, comparing between solutions, rise time was not significantly different during control or ischemia (Figure 5.2B, Right Panel). Finally, consistent with previous studies,[21,23] all solutions

were associated with increased RT during ischemia relative to control (Figure 5.2C, Right Panel).

Perinexal Width: Representative perinexal electron micrographs are presented in Figure 5.3A and W_P measured between 30 and 105 nm from the edge of the GJ edge was averaged and reported in Figure 5.3B.

During control conditions, all solutions produced similar W_P. During ischemia however, perfusates with lower $[Ca^{2+}]_o$ and/or mannitol (Solutions C, D and E) were associated with a wider W_P relative to Solution A (29.5±4.0, 28.8±3.7 and 28.2±3.3 nm respectively relative to 21.2±0.6nm). Even though such small changes in $[Ca^{2+}]_o$ and mannitol do not have any significant impact on W_P during control conditions here as well as in our previous studies,[17] it has a dramatic effect on W_P during ischemia. These effects during ischemia are on par with the W_P modulation induced by much larger changes in $[Ca^{2+}]_o$ and mannitol during control conditions in the previous studies. Therefore, these results could contribute to a very important therapy for preventing ischemic conduction slowing and arrhythmias without significant impact during healthy conditions.

Importantly, W_P was only transiently increased during ischemia with $[Ca^{2+}]_o$ between 1.25 to 1.63mM evidenced by the finding that W_P returned to control values during reperfusion with Solutions C and D. However, the perfusate with mannitol (Solution E) was still associated with wider W_P after reperfusion (24.5±1.2 nm versus 19.3±0.7 nm). Interestingly, the highly arrhythmogenic Solution B – high $[Ca^{2+}]_o$ and high $[Na^+]_o$, was also associated with wider W_P during reperfusion (25.5±2.2 nm) suggesting that ischemia with this solution may produce some kind of persistent intercalated disc remodeling.

To bring this into context with the CV results above, solutions that widened W_P during ischemia also attenuated CV slowing (Solutions C,D and E).

Cx43 Expression: Representative Western blots of total and Ser368 phosphorylated Cx43 is exhibited in Figure 5.4A along with N-Cadherin which was used as a loading control. The ratio of pCx43/total Cx43 as well as total Cx43/N-Cadherin is summarized in Figure 5.4B in tissue perfused with Solutions A – E during control, ischemia and reperfusion. No significant differences were observed in either the pCx43/total Cx43 ratio or total Cx43 expression due to

varying perfusate composition. Additionally, ischemia and reperfusion did not significantly alter either the pCx43/total Cx43 ratio or total Cx43 expression relative to control. Two results can be interpreted from this data, 1) CV modulation by perfusates during ischemia was probably not an effect of changes in Cx43 coupling and, 2) 30 minutes of the metabolic ischemia model and reperfusion, described in this study, did not significantly modulate Cx43 coupling.

Arrhythmias: All hearts went into asystole during ischemia, and the time to asystole was measured. The Kaplan Meier curves for the different solutions are presented in Figure 5.5. Notably, intrinsic rhythm ceased at approximately the same time with all solutions except for hearts perfused with Solution D. Specifically, hearts perfused with the solution containing low $[Ca^{2+}]_o$ and high $[Na^+]_o$ – Solution D – continued to exhibit intrinsic activity for a significantly longer period relative to Solution A. Note that this was also the perfusate associated with improved CV during ischemia and a wider W_P relative to solution A.

Next, ischemia induced ventricular fibrillation and tachycardia (VF and VT) in hearts was quantified. Solution A with high $[Ca^{2+}]_o$ and low $[Na^+]_o$ never produced VF or VT during ischemia (Figure 5.5B, Upper Panel). In contrast, increasing $[Ca^{2+}]_o$ and $[Na^+]_o$ independent of the presence or absence of mannitol – Solutions B and E – produced significantly more VT/VF. However, VT/VF was significantly reduced with mannitol –Solution B relative to E. Using mid $[Ca^{2+}]_o$ still produced VT/VF, but this was not significantly different from hearts perfused with Solution A. Finally, the solution with the lowest $[Ca^{2+}]_o$ and highest $[Na^+]_o$ – Solution D – used in this study did not produce any arrhythmias similar to Solution A.

In summary, low $[Ca^{2+}]_o$ and high $[Na^+]_o$ – Solution D – was associated with a wide W_P, and this solution performed best, because it attenuated CV slowing, prolonged time to asystole, and did not cause VF/VT during ischemia in guinea pig whole-heart preparations.

DISCUSSION:

This is the first study that demonstrates that the CV response due to myocardial ischemia can be modulated by perfusion composition. Specifically, increasing $[Na^+]_o$ and decreasing $[Ca^{2+}]_o$ performed best during ischemia in terms of greater attenuation of CV slowing while also preventing arrhythmias. Additionally, solutions that were associated with wider perinexi during ischemia were also associated with better outcomes. Finally, the acute beneficial effects of

reducing $[Ca^{2+}]_o$ (<30 mins) was not entirely due to lower metabolic demand, but may also have been due to the effect on increasing perinexal width.

Solutions and Ischemic Conduction:

Ischemia is a complex disease that results in alterations in several parameters that can detrimentally affect cardiac conduction. For example, ischemia has been associated with gap junctional uncoupling, elevated extracellular potassium ion concentration, acidosis, hypoxia and aglycemia among several others effects.[21] Any of these changes could then affect conduction in the heart and cause CV to be slow and aberrant which has been associated with increased arrhythmogenecity.[7] Of these effects, gap junctional uncoupling during ischemia has been extensively studied. Studies have also demonstrated that preserving GJ coupling during ischemia can attenuate CV slowing and prevent arrhythmias.[9,10]

Our previous studies identified an alternative form of electrical coupling between myocytes, ephaptic coupling, that is dependent on extracellular electric fields in nanodomains like the perinexus.[16,17] We determined that altering the solution composition, which may in turn modulate EpC, can vary CV in normal hearts and in diseased hearts with 50% reduced GJ coupling. Additionally, CV in hearts with reduced GJ coupling was more sensitive to changes in solution composition. This concept was applied in this study to determine if promoting EpC in hearts during ischemia can attenuate CV slowing similar to preserving GJ coupling.

As expected, modulating $[Na^+]_o$ and $[Ca^{2+}]_o$ in perfusates did not alter CV during control or reperfusion phases, but the solutions produced significantly different electrophysiologic effects during ischemia. In this study elevating $[Na^+]_o$ and reducing $[Ca^{2+}]_o$ improved conduction possibly by modulating EpC by two different mechanisms.

Extracellular Sodium Ion Concentration:

We previously demonstrated that increasing $[Na^+]_o$ increases CV in mice hearts with 50% reduced GJ and larger W_P.[16] In the present study, in the setting of ischemia, where GJ is reduced, increasing W_P by reducing $[Ca^{2+}]_o$ and increasing $[Na^+]_o$ also preserves CV in a similar manner. Specifically, solutions with elevated $[Na^+]_o$ were associated with faster CV during ischemia. One explanation may be that increasing $[Na^+]_o$ increases sodium current driving force, and a larger current could alter the extracellular potential (in nanodomains like the perinexi) faster. This then results in faster ephaptic transmission of impulses from one myocyte to its

downstream neighbor. However, one might expect this phenomenon to be even faster under conditions producing narrower W_P.

Extracellular Calcium Ion Concentration:

Our previous studies demonstrated that increasing $[Ca^{2+}]_o$ can reduce W_P in mice which we hypothesize promotes EpC and increases CV.[16] However, we also demonstrated in mice that during conditions associated with disease like hyponatremia, the role of $[Ca^{2+}]_o$ in modulating CV is more complex. Specifically, in our previous mouse study, we demonstrated that while increasing $[Ca^{2+}]_o$ increased CV during control conditions, increasing $[Ca^{2+}]_o$ slowed CV during hyponatremia. Therefore, the findings in the present study are consistent with a theoretical concept of ephaptic coupling called self-attenuation.

Briefly, ephaptic self-attenuation occurs when the driving force of the sodium current is greatly reduced in clefts within the intercalated disc, which then results in the slowing of ephaptic transmission of electrical impulses between neighboring myocytes. This theory has been predicted by several mathematical models,[24-26] which demonstrated greatly reducing W_P at low GJ coupling, slows CV. Experimental evidence that supports this concept was also demonstrated in our previous study in mice. In this study, perfusates with narrower W_P during ischemia-induced GJ uncoupling were associated with greater CV slowing consistent with the theoretical predictions of ephaptic self-attenuation.

Alternative Mechanisms:

Calcium is a key modulator of several cellular functions in the heart,[27] and it could be argued that one mechanism by which reducing $[Ca^{2+}]_o$ is beneficial during ischemia is due to reduced metabolic demand. While this may be true, our data suggests that the effect of $[Ca^{2+}]_o$ modulated W_P could also contribute to acute CV preservation during ischemia. For example, while Solution B (high $[Ca^{2+}]_o$) is highly arrhythmogenic, Solution E (high $[Ca^{2+}]_o$ + Mannitol) reduces arrhythmias and also attenuates CV slowing similar to reducing $[Ca^{2+}]_o$ in Solutions C and D.

It has also been demonstrated that altering $[Ca^{2+}]_o$ can affect other determinants of CV like membrane excitability and GJ coupling.[28-30] Changes in membrane excitability can be determined by measuring RT of the action potential upstroke and prolonged RT would denote reduced excitability as the myocyte takes longer to depolarize. However, we provide evidence

here that physiological changes in ionic composition as in this study does not significantly alter RT during control or ischemic conditions.

Additionally, the data also suggests that this change in ionic composition does not significantly modulate Cx43 expression or phosphorylation suggesting that GJ coupling is not measurably modulated by the solutions. Furthermore, Cx43 expression and phosphorylation was not altered by either ischemia or reperfusion. This is consistent with previous studies that have demonstrated that pCx43 expression in ventricular myocytes decrease only after 8 hours of exposure to hypoxia and reduced glucose and no significant differences are observed at earlier time points.[31] This study also demonstrated that hypoxia alone increases pCx43 expression. On the other hand, other studies have also reported reduction in pCx43 induced by acidosis.[32,33] Additionally, a dynamic response in Cx43 expression and phosphorylation during ischemia has also been previously reported where significant reduction in Cx43 was reported much beyond the ischemic time course of the current study (30 minutes compared to >2 hours).[2,3] Therefore, several results have emerged that report different Cx43 expression and phosphorylation during ischemia. However, the combined effects of the three factors that contribute to our model of metabolic ischemia – acidosis, aglycemia and hypoxia over 30 minutes is not clear from these previous studies. The present study demonstrates that 30 minutes of metabolic ischemia with various extracellular ionic compositions do not produce significant changes in Cx43 expression or phosphorylation.

Therefore, while $[Ca^{2+}]_o$ may have innumerable effects on cellular processes during control and ischemic conditions, we provide evidence that simply modulating W_P during ischemia, which can be accomplished by reducing $[Ca^{2+}]_o$ or perfusing mannitol can profoundly alter CV dependence on $[Na^+]_o$. This study provides continued evidence that $[Na^+]_o$ and W_P are modulators of EpC particularly under conditions of reduced GJ coupling.

LIMITATIONS:

The W_P values reported here are different from those we previously reported in control guinea pig heart preparations[17] with similar, but not identical Langendorff perfusates. These differences may be due to experimental differences such as the fact that tissue in this study was processed by a different electron microscopist using different fixation, embedding, and sectioning protocols for use in a different EM facility. However, the W_P values from guinea pig hearts reported here are similar to those from our previous study in mice[16] that were processed identically to the

tissue in this manuscript. More importantly, mannitol in this study still expanded the perinexus, consistent with mannitol induced perinexal expansion in the previous study.[17] On a final note, these and previous data demonstrate that W_P can be modulated by a variety of conditions and affect cardiac conduction particularly during the loss of functional gap junction coupling.

CONCLUSIONS:

Extracellular ionic composition is a very important determinant of the conduction response during myocardial ischemia. Solutions that promote ephaptic coupling with elevated $[Na^+]_o$ and wider perinexi attenuates conduction slowing during ischemia and reduces arrhythmia incidences. This study is the first to demonstrate that simply altering extracellular ionic composition is a possible therapy for conduction mediated arrhythmias during myocardial ischemia.

REFERENCES:

1. Mozaffarian D, Benjamin EJ, Go AS, et al. Heart disease and stroke statistics--2015 update: a report from the American Heart Association. *Circulation.* 2015;131:e29-322.

2. Matsushita T, Takamatsu T. Ischaemia-induced temporal expression of connexin43 in rat heart. *Virchows Archiv : An International Journal of Pathology.* 1997;431:453-458.

3. Huang XD, Sandusky GE, Zipes DP. Heterogeneous loss of connexin43 protein in ischemic dog hearts. *Journal of Cardiovascular Electrophysiology.* 1999;10:79-91.

4. Nattel S, Maguy A, Le Bouter S, et al. Arrhythmogenic ion-channel remodeling in the heart: heart failure, myocardial infarction, and atrial fibrillation. *Physiological Reviews.* 2007;87:425-456.

5. Pinto JM, Boyden PA. Electrical remodeling in ischemia and infarction. *Cardiovascular Research.* 1999;42:284-297.

6. Janse MJ, Kleber AG, Capucci A, et al. Electrophysiological basis for arrhythmias caused by acute ischemia. Role of the subendocardium. *Journal of Molecular and Cellular Cardiology.* 1986;18:339-355.

7. Wit AL, Hoffman BF, Cranefield PF. Slow conduction and reentry in the ventricular conducting system. I. Return extrasystole in canine Purkinje fibers. *Circulation Research.* 1972;30:1-10.

8. Sun B, Qi X, Jiang J. Heptanol decreases the incidence of ischemia-induced ventricular arrhythmias through altering electrophysiological properties and connexin 43 in rat hearts. *Biomedical Reports.* 2014;2:349-353.

9. Kjolbye AL, Dikshteyn M, Eloff BC, et al. Maintenance of intercellular coupling by the antiarrhythmic peptide rotigaptide suppresses arrhythmogenic discordant alternans. *American Journal of Physiology. Heart and Circulatory Physiology.* 2008;294:H41-49.

10. Eloff BC, Gilat E, Wan X, et al. Pharmacological modulation of cardiac gap junctions to enhance cardiac conduction: evidence supporting a novel target for antiarrhythmic therapy. *Circulation.* 2003;108:3157-3163.

11. Xing D, Kjolbye AL, Nielsen MS, et al. ZP123 increases gap junctional conductance and prevents reentrant ventricular tachycardia during myocardial ischemia in open chest dogs. *Journal of Cardiovascular Electrophysiology.* 2003;14:510-520.

12. Hatanaka K, Kawata H, Toyofuku T, et al. Down-regulation of connexin43 in early myocardial ischemia and protective effect by ischemic preconditioning in rat hearts in vivo. *Japanese Heart Journal.* 2004;45:1007-1019.

13. Sanchez JA, Rodriguez-Sinovas A, Fernandez-Sanz C, et al. Effects of a reduction in the number of gap junction channels or in their conductance on ischemia-reperfusion arrhythmias in isolated mouse hearts. *American Journal of Physiology. Heart and Circulatory Physiology.* 2011;301:H2442-2453.

14. Haugan K, Marcussen N, Kjolbye AL, et al. Treatment with the gap junction modifier rotigaptide (ZP123) reduces infarct size in rats with chronic myocardial infarction. *Journal of Cardiovascular Pharmacology.* 2006;47:236-242.

15. Hennan JK, Swillo RE, Morgan GA, et al. Rotigaptide (ZP123) prevents spontaneous ventricular arrhythmias and reduces infarct size during myocardial ischemia/reperfusion injury in open-chest dogs. *The Journal of Pharmacology and Experimental Therapeutics.* 2006;317:236-243.

16. George SA, Sciuto KJ, Lin J, et al. Extracellular sodium and potassium levels modulate cardiac conduction in mice heterozygous null for the Connexin43 gene. *Pflugers Archiv : European Journal of Physiology.* 2015;467:2287-2297.

17. Veeraraghavan R, Lin J, Hoeker GS, et al. Sodium channels in the Cx43 gap junction perinexus may constitute a cardiac ephapse: an experimental and modeling study. *Pflugers Archiv : European Journal of Physiology.* 2015;467:2093-2105.

18. Veeraraghavan R, Salama ME, Poelzing S. Interstitial volume modulates the conduction velocity-gap junction relationship. *American Journal of Physiology. Heart and Circulatory Physiology.* 2012;302:H278-286.

19. Smyth JW, Hong TT, Gao D, et al. Limited forward trafficking of connexin 43 reduces cell-cell coupling in stressed human and mouse myocardium. *The Journal of Clinical Investigation.* 2010;120:266-279.

20. Weiss J, Shine KI. [K+]o accumulation and electrophysiological alterations during early myocardial ischemia. *The American Journal of Physiology.* 1982;243:H318-327.

21. Shaw RM, Rudy Y. Electrophysiologic effects of acute myocardial ischemia: a theoretical study of altered cell excitability and action potential duration. *Cardiovascular Research.* 1997;35:256-272.

22. Stengl M, Ledvinova L, Chvojka J, et al. Effects of clinically relevant acute hypercapnic and metabolic acidosis on the cardiovascular system: an experimental porcine study. *Critical Care.* 2013;17:R303.

23. Franz MR, Flaherty JT, Platia EV, et al. Localization of regional myocardial ischemia by recording of monophasic action potentials. *Circulation.* 1984;69:593-604.

24. Kucera JP, Rohr S, Rudy Y. Localization of sodium channels in intercalated disks modulates cardiac conduction. *Circulation Research.* 2002;91:1176-1182.

25. Mori Y, Fishman GI, Peskin CS. Ephaptic conduction in a cardiac strand model with 3D electrodiffusion. *Proceedings of the National Academy of Sciences of the United States of America.* 2008;105:6463-6468.

26. Lin J, Keener JP. Microdomain effects on transverse cardiac propagation. *Biophysical Journal.* 2014;106:925-931.

27. Zarain-Herzberg A, Fragoso-Medina J, Estrada-Aviles R. Calcium-regulated transcriptional pathways in the normal and pathologic heart. *International Union of Biochemistry and Molecular Biology Life.* 2011;63:847-855.

28. Maurer P, Weingart R. Cell pairs isolated from adult guinea pig and rat hearts: effects of [Ca2+]i on nexal membrane resistance. *Pflugers Archiv : European Journal of Physiology.* 1987;409:394-402.

29. Kagiyama Y, Hill JL, Gettes LS. Interaction of acidosis and increased extracellular potassium on action potential characteristics and conduction in guinea pig ventricular muscle. *Circulation Research.* 1982;51:614-623.

30. Tan HL, Kupershmidt S, Zhang R, et al. A calcium sensor in the sodium channel modulates cardiac excitability. *Nature.* 2002;415:442-447.

31. Turner MS, Haywood GA, Andreka P, et al. Reversible connexin 43 dephosphorylation during hypoxia and reoxygenation is linked to cellular ATP levels. *Circulation Research.* 2004;95:726-733.

32. Jozwiak J, Dietze A, Grover R, et al. Desipramine prevents cardiac gap junction uncoupling. *Naunyn-Schmiedeberg's Archives of Pharmacology.* 2012;385:1063-1075.

33. Matsumura K, Mayama T, Lin H, et al. Effects of cyclic AMP on the function of the cardiac gap junction during hypoxia. *Experimental and Clinical Cardiology.* 2006;11:286-293.

Table 5.1: Ionic Composition of the solutions used in the Ischemia study is listed in mM.

	Solution A	Solution B	Solution C	Solution D	Solution E
$CaCl_2$	2.0	2.0	1.625	1.25	2.0
NaCl	141.5	147.5	147.5	147.5	147.5
NaOH	5.5	5.5	5.5	5.5	5.5
KCl	6.9	6.9	6.9	6.9	6.9
$MgCl_2$	0.7	0.7	0.7	0.7	0.7
Glucose	5.5	5.5	5.5	5.5	5.5
HEPES	9.99	9.99	9.99	9.99	9.99
BDM	7.5	7.5	7.5	7.5	7.5
Mannitol	0	0	0	0	45.3

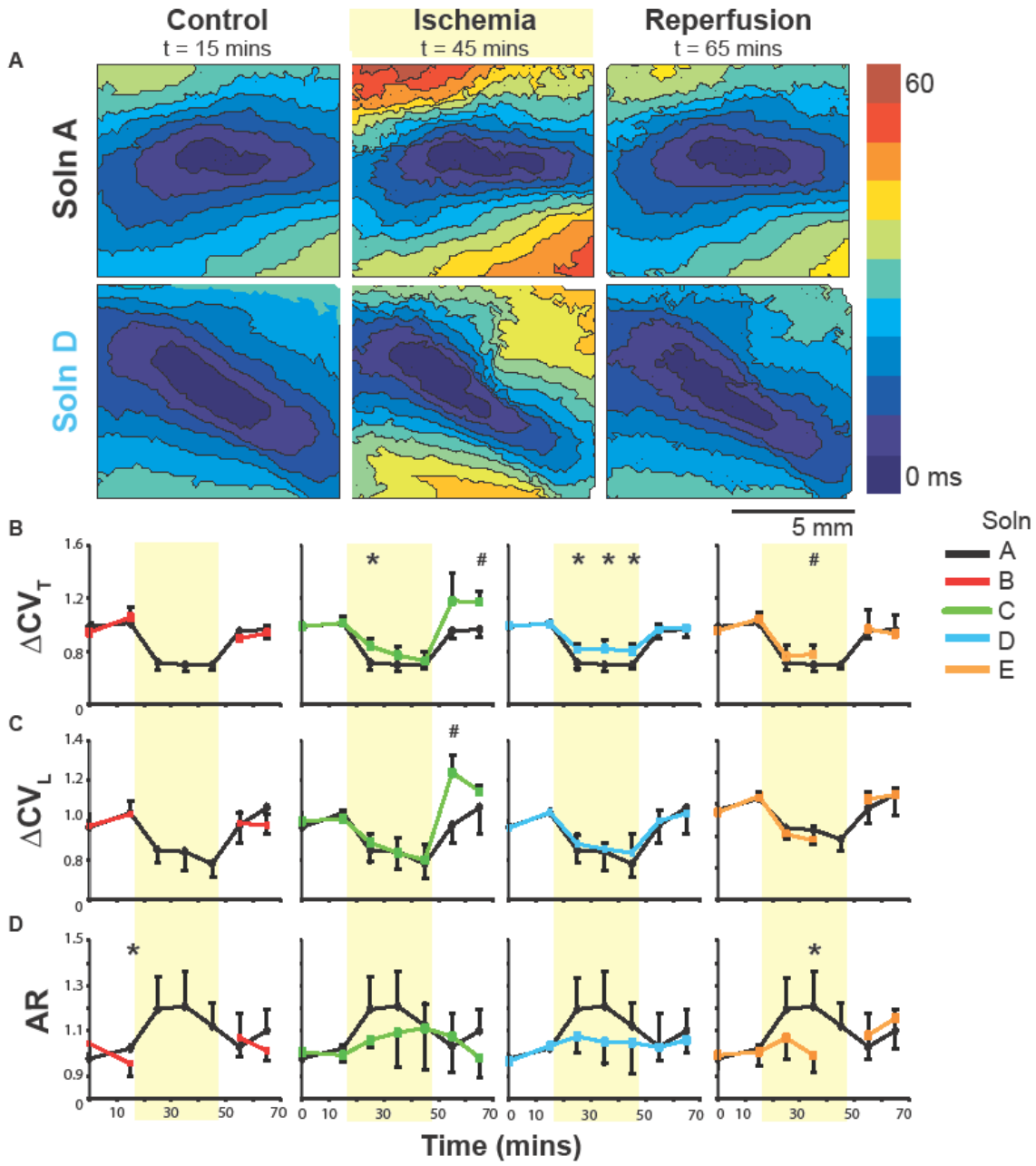

Figure 5.1: Conduction Velocity during Ischemia and Reperfusion. A) Representative isochrones maps of conduction in hearts perfused with Solution A and D where Solution A has most CV slowing and Solution D has least CV slowing. B,C,D) Percent change in CV_T, CV_L and AR in hearts perfused with Solutions A through E. * indicates $p<0.05$ relative to Solution A.

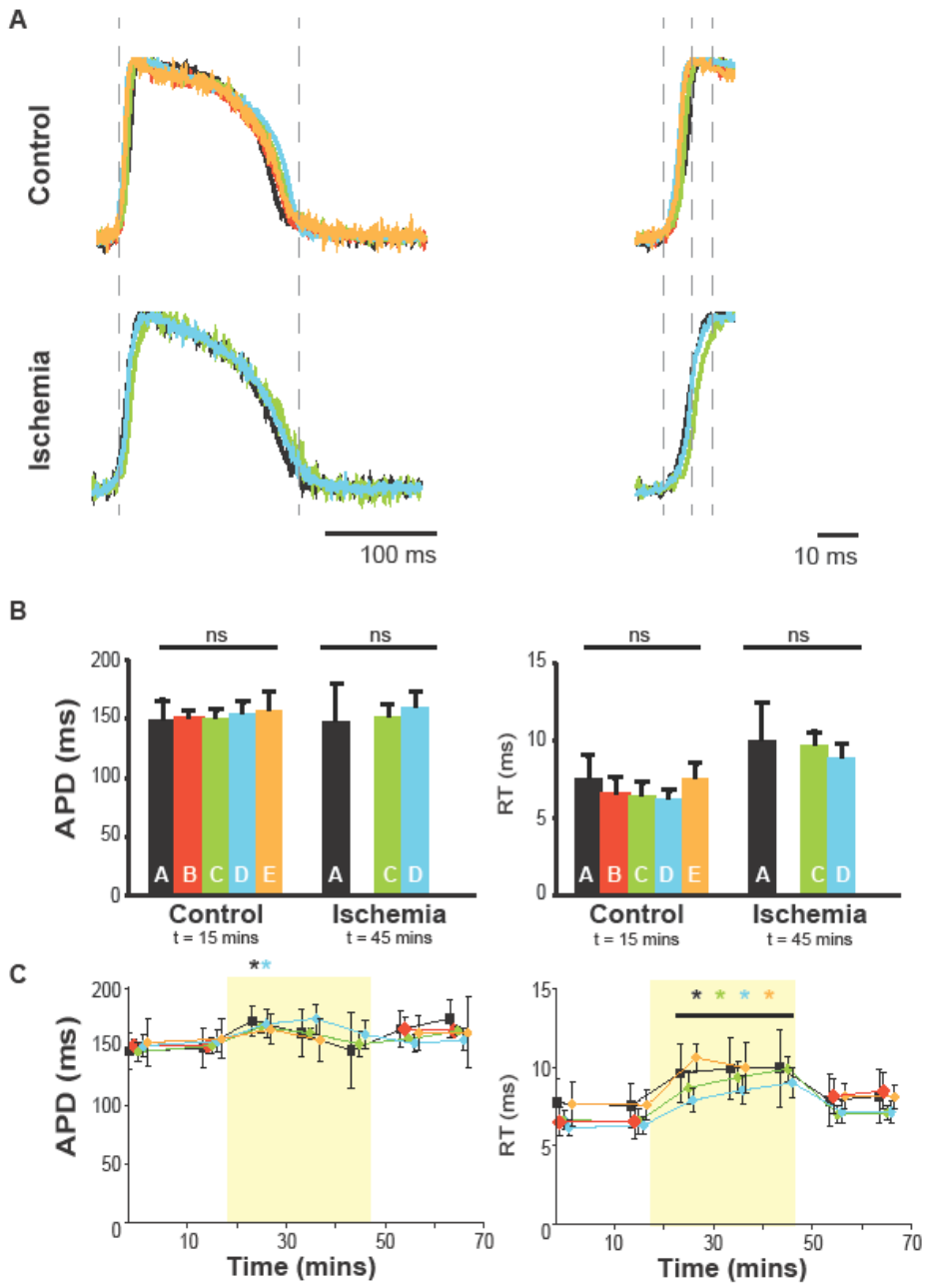

Figure 5.2: Action Potential Characteristics. A) Representative action potential and the zoomed in upstroke of the action potential from hearts perfused with various solutions. B) Summary of APD and RT during control (t=0) and ischemia (t=45) compared by solutions. C) Time response of APD and RT from hearts perfused with various solutions. * indicates $p<0.05$ relative to t=0.

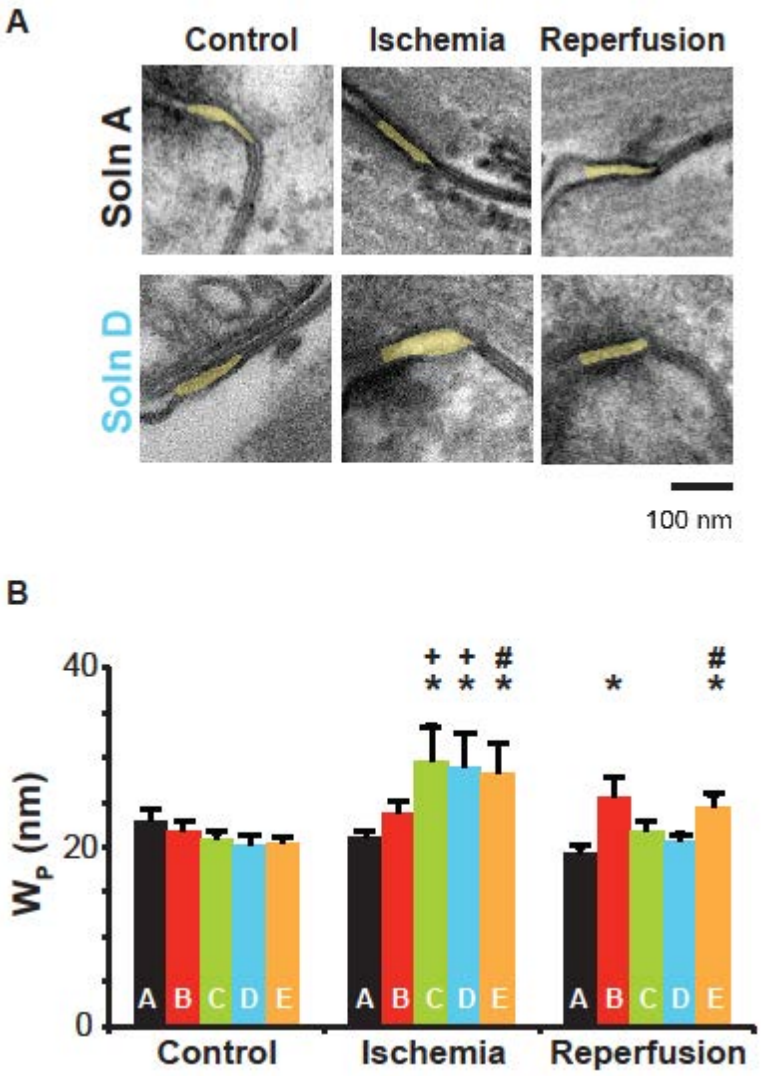

Figure 5.3: Perinexal Width during Ischemia and Reperfusion. A) Representative electron micrographs of perinexi from hearts perfused with solution A and D where Solution A demonstrates no change in W_P during ischemia and reperfusion while Solution D perfused hearts demonstrate W_P widening during ischemia and return to control during reperfusion. B) Summary of W_P values averaged over a distance of 30 to 105 nm away from the edge of the GJ plaque. * indicates $p<0.05$ relative to Solution A

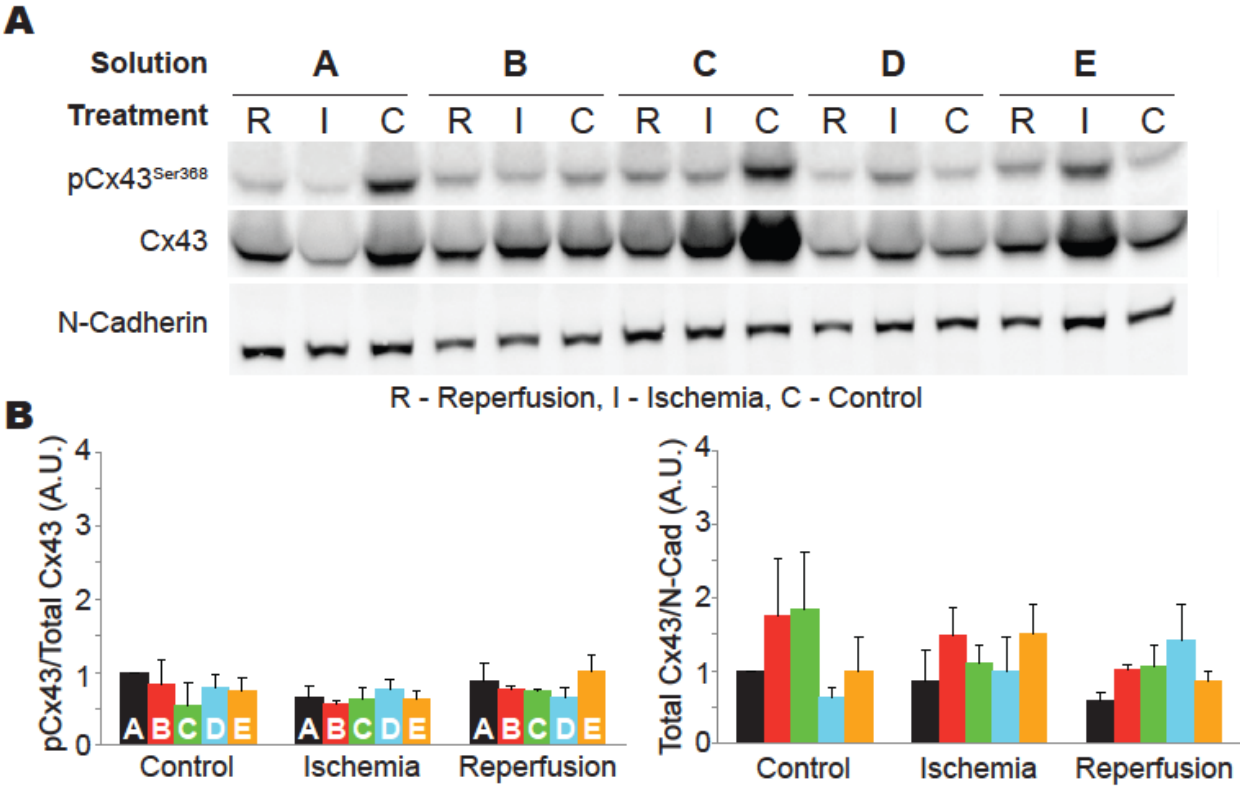

Figure 5.4: Connexin43 expression and phosphorylation. A) Representative Western blots probed for Cx43 phosphorylated at Ser368, total Cx43 and N-Cadherin (loading control) is exhibited during Control, Ischemia and Reperfusion conditions from hearts perfused with Solutions A through E. **B)** Summary of pCx43/Total Cx43 as well as Total Cx43/N-Cadherin ratio normalized to Control hearts perfused with Solution A.

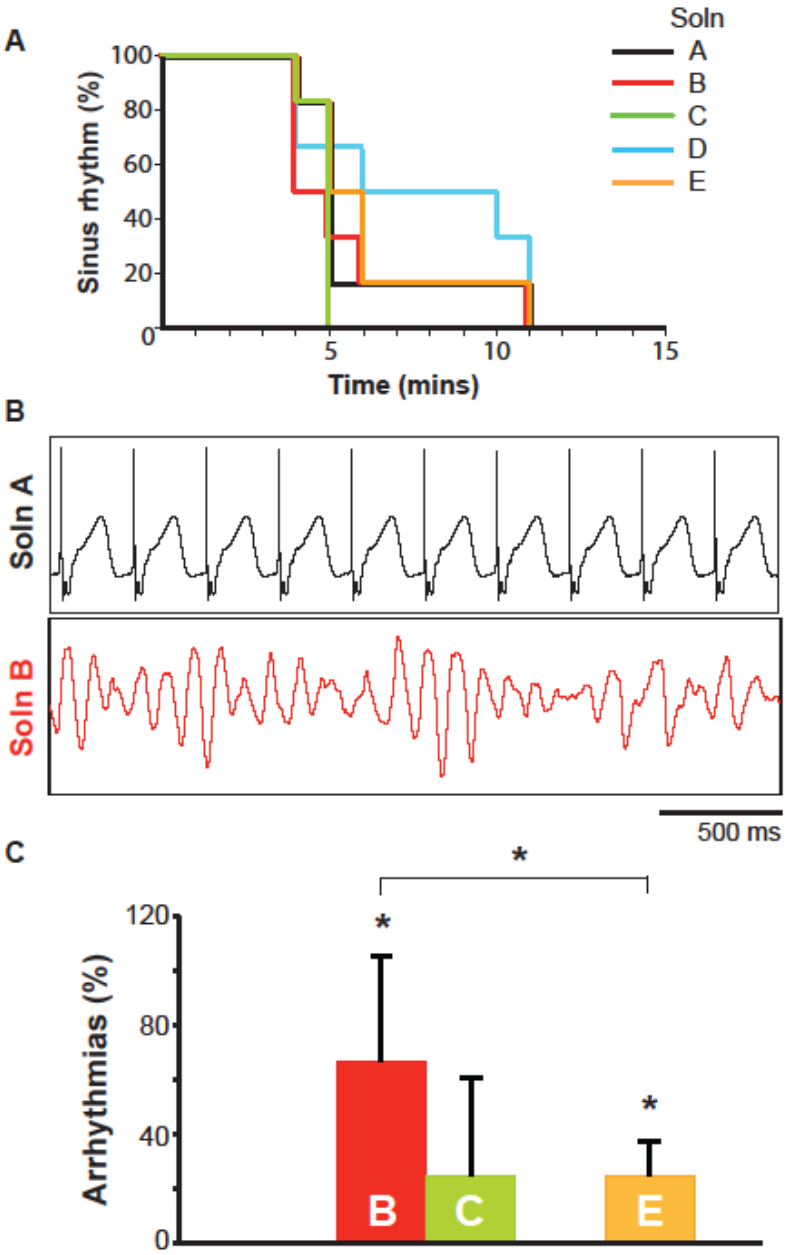

Figure 5.5: Arrhythmias. A) Kaplan Meier curve demonstrating the time to asystole in hearts perfused with various solutions. B) Representative ECGs demonstrating normal paced rhythm (Upper Panel) during solution A perfusion and ventricular fibrillation during Solution B perfusion. C) Summary of arrhythmia incidences in hearts perfused with various solutions. * indicates $p<0.05$ relative to Solution A.

CHAPTER - 6

SUMMARY AND FUTURE DIRECTIONS

Great strides have been made in identifying the complex processes involved in cardiac conduction and the intricate balance of elements that sustain it. However, the studies described above testify that there are still gaps in knowledge that need to be addressed to improve our understanding of conduction and to further current therapeutic approaches. This work provides evidence that supports a theory of a new form of electrical coupling between cardiac myocytes – Ephaptic Coupling, and identifies modulators of this phenomenon. This concept is then applied in the two arms of cardiac science, 1) to classify and identify trends in previously published inconsistent results in cardiac research and 2) to understand how therapy based on ephaptic coupling can be implemented in cardiac therapy.

The first part of this work focuses on identifying ionic modulators of CV based on the theoretical concept of ephaptic coupling. The study described in Chapter 2 was aimed at addressing a controversy in cardiac research where studies that used different perfusates but were otherwise similar reported inconsistent CV-GJ relationships. We reported how different CV-GJ relationships can be demonstrated in the same heart by altering just the perfusate composition. Specifically, we chose two solutions and modified its sodium and potassium ion composition to match that of the other. In short the results of this study demonstrated that,

1. CV was slower in both wild type (WT – 100% Cx43) and heterozygous (HZ – 50% Cx43) hearts when perinexal separation was large.
    - Increased perinexal separation preferentially slowed CV in HZ hearts.
2. Increasing $[Na^+]_o$ increased CV preferentially in HZ hearts.
3. Increasing $[K^+]_o$ slowed CV,
    - Independent of Cx43 expression in hearts with wide perinexi.
    - Dependent on both Cx43 expression and $[Na^+]_o$ in hearts with narrow perinexi.

The role of extracellular ion accumulation and depletion in modulating EpC has been theorized previously.[1] Briefly, varying extracellular sodium ion concentration in narrow clefts like the perinexi can modulate sodium current driving force.[2] Similarly, increasing potassium has been reported to increase resting membrane potential (RMP), which can result in inactivation of sodium channels and reduced sodium channel availability.[3,4] Either of these factors may then reduce the influx of sodium ions into the upstream myocyte, rate of cleft depletion and thereby rate of change of transmembrane potential in the downstream myocyte. Thus, modulating sodium and potassium ion concentration can alter CV.

The next part of this work identifies the role of extracellular calcium ion concentration in modulating CV during health and disease. Calcium ions play a crucial role in several cellular functions and pathophysiologic fluctuations in calcium can be detrimental.[5] In Chapter 3, the role of extracellular calcium ion concentration in modulating electrical coupling between myocytes is demonstrated. The specific results of this study are,

1) Extracellular calcium ion concentration is directly correlated to perinexal width (W_P) during normonatremia as well as hyponatremia.
2) CV, on the other hand, has a dual response to increasing extracellular calcium at different sodium concentrations. Specifically,
    - Increasing calcium increased CV during normonatremia.
    - Increasing calcium slowed CV during hyponatremia.
3) GJ coupling modulation was not a major determinant the CV-$[Ca^{2+}]_o$ relationship.

The differential CV response to varying extracellular calcium also provides evidence for concepts of ephaptic coupling. Specifically, during normonatremia, increasing calcium reduces perinexal width which has been theoretically hypothesized to improve EpC between myocytes.[6] This could then increase CV. On the other hand, when sodium ion concentration is decreased, reducing W_P, further reduces the pool of sodium ions available in this space, thereby greatly decreasing sodium driving force. This then results in slow transmission of impulses as explained by the concept of ephaptic self-attenuation.[7]

PERFUSATE CLASSIFICATION BY IONIC COMPOSITION:

The results from these two studies were then implemented to identify a classification method for CV-GJ studies in literature, to identify if differences in solution composition can explain their different results. Studies were categorized according to the effect we hypothesized each solution would have on the CV-GJ relationship with focus on sodium, potassium and calcium ion composition.

Group A-Perfusate: Perfusates with lower $[Na^+]_o$ and higher $[K^+]_o$ were classified as Group A.[8-11] Many of the Group A perfusates were hypocalcemic with the exception of the Eloff et al.[9] perfusate, which was hypercalcemic.

Group B-Perfusate: Perfusates with higher $[Na^+]_o$ and lower $[K^+]_o$ were classified as Group B.[12-14] $[Ca^{2+}]_o$ was uniform at 1.8 mM within Group B, which fell in the lower physiologic bounds for mice.

Group C-Perfusate: Perfusates with the lowest $[Na^+]_o$, low $[K^+]_o$, and physiologic $[Ca^{2+}]_o$ were classified as Group C.[15-17] Importantly, these solutions differed from Group A and B in that Group C solutions included additional non-ionic solutes such as creatine, taurine and insulin.

To summarize the results of this classification, studies that used Group A solutions reported significant conduction slowing and elevated arrhythmia risk in hearts with ~50% reduced Cx43 expression. In contrast, studies that used Group B solutions did not observe differences in CV or arrhythmia risk between hearts with reduced Cx43 and wild type controls. Under these conditions, no significant CV changes were observed when Cx43 was reduced by approximately 50%. Neither was arrhythmia risk significantly higher relative to control groups. Finally, studies in Group C behaved similarly to studies in Group B. However, the perfusate used in the studies categorized in Group C are more difficult to discuss in context of simple ionic composition because the solutions contained non-ionizable solutes which may have additional effects on electrophysiology. Thus when the studies are classified based on perfusate composition, a clear trend in the CV-GJ relationship can be identified.

PERFUSATE ION MODULATION IN CARDIAC DISEASE:

The next step was then to identify the therapeutic consequences of Ephaptic Coupling. One major point to be noted from the discrepancies in previous studies is that there are ideal perfusate compositions that can conceal the functional manifestations of cardiac diseases. Understanding the mechanism involved could therefore provide important new targets for cardiac arrhythmia therapy. In Chapter 4, we describe acute TNFα exposure as a model of myocardial inflammation and identify a perfusate composition that can conceal TNFα induced CV slowing in guinea pig hearts. Briefly,

1) TNFα slowed CV relative to control.
2) CV slowing was associated with increased W_P with no significant change in GJ coupling.
3) Increasing extracellular calcium ion concentration, reduced W_P and preserved CV in the presence of TNFα.

4) Interestingly, increasing calcium also improved GJ coupling in these hearts which could also contribute to faster CV.
5)

In short, preserving the cardiac ephapse – perinexus, as well as gap junctions, by modulating perfusate calcium concentration, concealed CV slowing in TNFα treated hearts.

Finally, in Chapter 5, we implemented a similar approach in attenuating CV slowing induced by metabolic ischemia in the heart. The results of this study can be summarized as follows.

1) Five different perfusates with varying physiologic sodium and calcium concentration that produced similar CV responses during control and reperfusion, reduced CV to significantly different extents during ischemia.
2) Solutions with higher sodium ion concentration and wider W_P performed best during ischemia, in terms of greatest CV slowing attenuation, reduced arrhythmias and longer time to asystole.
3) CV modulation by perfusates was not associated with changes in GJ coupling.
4)

In addition to the above two disease conditions, the concept of perfusate composition modulation as cardiac arrhythmia therapy was applied in a model of Brugada syndrome, which is often characterized by a loss of function mutation in the cardiac sodium channel.[18] This results in a reduction in the sodium current which could be arrhythmogenic. In a pilot study, Brugada syndrome was simulated by perfusing the hearts with 0.5μM Flecainide, a sodium channel blocker. Perfusate calcium ion composition was modulated between 1.25 and 2.0 mM in the same heart in the presence of flecainide and CV was measured. As illustrated in Figure 6.1, CV slowed relative to control in hearts with Flecainide and low calcium. On the other hand, CV slowing was attenuated in hearts treated with Flecainide and high calcium. These initial data describe another cardiac disease where perfusate ion modulation can attenuate arrhythmogenic conduction alterations.

In this section, we discuss evidence for the complete or partial concealment of the effects of three very different cardiac diseases – myocardial inflammation, metabolic ischemia and Brugada's syndrome, by simply modulating the perfusate ion composition.

CONCLUSIONS:

The findings described here can have significant impacts not only in cardiac research but also in clinical diagnosis and treatment of cardiac diseases. On the research side, perfusate ion composition has been identified as a novel determinant of conduction that has to be accounted for in cardiac electrophysiology research. Using a classification system based on the ionic modulators of Ephaptic coupling, such as that described above, could shed light on several unanswered questions that have existed over the last several decades. The effects of ephaptic coupling have to be considered in clinical settings as well as in the diagnosis and treatment of cardiac diseases. As demonstrated above, serum ion concentration could vary the manifestation of diseases like myocardial inflammation, metabolic ischemia and Brugada syndrome, complicating diagnostic procedures. Fortunately, this very process can be applied in the treatment of the above diseases to keep the electrophysiologic effects of cardiac diseases in a concealed state.

FUTURE DIRECTIONS:

The concept of Ephaptic coupling is still novel and several aspects of this phenomenon are not completely understood. Ephaptic coupling has to be further researched by a threefold approach.

1) To identify how the interaction between the two forms of electrical coupling described here translates to *in vivo* conditions as well as to other species during age, health and disease.
2) To develop methodology that would directly enable the measurements of electric potential changes in cardiac ephapses, during an AP, as predicted by ephaptic coupling models.
3) To identify mechanisms that already exist in the body that can regulate serum ion composition and how they can be integrated to achieve ideal cardiac conduction during health and disease.

Clinical application of Ephaptic coupling may not only provide a new therapeutic tool in itself, but also a means to improve the efficiency of current approaches. The field of cardiac research and therapy could then take one more step towards preventing the disastrous estimates of deaths due to cardiovascular cardiac diseases predicted for 2030.

REFERENCES:

1. Sperelakis N, McConnell K. Electric field interactions between closely abutting excitable cells. *Institute of Electrical and Electronic Engineers - Engineering in Medicine and Biology Magazine.* 2002;21:77-89.

2. Hodgkin AL, Huxley AF. Currents carried by sodium and potassium ions through the membrane of the giant axon of Loligo. *The Journal of Physiology.* 1952;116:449-472.

3. Maruyama T, Ejima J, Kaji Y, et al. [The nature of the external ionic modulation of the myocardial electrical propagation: importance of the safety factor]. *Nihon seirigaku zasshi. Journal of the Physiological Society of Japan.* 1994;56:415-424.

4. Kagiyama Y, Hill JL, Gettes LS. Interaction of acidosis and increased extracellular potassium on action potential characteristics and conduction in guinea pig ventricular muscle. *Circulation Research.* 1982;51:614-623.

5. Zarain-Herzberg A, Fragoso-Medina J, Estrada-Aviles R. Calcium-regulated transcriptional pathways in the normal and pathologic heart. *International Union of Biochemistry and Molecular Biology Life.* 2011;63:847-855.

6. Veeraraghavan R, Lin J, Hoeker GS, et al. Sodium channels in the Cx43 gap junction perinexus may constitute a cardiac ephapse: an experimental and modeling study. *Pflugers Archiv : European Journal of Physiology.* 2015;467:2093-2105.

7. Kucera JP, Rohr S, Rudy Y. Localization of sodium channels in intercalated disks modulates cardiac conduction. *Circulation Research.* 2002;91:1176-1182.

8. Guerrero PA, Schuessler RB, Davis LM, et al. Slow ventricular conduction in mice heterozygous for a connexin43 null mutation. *The Journal of Clinical Investigation.* 15 1997;99:1991-1998.

9. Eloff BC, Lerner DL, Yamada KA, et al. High resolution optical mapping reveals conduction slowing in connexin43 deficient mice. *Cardiovascular Research.* 2001;51:681-690.

10. Danik SB, Rosner G, Lader J, et al. Electrical remodeling contributes to complex tachyarrhythmias in connexin43-deficient mouse hearts. *Federation of American Societies for Experimental Biology Journal.* 2008;22:1204-1212.

11. Lubkemeier I, Requardt RP, Lin X, et al. Deletion of the last five C-terminal amino acid residues of connexin43 leads to lethal ventricular arrhythmias in mice without affecting coupling via gap junction channels. *Basic Research in Cardiology.* 2013;108:348.

12. Morley GE, Vaidya D, Samie FH, et al. Characterization of conduction in the ventricles of normal and heterozygous Cx43 knockout mice using optical mapping. *Journal of Cardiovascular Electrophysiology.* 1999;10:1361-1375.

13. Gutstein DE, Morley GE, Tamaddon H, et al. Conduction slowing and sudden arrhythmic death in mice with cardiac-restricted inactivation of connexin43. *Circulation Research.* 2001;88:333-339.

14. Danik SB, Liu F, Zhang J, et al. Modulation of cardiac gap junction expression and arrhythmic susceptibility. *Circulation Research.* 2004;95:1035-1041.

15. van Rijen HV, Eckardt D, Degen J, et al. Slow conduction and enhanced anisotropy increase the propensity for ventricular tachyarrhythmias in adult mice with induced deletion of connexin43. *Circulation.* 2004;109:1048-1055.

16. Stein M, van Veen TA, Remme CA, et al. Combined reduction of intercellular coupling and membrane excitability differentially affects transverse and longitudinal cardiac conduction. *Cardiovascular Research.* 2009;83:52-60.

17. Stein M, van Veen TA, Hauer RN, et al. A 50% reduction of excitability but not of intercellular coupling affects conduction velocity restitution and activation delay in the mouse heart. *PloS One.* 2011;6:e20310.

18. Chen Q, Kirsch GE, Zhang D, et al. Genetic basis and molecular mechanism for idiopathic ventricular fibrillation. *Nature.* 1998;392:293-296.

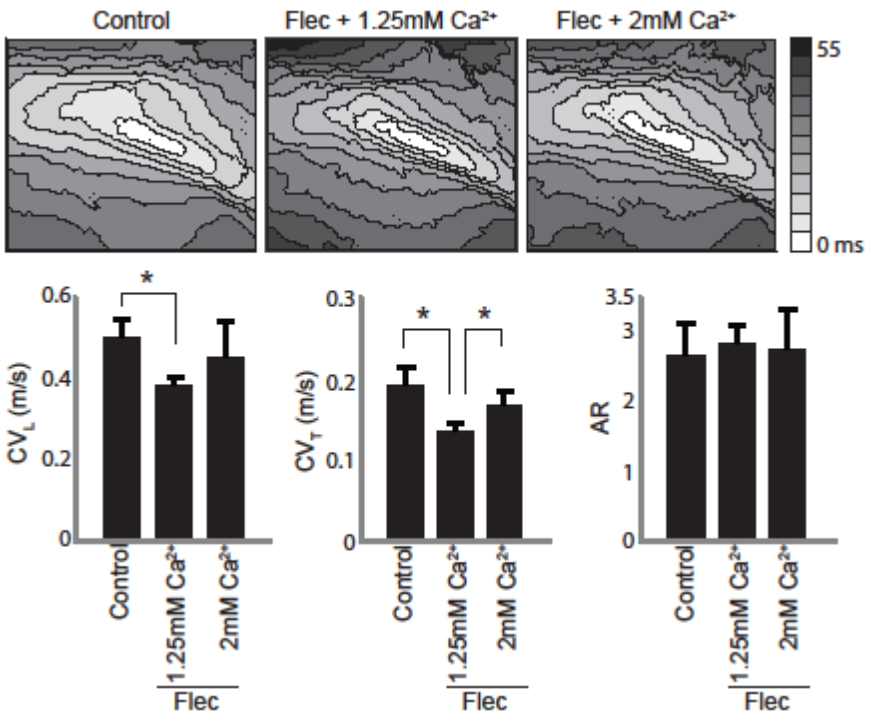

Figure 6.1 Perfusate Composition Modulates CV during Flecainide Exposure A) Representative isochrones maps from hearts perfused with Control tyrode, 0.5μM Flecainide + 1.25mM $[Ca^{2+}]_o$ and 0.5μM Flecainide + 2mM $[Ca^{2+}]_o$. **B)** Summary of CVL, CVT and AR values measured from hearts treated as mentioned above. * indicates $p<0.05$.

APPENDIX A
COPYRIGHTS AND LICENSES

Chapter 1 & 6 Excerpts © Progress in Biophysics and Molecular Biology

George SA, Poelzing S. Cardiac conduction in isolated hearts of genetically modified mice - Connexin43 and salts. 2015.

Chapter 2 © Pflugers Archiv European Journal of Physiology

George SA, Sciuto KJ, Lin J, Salama ME, Keener JP, Gourdie RG, Poelzing S. Extracellular sodium and potassium levels modulate cardiac conduction in mice heterozygous null for the Connexin43 gene. 2015

Chapter 3 is a manuscript that is currently under final stages of review for publication in the American Journal of Physiology – Heart and Circulatory Physiology.

SPRINGER LICENSE
TERMS AND CONDITIONS

Jan 04, 2016

This is a License Agreement between Sharon A George ("You") and Springer ("Springer") provided by Copyright Clearance Center ("CCC"). The license consists of your order details, the terms and conditions provided by Springer, and the payment terms and conditions.

All payments must be made in full to CCC. For payment instructions, please see information listed at the bottom of this form.

License Number	3782070648151
License date	Jan 04, 2016
Licensed content publisher	Springer
Licensed content publication	Pflügers Archiv European Journal of Physiology
Licensed content title	Extracellular sodium and potassium levels modulate cardiac conduction in mice heterozygous null for the Connexin43 gene
Licensed content author	Sharon A. George
Licensed content date	Jan 1, 2015
Volume number	467
Issue number	11
Type of Use	Thesis/Dissertation
Portion	Full text
Number of copies	10
Author of this Springer article	Yes and you are the sole author of the new work
Order reference number	None
Title of your thesis / dissertation	Interplay between Ephaptic and Gap Junctional Coupling in Cardiac Conduction
Expected completion date	May 2016
Estimated size(pages)	100
Total	0.00 USD
Terms and Conditions	

Introduction

The publisher for this copyrighted material is Springer. By clicking "accept" in connection with completing this licensing transaction, you agree that the following terms and conditions apply to this transaction (along with the Billing and Payment terms and conditions established by Copyright Clearance Center, Inc. ("CCC"), at the time that you opened your Rightslink account and that are available at any time at http://myaccount.copyright.com).

Limited License

With reference to your request to reuse material on which Springer controls the copyright,

ELSEVIER LICENSE
TERMS AND CONDITIONS

Jan 29, 2016

This is an Agreement between Sharon A George ("You") and Elsevier ("Elsevier"). It consists of your order details, the terms and conditions provided by Elsevier, and the payment terms and conditions.

All payments must be made in full to CCC. For payment instructions, please see information listed at the bottom of this form.

Supplier	Elsevier Limited The Boulevard,Langford Lane Kidlington,Oxford,OX5 1GB,UK
Registered Company Number	1982084
Customer name	Sharon A George
Customer address	2 Riverside Circle ROANOKE, VA 24016
License number	3798200788417
License date	Jan 28, 2016
Licensed content publisher	Elsevier
Licensed content publication	Progress in Biophysics and Molecular Biology
Licensed content title	Cardiac conduction in isolated hearts of genetically modified mice – Connexin43 and salts
Licensed content author	Sharon A. George,Steven Poelzing
Licensed content date	Available online 25 November 2015
Licensed content volume number	n/a
Licensed content issue number	n/a
Number of pages	1
Start Page	None
End Page	None
Type of Use	reuse in a thesis/dissertation
Portion	excerpt
Number of excerpts	3
Format	electronic
Are you the author of this Elsevier article?	Yes
Will you be translating?	No
Title of your thesis/dissertation	Interplay between Ephaptic and Gap Junctional Coupling in Cardiac Conduction
Expected completion date	May 2016
Estimated size (number of pages)	
Elsevier VAT number	GB 494 6272 12
Price	0.00 USD
VAT/Local Sales Tax	0.00 USD / 0.00 GBP